



Helmholtz-Zentrum für Ozeanforschung Kiel

RV PELAGIA

Fahrtbericht / Cruise Report

64PE350/64PE351

- JEDDAH-TRANSECT -

08.03. – 05.04.2012

Jeddah - Jeddah

06.04 - 22.04.2012

Jeddah - Duba



Berichte aus dem Helmholtz-Zentrum
für Ozeanforschung Kiel (GEOMAR)

Nr. 5 (N. Ser.)

März 2013



Helmholtz-Zentrum für Ozeanforschung Kiel

RV PELAGIA

Fahrtbericht / Cruise Report

64PE350/64PE351

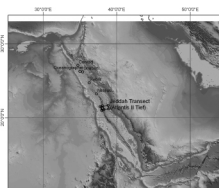
- JEDDAH-TRANSECT -

08.03. – 05.04.2012

Jeddah - Jeddah

06.04 - 22.04.2012

Jeddah - Duba



Nr. 5 (N. Ser.)

März 2013

ISSN Nr.: 2193-8113

Das Helmholtz-Zentrum für Ozeanforschung Kiel (GEOMAR)
ist Mitglied der Helmholtz-Gemeinschaft
Deutscher Forschungszentren e.V.

The Helmholtz Centre for Ocean Research Kiel (GEOMAR)
is a member of the Helmholtz Association of
German Research Centres

Herausgeber / Editor:

M. Schmidt, R. Al-Farawati, A. Al-Aidaroos, B. Kürten and the shipboard scientific party

GEOMAR Report

ISSN Nr.: 2193-8113, DOI 10.3289/GEOMAR_REP_NS_5_2012

Helmholtz-Zentrum für Ozeanforschung Kiel / Helmholtz Centre for Ocean Research Kiel

GEOMAR
Dienstgebäude Westufer / West Shore Building
Düsternbrooker Weg 20
D-24105 Kiel
Germany

Helmholtz-Zentrum für Ozeanforschung Kiel / Helmholtz Centre for Ocean Research Kiel

GEOMAR
Dienstgebäude Ostufer / East Shore Building
Wischhofstr. 1-3
D-24148 Kiel
Germany

Tel.: +49 431 600-0
Fax: +49 431 600-2805
www.geomar.de

Table of contents

Part A: Cruise 64PE350

1. Abstract.....	A-1
2. Scientific crew lists.....	A-2
3. Cruise track	A-3
4. Work performed and preliminary results.....	A-5
4.1 List of stations.....	A-5
4.2 Hydroacoustic measurements.....	A-12
4.3 Seismic measurements	A-19
4.4 Water column sampling.....	A-24
4.5 Seafloor observations	A-33
4.6 Petrology and seafloor rock sampling	A-44
4.7. Sediment sampling and porewater geochemistry	A-54
4.8 Organic-geochemical chracterisation of sediments from brine-filled Red Sea deeps.....	A-96
4.9 Microbiological investigations.....	A-104
5. Acknowledgements	A-109

Part B: Cruise 64PE351

1. Abstract	B-1
2. Cruise narrative.....	B-1
3. Crew lists.....	B-4
4. List of stations.....	B-6
5. Individual reports of the Subprojects	B-8
5.1 Subproject 3.1.....	B-8
5.1.1 Nutrient gradients in the Red Sea	B-8
5.2 Subproject 4.....	B-13
5.2.1 Buoy deployments.....	B-13
5.2.2 Nutrient dynamics	B-14
5.2.3 ADCP data recording.....	B-16
5.3 Subproject 2.....	B-17
5.3.1 Sea Floor Imaging	B-17
5.3.2 Petrology and seafloor sampling.....	B-20
5.4 Subproject 3.2.....	B-23
5.4.1 Submersible JAGO Dives.....	B-23
6. Acknowledgements	B-27
7. References	B-27

Appendix

RV PELAGIA cruise No. 64PE350

Dates, Ports: 8 March 2012, Jeddah, - 5 April 2012, Jeddah

Chief Scientist: Dr. Mark Schmidt, GEOMAR, Kiel; Dr. Radwan Al-Farawati, KAU, Jeddah

Number of Scientists: Leg a: 18; Leg b: 16; Leg c: 8

Project: The Jeddah Transect

1. Abstract

The multidisciplinary research cruise 64PE350 was conducted in the central part of the Red Sea to strengthen our understanding of volcanism and tectonics and related hydrothermal processes in this young rifting system. Therefore we extended our intense multibeam mapping campaign, which had started during the PO408 cruise in 2011, by mainly focusing on the hydrothermally active “Multi Deep” area. Detailed geological mapping was performed by selective rock sampling (dredging, coring) in areas of special interest (i.e. fresh basalt flows, or zones with signals of recent volcanic activities).

Moreover, a geochemical sampling campaign (i.e. gravity coring, Niskin water sampling) was conducted in brine-filled Red Sea deeps where variable hydrothermal activity is expected. The geochemical characteristics of sediment (pore water and mineral composition) and brine will help to identify sources and sinks relative to hydrothermal activity (e.g. hydrocarbon inflow, heavy metal concentrations in brine and sediment, etc.). Transport and degradation processes (biogeochemical cycles) at the brine-seawater interfaces were investigated by high-resolution water sampling and subsequent onboard membrane inlet mass spectrometry, gas chromatography, and major and trace element sampling. Biomarker studies are being performed by sampling/ filtering water column and brine to decipher allochthonous from autochthonous organic matter input to the Red Sea Deep. Moreover, microbiological studies will be performed on selected brine and sediment samples.

Hydrocarbon seepage at the pockmark area was investigated by hydroacoustic and geophysical methods (water column imaging, sparker reflection seismics). Additionally, sediment cores were retrieved from selected pockmark structures to investigate gas/ fluid seepage activities during Holocene.

The recently described subsea salt glacier phenomenon was investigated by seismic reflection studies and comparative multibeam profiling (salt glacier flow velocities will be calculated).

2. Scientific crew lists

Leg a, 7 – 27 March 2012		
No	Name	Nationality
1	Dr. Mark Schmidt	Germany
2	Dr. Peter Linke	Germany
3	Sergiy Cherednichenko	Ukraine
4	Dr. Stefan Sommer	Germany
5	Dr. Thorsten Bauersachs	Germany
6	Dr. Peter Feldens	Germany
7	Dr. Nico Augustin	Germany
8	Froukje van der Zwan	The Netherlands
9	Stefanie Walther	Germany
10	Svetlana Tsarichenko	Russia
11	Dr. Tomas Lundälv	Sweden
12	Dr. Radwan Farawati	Saudi Arabia
13	Dr. Alaa Barakati	Saudi Arabia
14	Dr. Mamdouh Jamal	Saudi Arabia
15	Dr. ElGasim Elgarafi	Sudan
16	Waleed Al Mehana	Saudi Arabia
17	Salim Al-Nomani	Saudi Arabia
18	Dr. Rashad Bantan	Saudi Arabia

Leg b, 27 March – 3 April 2012		
No	Name	Nationality
1	Dr. Mark Schmidt	Germany
2	Tom Kwasnitschka	Germany
3	Sergiy Cherednichenko	Ukraine
4	Dr. Thorsten Bauersachs	Germany
5	Dr. Peter Feldens	Germany
6	Dr. Nico Augustin	Germany
7	Froukje van der Zwan	The Netherlands
8	Stefanie Walther	Germany
9	Karen Hissmann	Germany
10	Jürgen Schauer	Germany
11	Dr. Radwan Farawati	Saudi Arabia
12	Dr. Alaa Barakati	Saudi Arabia
13	Dr. Mohammed Orif	Saudi Arabia
14	Ibrahim Omar Aldhuyan	Saudi Arabia
15	Salim Al-Nomani	Saudi Arabia
16	Dr. Ali Basaham	Saudi Arabia

Leg c, 3 – 5 April 2012		
No	Name	Nationality
1	Dr. Mark Schmidt	Germany
2	Tom Kwasnitschka	Germany
3	Karen Hissmann	Germany
4	Jürgen Schauer	Germany
5	Dr. Nico Augustin	Germany
6	Dr. Yvonne Sawall	Germany
7	Froukje van der Zwan	The Netherlands
8	Ibrahim Omar Al-Dhouyan	Saudi Arabia

Guests: Prof.. Peter Herzig, Dr. Jürgen Mlynek, Dr. Warner Brückmann, Dr. Georg Teutsch



Figure A-3.1: Science crew of 64PE350 leg b.

3. Cruise track

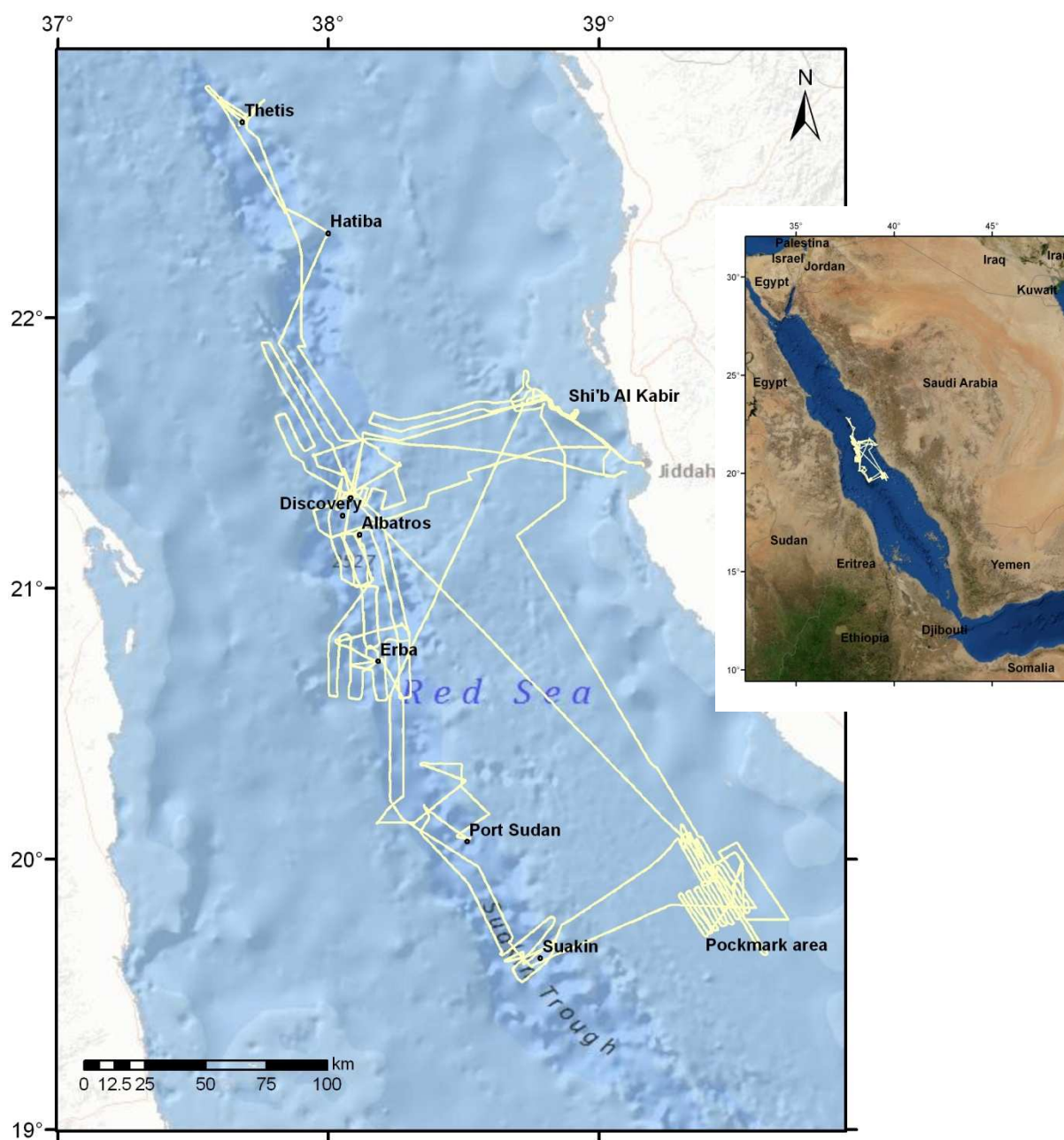


Figure A-2.1: Overview map and cruise track (yellow line) of cruise 64PE350.

For details and some non-scientific information we refer to the 64PE350 weblog (special thanks to Nico Augustin):

March 7th – March 8th

<http://www.jeddah-transect.org/deutsch/news-announcements/single-darstellung-blogeintrag/artikel/wed-07-thu-08-march-2012/>

March 9th – March 11th

<http://www.jeddah-transect.org/deutsch/news-announcements/single-darstellung-blogeintrag/artikel/fr-09-su-11032012/>

March 12th – March 14th

<http://www.jeddah-transect.org/deutsch/news-announcements/single-darstellung-blogeintrag/artikel/mon-12-wed-14-march-2012/>

March 15th – March 18th

<http://www.jeddah-transect.org/deutsch/news-announcements/single-darstellung-blogeintrag/artikel/thu-15-sun-18-march-2012/>

March 17th – March 21st

<http://www.jeddah-transect.org/deutsch/news-announcements/single-darstellung-blogeintrag/artikel/mon-17-march-wed-21-march-2012/>

March 22nd - March 27th

<http://www.jeddah-transect.org/deutsch/news-announcements/single-darstellung-blogeintrag/artikel/thu-22-tue-27-march-2012/>

March 28th - April 2nd

<http://www.jeddah-transect.org/deutsch/news-announcements/single-darstellung-blogeintrag/artikel/wed-28-tue-2-april-2012/>

4. Work performed and preliminary results

4.1 List of stations

Station No.	Gear	Gear No.	Area	Date	Deploy time (UTC)	Latitude N	Longitude E	Water depth	Recovery time (UTC)	Latitude N	Longitude E	Water depth	Remarks
64PE350-a													
1	Brine CTD	1	Salty Sediment	8.3.12	1206	21 34.419	38 49.626	760	-	-	-	-	
2	ROV	1	Salty Sediment	8.3.12	-	21 34.419	38 49.626	-	-	-	-	-	Balancing test
3	MB	1	Salty Sediment	8.3.12	1529	21.624	38.806	753	0457	21.525	38.872	720	Across first ROV target area
4	ROV	2	Salty Sediment	9.3.12	1208	21 34.526	38 49.449	794	1806	21 34.6	38 49.262	792	+CTD
5	MB	2	Transect to gas site	9.3.12	1914	21 36.02	38 49.14	749	0211	21 29.82	38 11.96	1317	
6	MB+SS	1	Gas site	9.3.12	0300	21 33.42	38 14.6	1100	0800	-	-	-	NS profile crossing the gas site
7	ROV	7	Gas site	10.3.12	1130	21 26.87	38 11.64	1080	1150	21 25.394	38 11.463	-	Cable test
8	Hatlapa winch	1	Gas site	10.3.12	1200	-	-	-	1232	-	-	-	Test with weight
9	VCTD	1	Gas site	10.3.12	1404	21 28.96	38 14.848	694	1733	21 26.865	38 16.541	857	+CO2 sensor
10	MB+SS	2	Gas site, track 2	10.3.12	1815	21 26.18	38 16.09	950	0000	-	-	-	
11	MB	3	Atlantis II	10.3.12	1010	21 31	38 7.8	1486	0241	21 23.68	37 55.17	1220	
12	VCTD	2	Gas site	11.3.12	0551	21 27.876	38 16.009	784	-	21 27.624	38 15.738	838	+CO2 sensor
13	Dredge	1	Gas site	11.3.12	1059	21 27.702	38 15.708	835	1256	21 27.791	38 15.667	810	
14	Dredge	2	Gas site	11.3.12	1340	21 27.724	38 15.731	840	1446	21 27.896	38 15.794	700	

15	MB+SS	3	Atlantis II	11.3.12	0017	21 23.911	38 15.535	2000	0354	21 21.63	38 5.84	2084	
16	GC	1	Gas Site	12.3.12	0511	21 27.518	38 15.812	834	-	-	-	-	
17	GC	2	Gas Site	12.3.12	0614	21 27.214	38 15.925	839	-	-	-	-	
18	MB	4	All-N / Thetis	12.3.12	0713	21.47	38.24	800	2020	22.81	37.60	1700	
19	MB+SS	4	Thetis (N-S)	12.3.12	2045	22 48.82	37 35.88	-	0120	22.73	37.68	1600	
20	MB+SS	5	Thetis	13.3.12	0120	22.725	37.680	1600	0335	22.802	37.758	1000	
21	Dredge	3	Thetis Deep (E-basin)	13.3.12	0450	22 43.630	37 41.771	2007	0645	22 43.892	37 41.848	1980	
22	GC	3	Thetis Deep	13.3.12	0755	22 48.171	37 35.682	1818	0846	22 48.205	37 35.707	1816	
23	Dredge	4	Hadarba Deep (southern volcano)	13.3.12	1222	22 23.524	37 58.334	2081	1510	22 23.946	37 50.428	2000	
24	VCTD	3	Hatiba Deep	13.3.12	1655	22 18.829	37 59.973	1886	1950	22 18.559	37 59.768	1891	
25	MB	5	Hatiba+All Deeps	13.3.12	2028	22 18.4	37 59.8	1900	0212	21 33.11	38 2.5	1600	
26	ROV	3	Near Jeddah	14.3.12	-	21 28.587	38 47.704	690	0900	21 28.714	38 47.544	682	
27	MB	6	Jeddah Transect	14.3.12	15.31	21.48	39.02	690	0451	21.34	38.07	2100	
28	VCTD	4	Atlantis II S.	15.3.12	0530	21 20.612	38 4.748	2152	0740	21 20.565	38 4.755	2148	28VCTD4
29	GC	4	Atlantis II N.	15.3.12	1018	21 26.472	38 3.403	2074	1115	21 26.462	38 3.420	2074	
30	MB	7	S. Atlantis II	15.3.12	1348	21.25	38.20	~1000	0311	21.18	38.06	~1500	
31	Brine CTD	2	Atlantis II S.	16.3.12	0525	21 20.595	38 4.727	2150	0723	21 20.612	38 4.739	2150	64PE350CT31.cnv

32	Dredge	5	Western most ridge W. from Atlantis II	16.3.12	0849	21 18.103	38 1.71	1768	1130	21 17.945	38 1.843	1860	
33	Dredge	6	N point of W ridge from A II	16.3.12	1351	21 23.991	38 3.043	2145	1546	21 24.009	38 3.034	2011	Dredge started in brine
34	MB	8	Shagara Deep area	16.3.12	1742	21.20	38.01	1100	0312	20.99	38.12	1500	
35	Brine CTD	3	Albatross	17.3.12	0613	21 11.952	38 6.923	2106	0755	21 11.904	38 6.935	2107	64PE350CT35.cnv
36	GC	5	South Albatross Deep	17.3.12	10.16	21 5.586	38 7.087	2255	1132	21 9.726	38 7.392	2972	
37	Dredge	7	Southern Shagara Deep	17.3.12	1306	21 1.797	38 9.871	2290	1620	21 1.948	38 9.862	2270	
38	MB	9	Erba Deep area	17.3.12	1701	20.84	38.01	-	0700	20.73	38.18	2395	
39	Brine CTD	4	Erba Deep	18.3.12	0651	20 37.605	38 0.08	2372	0840	20 43.802	38 10.991	2372	64PE350CT39.cnv
40	GC	6	Erba Deep	18.3.12	1112	20 47.992	38 2.410	1866	1203	20 48.042	38 2.471	1866	
41	Dredge	8	valley north of Erba	18.3.12	1354	20 51.992	38 16.148	2279	1514	20 52.226	38 16.126	2246	Empty Dredge
42	MB	10	Erba Deep area	18.3.12	1224	20.83	38.30	1200	0408	20.6000	38.2200	1000	
43	Dredge	9	Eastern Erba Deep	19.3.12	0506	20 44.037	38 11.728	2306	0715	20 44.406	38 11.727	2283	
44	MB	11	Transect Erba-Port Sudan	19.3.12	0801	20.72	38.20	2200	1435	20.13	38.30	1200	
45	MB+SS	6	Port Sudan Deep	19.3.12	1515	20 9.47	38 20.87	1200	2024	20 20.7	38 21.02	1670	

46	MB+SS	7	Port Sudan Deep	19.3.12	2024	20 20.07	38 21.02	1670	0115	20 20.91	38 29.57	2000	
47	MB	12	Port Sudan Deep	19.3.12	0115	20 20.31	38 29.57	1000	0400	20 10.0	38 36.0	1055	
48	Brine CTD	5	Port Sudan Deep	20.3.12	0614	20 4.603	38 30.745	2798	0744	20 4.613	38 30..758	2795	64PE350CT48.cnv
49	GC	7	Port Sudan Deep	20.3.12	0801	20 4.196	38 30.605	2649	0912	20 4.303	38 30 6.39	2667	Failed (Basalt+glass)
50	GC	8	Port Sudan Deep	20.3.12	1016	20 4.610	38 30.715	2767	1135	20 4.585	38 30.706	2767	
51	Dredge	10	Volcanoes Port Sudan Deep	20.3.12	1316	20 11.431	38 21.394	1942	1442	20 11.586	38 21.306	1890	
52	MB	13	Transect to Suakin Deep	20.3.12	1530	19.61	38.72	2290	0500	20.19	38.35	2820	
53	MB	14	Suakin Deep	20.3.12	-	-	-	-	-	-	-	-	
54	Brine CTD	6	Suakin Deep	21.3.12	0507	19 36.677	38 43.164	2821	0733	19 36.722	38 43.169	2823	64PE350CT54.cnv
55	GC	9	Suakin Deep	21.3.12	0807	19 36.722	38 43.174	2774	0925	19 36.728	38 43.170	2776	
56	Dredge	11	Suakin Deep	21.3.12	1010	19 38.746	38 43.263	2604	1230	19 38.996	38 43.238	2625	Empty Dredge
57	Dredge	12	Suakin Deep	21.3.12	1256	19 38.776	38 43.229	2638	1512	19 38.966	38 43.269	2626	Empty, some small glass pieces
58	MB	15	Pockmark area	21.3.12	2058	20 2.3	39 15.7	470	0530	20 5.2	39 19.5	460	
59	ROV	4	Pockmark area	22.3.12	0630	20 2.658	39 18.943	499	0852	20 2.303	39 18.842	505	

60	VCTD	5	Pockmark area	22.3.12	1019	20 2.51	39 18.511	507	1247	20 3.57	39 18.27	469	
61	MB+SS	8	Pockmark area	22.3.12	1330	20 6.7	39.19.0	450	1126	19 39.26	39 37.32	400	
62	MB	16	Pockmark area	22.3.12	23.26	19 39.2	39 37.4	400	0407	20 4.2	39 21.9	450	
63	GC	10	Pockmark area	23.3.12	0508	19 57.748	39 24.603	483	0526	19 57.09	39 24.618	481	
64	VCTD	6	Pockmark area	23.3.12	0600	19 57.056	39 24.741	481	1100	19 58.645	39 23.823	467	
65	MB+SS	9	Pockmark area	23.3.12	1145	19 57.17	39 23.13	470	1715	19 53.56	39 29.18	426	
66	Brine CTD	7	Atlantis II South	24.3.12	0539	21 20.628	38 4.735	2172	0742	21 20.642	38 4.736	2174	64PE350CT66.cnv
67	MB+SS	10	Atlantis II	24.3.12	0910	21 32.93	38 7.27	1490	1713	21 32.50	37 59.94	1700	
68	MB	17	N. of Atlantis II Deep	24.3.12	1707	21 32.1	38 0.6	1500	0400	21 30.7	37 51.4	1300	
69	Brine CTD	8	Atlantis II South-East	25.3.12	0544	21 20.247	38 5.59	2165	0800	21 20.249	38 5.603	2164	64PE350CT69.cnv
70	GC	11	Atlantis II South-East	25.3.12	0810	21 20.261	38 5.601	2145	0908	21 20.212	38 5.565	2143	
71	MB	18	NW of Jeddah, Jeddah transect	25.3.12	1112	21 34.5	38 7.8	1100	0158	21 37.5	38 54.4	750	
72A	MB+SS	11	Jeddah Transect	27.3.12	1200	21 42.02	38 48.78	560	0110	21 39.24	38.36.20	970	
72B	MB	19	Jeddah Transect	28.3.12	0115	21 39.24	38 36.20	970	1100	21 43.2	38 47.7	530	

73	Huge CTD	1	Sea Peak	28.3.12	1145	21 40.853	38 43.494	844	1239	21 40.853	38 43.512	844	64PE350CT73.cnv
74	GC	12	Sea Peak	28.3.12	1343	21 40.848	38 43.402	839	1406	21 40 843	38 43.410	839	
75	MB	20	Transit to Suakin Deep	28.3.12	1940	20 57.1	38 23.6	900	0550	19 42.7	38 41.2	2600	
76	Dredge	13	N Suakin Deep, Volcanic area	29.3.12	0629	21 41.438	38 40.066	2456	0844	19 41.791	38 40.212	2451	
77	Dredge	14	Hummocky volcanic area in middle of S Suakin Deep	29.3.12	1024	19 36.074	38 45.183	2546	1251	19 36.276	38 45.180	2477	
78	MB	21	Pockmark	30.3.12	0108	-	-	-	0517	19 59.569	39 31.848	471	
79	GC	13	Pockmark	30.3.12	0530	19 59.544	39 31.808	465	0543	19 59.549	39 31.847	463	
80	GC	14	Pockmark	30.3.12	0653	19 55.121	39 30.387	450	0706	19 55.102	39 30.385	454	
81	GC	15	Pockmark	30.3.12	0800	19 50.694	39 29.813	420	0812	19 50.714	39 29.769	420	
82	MB	22	Pockmark	30.3.12	0530	19 42.3	39 29.5	450	1008	19 59.009	39.26.493	434	
83	MB	23	Pockmark-> Seamount	31.3.12	1012	19 59.33	39 15.99	437	0450	21 44.0	38 45.3	870	
84	Jago	n.a.	Sea Peak	1.4.12	0600	21 41.208	38 45.267	100	0700	-	-	-	Jago handling test
85	Jago	1	Sea Peak	1.4.12	0908	21 41.136	38 45.289	295	1145	-	-	-	Jago No. 1178-1
86	MB	24	Eliza Shoals	1-2.4.12	1238	21 44.9	38 44.5	850	0140	21 42.2	38 37.6	860	
64PE350-b													
1	Jago	2	Shi'b Al Kabir	05.04.12	0421	21 40.109	38 50.396	300	0720	21 39.828	38 50.398	400	Jago No. 1179-2

2	Jago	3	Shi'b Al Kabir	05.04.12	0845	21 40.041	38 50.516	400	1130	21 40.010	38 50.605	316	Jago No. 1180-3
3	Huge-CTD	2	Shi'b Al Kabir	05.04.12	1130	21 40.041	38 50.516	100	1200	21 39.525	38 51.266	560	

VCTD – Video (Sea and Sun Technology); 11 Niskin bottles (Hydrobios)

Brine CTD/Huge CTD – Seabird 9plus, 24 Niskin bottles (RV PELAGIA)

GC – Gravity corer 4m (GEOMAR)

MB – Multibeam (RV PELAGIA)

SS – Sparker reflection seismic (Applied Acoustics)

Jago – Submersible Jago (GEOMAR)

ROV – Remotely Operated Vehicle Ocean Modules V8 (Sven Lovén Centre for Marine Sciences, Sweden)

Dredge – Chain bag dredge (GEOMAR)

4.2 Hydroacoustic measurements

Nico Augustin, Rashad Bantan, Peter Feldens

During PELAGIA cruise 64PE350, extensive multibeam mapping provided new bathymetric data of the Red Sea between 22°48'N and 19°3'N and 37°34'E and 39°42'E including parts of the Thetis and Hadarba Deeps north of Jeddah (KSA) as well as the Erba and Suakin Deeps in the southern working area of 64PE350. Mapping was carried out with a hull-mounted EM302 echo sounder system provided by Kongsberg Maritime AS. The EM302 multibeam echo sounder collects bathymetric, corrected backscatter and water column imaging (WCI) deep-water data over a wide swath with a maximum excess of 130 degrees (2 x 65°). The configuration installed on RV PELAGIA operates in the 30 kHz frequency band at water depths of up to 7,000 m. It has an across-ship swath width of up to 5.5x the depth, to approximately 8 km with 288 beams and 32 soundings per swath. In addition, the EM302 is equipped with a function to reduce the transmission power in order to avoid hurting mammals if they are close by. Data acquisition has been done using the Kongsberg Seafloor Information System (SIS) Version 3.7.5, Build 93 running in a Microsoft Windows XP environment (Fig. A-4.2.1).

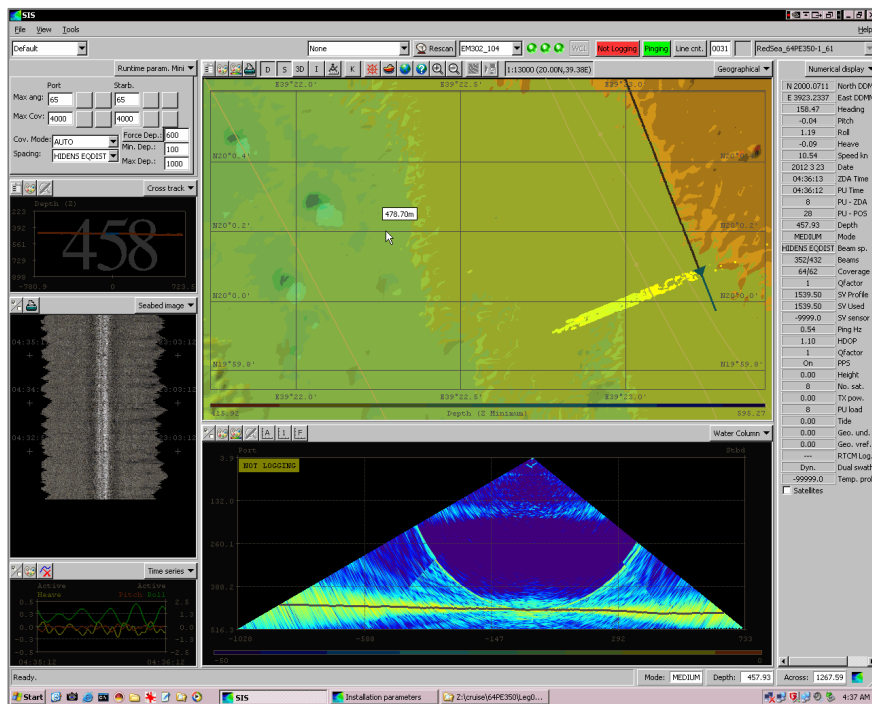


Figure. A-4.2.1: Graphical user interfaces of the Seafloor Information System (SIS) during EM302 bathymetric survey in the vicinity of pockmark fields at 20°N, offshore Saudi Arabia. The water column window is seen at the bottom.

While the northern mapping surveys were generally used to stitch information to the existing dataset of Poseidon Cruise 408 (Jan. – Mar. 2011) and extend this dataset, the bathymetric surveys south of the Atlantis II Deep recorded new bathymetric data of the Red Sea spreading centers. The approximate spatial acoustic resolution of the deeps is 25-30m. Additionally, higher resolution EM302 data (10-20m) were collected from the shelf areas at the shores of Jeddah (KSA) and the northern Pockmark fields, which were newly discovered during Poseidon cruise 408, leg 3 in 2011. The average ship speed during the bathymetric surveys was 6-7 kns. Due to bad weather conditions and strong winds from the north (5-7 bft, spikes up to 8 bft) with a high swell during large parts of the expedition, speed had to be decreased to 5-6 kns. Due to the weather conditions, large parts of the data contain errors and only have an acceptable quality. However,

thanks to partial second surveys during transits, extensive postprocessing and data cleaning, the resulting maps are of good quality and show many new details of the Red Sea floor.

The beam angle was mostly set in SIS to automatic mode, but manually limited if necessary (e.g., because of less overlap of the mapped track lines). The Pingmode was also set to Auto since this resulted in the best data quality. Source Level, Pulse Length and Desired Ping Rate were also set to Automatic. For bottom search the gates were set manually and, if required, a Force Depth command was given until the bottom signal was found.

Area-based editing of large parts of the collected data sets has been carried out using PFM container files created by DMagic as well as the 3DEditor modules included in the IVS 3D Fledermaus Professional software package (Fig. A-4.2.2). The cleaning and postprocessing performed aboard PELAGIA is preliminary and will be finished on shore. The IVS 3D FM Midwater module was used to evaluate the collected water column data and for imaging. During cruise 64PE350, water column data were only collected at stations 06MB (partially) and 58MB (pockmark survey).

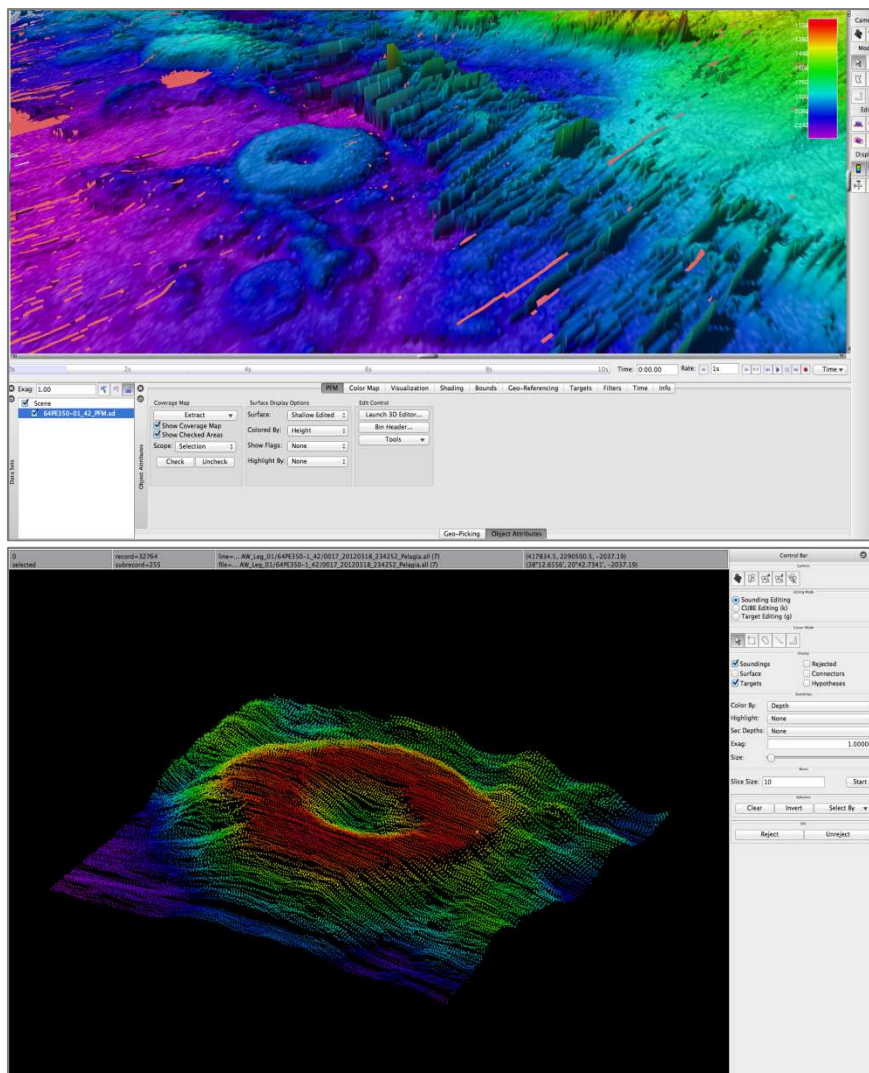


Figure A-4.2.2:

(a) Fledermaus screenshot of partially post-processed data of the Erba Deep region. The parallel errors seen in the lower right to the upper half were induced by too heavy movements of the ship due to strong winds during 64PE350/1. A volcano chain in the middle part is almost cleaned.

(b) Fledermaus 3-D Editor screen grab of a cratered, flat-rimmed volcano (see also Fig. A-4.2.2a, middle) in the Erba Deep bathymetric data set. PFM files and the 3-D Editor module allow the operator to filter and clean the dataset very accurately from wrong soundings and export a fully pos processed xyz dataset for usage in many DEM & GIS software packages.

Since the ground truthing of high-intensity multibeam backscatter signals of the southern Hatiba Deep area revealed glassy basalts in 2011, the EM302 backscatter data were used by default for targeting dredge tracks during 64PE350. By processing and mosaicking of the Kongsberg backscatter data with the FMGT module, it was possible to distinguish between harder seafloor of higher reflectivity (which was interpreted to be basaltic) from more sedimented or encrusted, restraining seafloor (Fig. A-4.2.3).

Preliminary gridding and bathymetric map production was realized using the Fledermaus DMagic module as well as Global Mapper. The data were gridded with cell sizes of 15-30m and could be exported to many data formats such as ArcView asc-files or Google Earth file format to provide the science party aboard the vessel with preliminary maps.

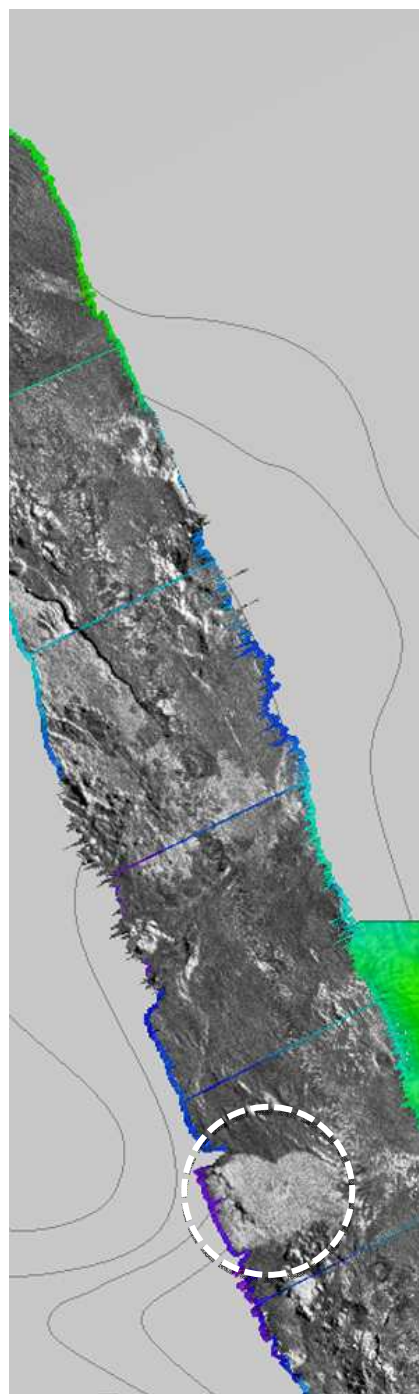
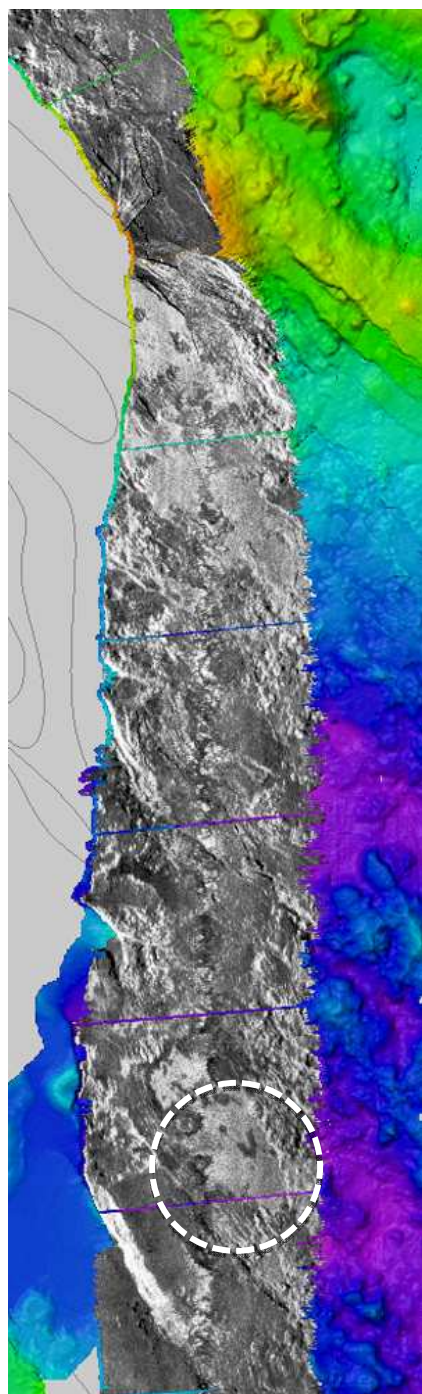


Figure A-4.2.3:

Visualization of backscatter data was mainly used for dredge track planning.

Left: Bright reflectors in the southern and northern area of the Hatiba Deep. The dashed circle shows the area in which basalt samples were recovered during R/V Poseidon expedition P408-1 in 2011. The northern part of the Hatiba deep reveals structures which are most likely to be recent lava flows to the south of a 10-km-wide volcano physically delimitating the Hatiba and Hadarba Deeps.

Right: Eastern flank of the Hadarba Deep with brighter backscatter reflectors in the north and south. The sharp-edged, very well defined area in the south of the shown stripe (dashed circle) was sampled by dredge, which revealed glassy basaltic rocks.

Preliminary Results

During R/V PELAGIA cruise 64PE350 new bathymetric data could be stitched to and around the existing dataset of R/V Poseidon cruise P408 in 2011 (Fig. A-4.2.4). The existing data covered large parts of the Hatiba and Atlantis II Deep as well as parts of the Port Sudan Deep and the so-called Jeddah-Transect area between Jeddah (KSA) and the Red Sea Rift. During the first part of 64PE350 the bathymetric works mainly remapped areas already known in the vicinity of the Atlantis II Deep (Fig. A-4.2.5) and stitched some bathymetric information to the dataset north of Atlantis II (e.g., Hatiba Deep). North of the Hatiba Deep small parts of the Hadarba and Thetis Deeps could be mapped mainly during transit. In the second part of 64PE350 large parts of the Shagara-Erba Deep area as well as the northern Suakin Deep could be mapped. In addition, the pockmarks, which had been newly discovered during R/V Poseidon cruise P408, were mapped with a larger extension and higher resolution than in 2011. Finally, large parts of the area around the Eliza shoals in front of the coast of Jeddah have been mapped.

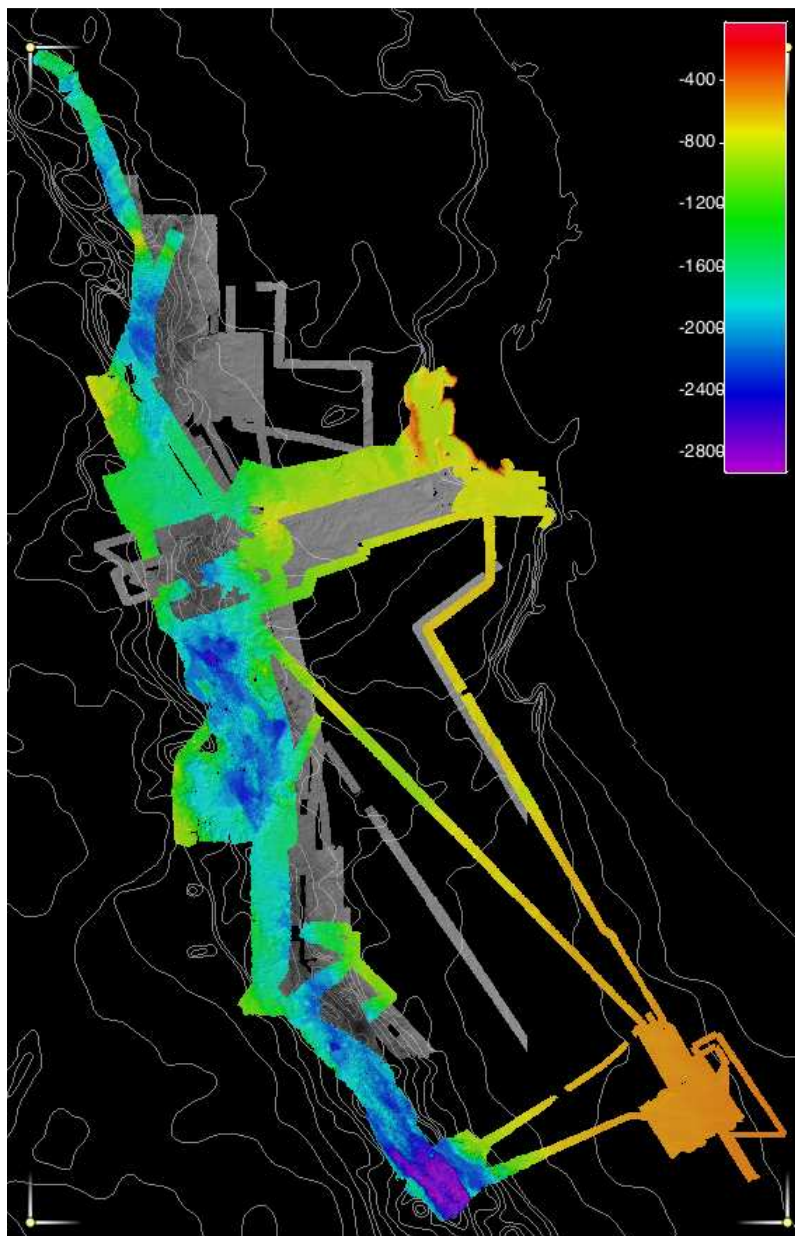


Figure A-4.2.4: New bathymetric data could be stitched to and around the existing dataset from R/V Poseidon cruises P408-1 and -2 (gray shading). Areas of completely new coverage are the Shagara-Erba through south of the Atlantis II Deep and small parts of the Suakin Deep area south of the Port Sudan Deep.

Coral Seep Peak Area

The area around the site denominated “Gas Site” in 2011 was remapped in order to get additional data at a higher spatial resolution (10-15 m) than that of the bathymetric dataset of Poseidon Cruise P408 (20-30m). The Coral Seep Peak is a mound-like structure of 400m in diameter, accompanied by a small hummocky area in its south-east, steeply raised to about 100m above the surrounding seafloor (Fig. A-4.2.5). Its origin is most likely to be volcanic and represents a pillow basalt mound or comparable feature. Two dredges (13DR, 14DR) revealed that this structure is covered by fossil corals, which has lead to the conclusion that it hosted a deep water coral reef in ancient times, maybe during the last glacial, when sea level as well as water temperatures were lower. In the new bathymetric data, sediment flow structures, which were less visible in the old data set, can be clearly observed.

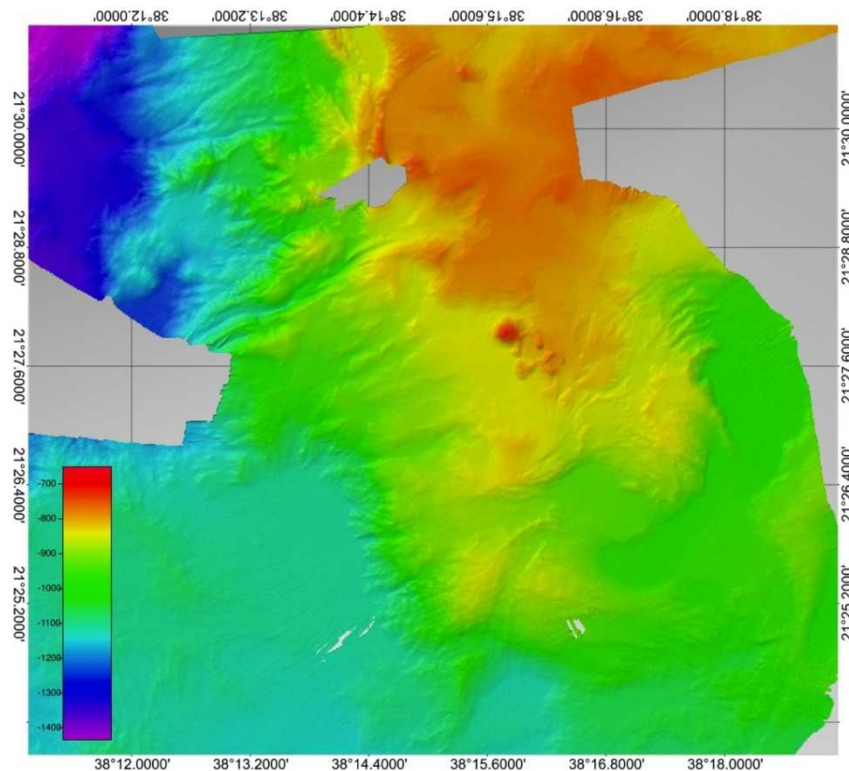


Figure 4.2.5: The Coral Seep peak (shallow, red mound in centre) area in the eastern vicinity of the Atlantis II Deep. The figure only shows the bathymetric dataset of cruise 64PE350/1.

Shagara – Erba Trough

South of the Atlantis II Deep the Shagara as well as the Erba Deep mark the northern and southern ends, respectively, of a long, slightly eastward bent, >60km N-S striking trough. This trough is limited by terraces at the western and eastern flanks, hosting individual volcanic edifices as well as proportions of sediments, migrating into the trough mainly in the south-eastern and north-eastern part of the mapped area. Several hummocky, NNW-SSE striking volcanic ridges divide the Shagara-Erba Through into at least 5 basins of an approximate water depth of 2500 m. While the two northernmost basins describe the area of the Shagara Deep, the southernmost basin is the so-called Erba Deep (Searle & Ross, 1975). Other than the Shagara Deep, which hosts metalliferous sediments but no brine pool, the Erba deep is brine-filled and shows recent volcanic activity, as indicated by very fresh basalt samples recovered during this cruise (43DR).

Suakin Deep

At a water depth of 2860 m, the northern part of the Suakin Deep marks the deepest part of the area mapped during cruise 64PE350. The structure of the Suakin deep seems to be simpler than that of the northern deeps, i.e. the Hatiba- or Erba Deep areas. The Suakin Deep consists of a NW-SE striking, 10-km-wide graben flanked by steep walls. The northeastern rim differs from the southwestern rim by the presence of at least two wide and relatively flat terraces. The centre of the deep hosts a chain of volcanoes and hummocky volcanic edifices. The deep hosts two small brine pools NE and SW of a volcano in the centre, which is prominent, but low in backscatter signal strength (Baumann et al., 1973). Dredges mainly yielded sediments, carbonate crusts and Mn-coated basaltic glass which could be an indication for a recent reduction of volcanic activity in this area, i.e. compared to the Port Sudan or Erba Deep north of it.

Eliza Shoals Reef

In order to prepare JAGO submersible dives along the reef north of Jeddah (KSA) it was necessary to create a detailed bathymetric dataset of the reef edges as there is only poor information provided by the nautical charts of this area. Therefore, we first followed the 100-m depth line given by the nautical charts to get a first impression of the real depths along the southern Eliza Shoals Reef edge (Fig. A-4.2.6). After that, a second bathymetric track closer to the reef could be performed. This resulted in detailed information about the shape of the reef edge at a high resolution of about 5m. During the survey a single, very steep seamount southwest of the Eliza Shoals was discovered. This seamount rises to about 650m above the surrounding seafloor at a depth of about 700m. The uppermost third of the mount shows very steep slopes of almost 90° in steepness. It is surrounded by its own talus, which makes a total diameter of the mount of about 1,800 m. A JAGO submersible dive at the southern flank of the mount revealed a reef on top of it. Due to reported basalts from the Eliza Shoals reef (Montaggioni et al., 1886) it is most likely to be an isolated pillow-mound covered by a carbonate reef, but no basaltic rocks could be observed during the dive.

Pockmarks and Water Column Data

During multibeam survey #58, we used the EM302 echo sounder to collect water column data to image possible degassing from the seafloor in the area of the pockmarks discovered in 2011. This was done in order to determine what has caused the immense number of pockmarks along more than 350km between 20°30'N and 17°40'N offshore Saudi Arabia, observed at water depths of less than 700 m in the P408-3 and P350-1 data. The origin of the pockmarks can be connected to seeping gas, oil or fluids; or have a more structural cause; e.g. salt collapse.

The collected water column data were processed in FM Midwater. Therefore the Kongsberg ".all data" format, which included the water column data after enabling water column data recording in the SIS, had to be converted into the Midwaters own WCI file format. The data quality appears to be good, but preliminary imaging shows no signals of degassing or other phenomena in the water column, which might indicate that the pockmarks are recently inactive or did not originate from the release of free gas.

However, bathymetric mapping shows numerous pockmarks widely spread over the covered area. The pockmarks are often connected to depressions or small channels in the sediment. Detailed analyses of pockmark density, position, and geometries as well as sparker seismic data and gravity core samples will provide additional information to determine their origin.

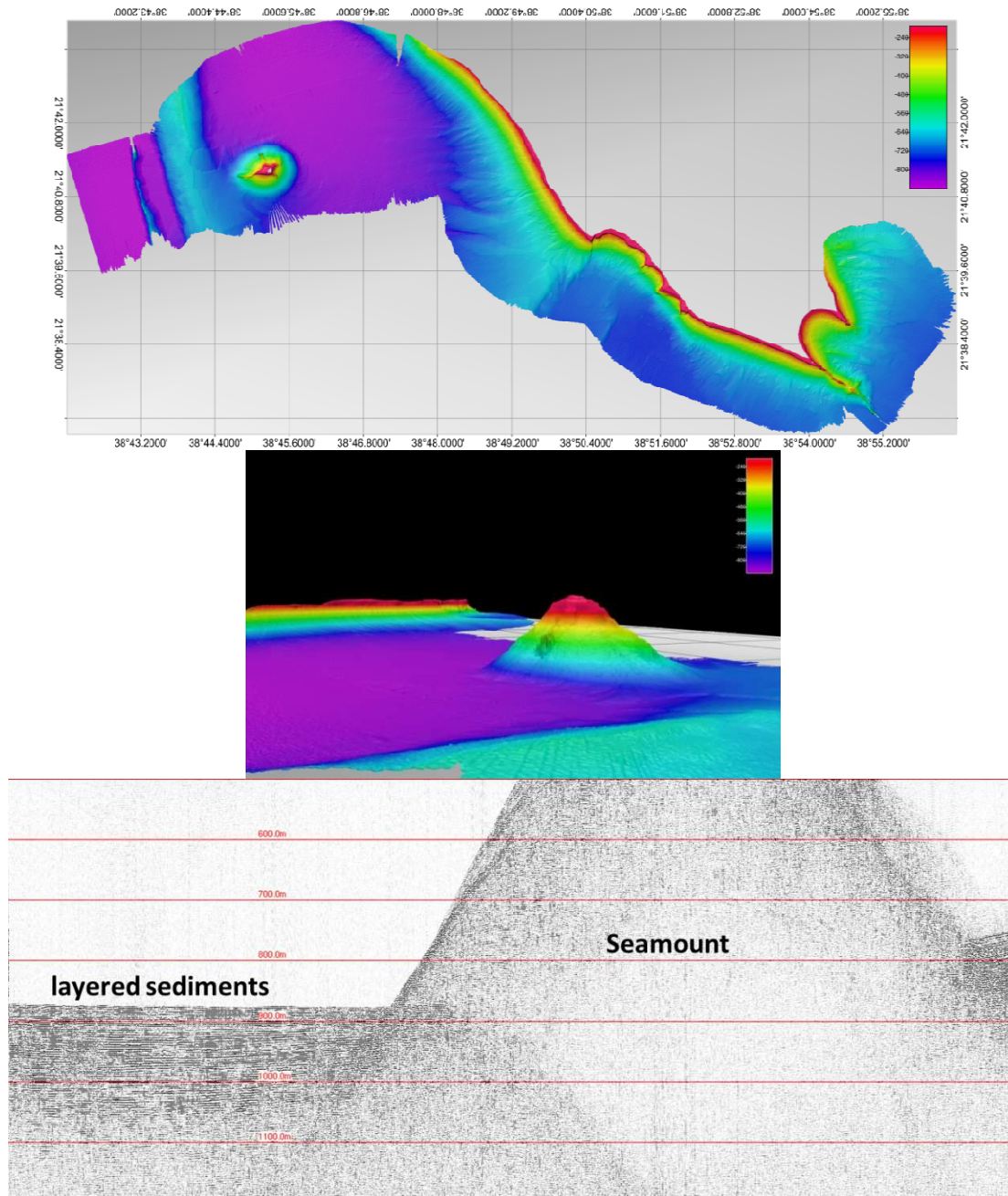


Figure A-4.2.6: *Top:* detailed mapping of reef structures close to Jeddah (KSA) revealed a very steep, single peak with an elevation of 650m above its surrounding seafloor. The structure is about 1,800 m in diameter.
Middle: 3-D view from NW to the sea peak (see map above) with the steep reef walls in the far background.
Bottom: Appearance of the seamount base in seismic data. Depth difference between red lines is 100 m.

4.3. Seismic measurements

Peter Feldens, Rashad Bantan

Seismic survey setup and first results

Reflection seismic data was acquired during the 64PE-350 cruise using a Delta Sparker system (rented from Applied Acoustics). The aim of these measurements was a) to detect gas emanations, b) to obtain further information on salt glaciers present along the Red Sea spreading axis, c) to help identifying the origin of uncertain morphological features and d) to identify soft sediments suitable as coring locations.

The Delta Sparker system comprises a power supply capable of discharging 12 kJ, a metallic frame towed behind the ship, and an 8-element single channel streamer. The acoustic signal is generated by rapidly discharging an electrical pulse between two electrodes, separated by seawater. By changing the electrodes (“tips”) on the metal frame, the frequency of the system can be changed. During the cruise, 9 electrodes were used, resulting in a peak release of the acoustic energy between approx. 300 and 500 Hz with a source sound level of 226dB at 6000kJ (according to the technical specification). This allowed for a maximum of several hundred meters of penetration into the subsurface, while maintaining a relatively high maximal resolution of a few meters. However, due to technical problems (see below) such a penetration was only achieved at water depths above 1000 m.

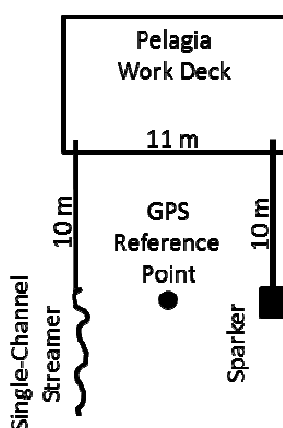


Figure A-4.3.1: Towing configuration of the Delta Sparker during 64PE350.

The schematic drawing of the towing configuration is given in Fig. A-4.3.1. The towing speed was between 3 and 4 kn, the towing depth of the sparker was 1 m. The depth of the streamer could not be controlled and depended on the survey speed; generally it was towed slightly submerged. The coordinates included in the *seggy*-files are referenced to the center between the sparker and streamer position.

Unfortunately, sparker operations were not without problems during the cruise:

- An electric safety circuit prohibiting the sparker from firing was open. It took several hours to locate the open circuit.
- The power cable leading to one of the three electrode sets on the sparker frame broke. This happened due to contact and subsequent friction with one of the two steel cables that attach the main power cable to the sparker frame. The cable could be repaired onboard.

Regardless of the fixing of the above problems, the system worked unreliably, stopping discharge at random time intervals. To rule out that the problem was related to the repaired line of the power cable, the line was detached from the power supply. The two remaining electrode sets were expected to reliably deliver a discharge of 6000J (half of the maximal energy), according to manufacturer information. However, the problem persisted, despite thorough inspection of all accessible cables and the construction of a large sea-earth to further improve the ground-earth connection. Ultimately, the cause of the failures could not be determined on board. The system randomly stopped at discharge rates as low as 4500J, causing a diminished penetration especially in deeper waters, while it was partly possible to measure with 6000J for several hours.

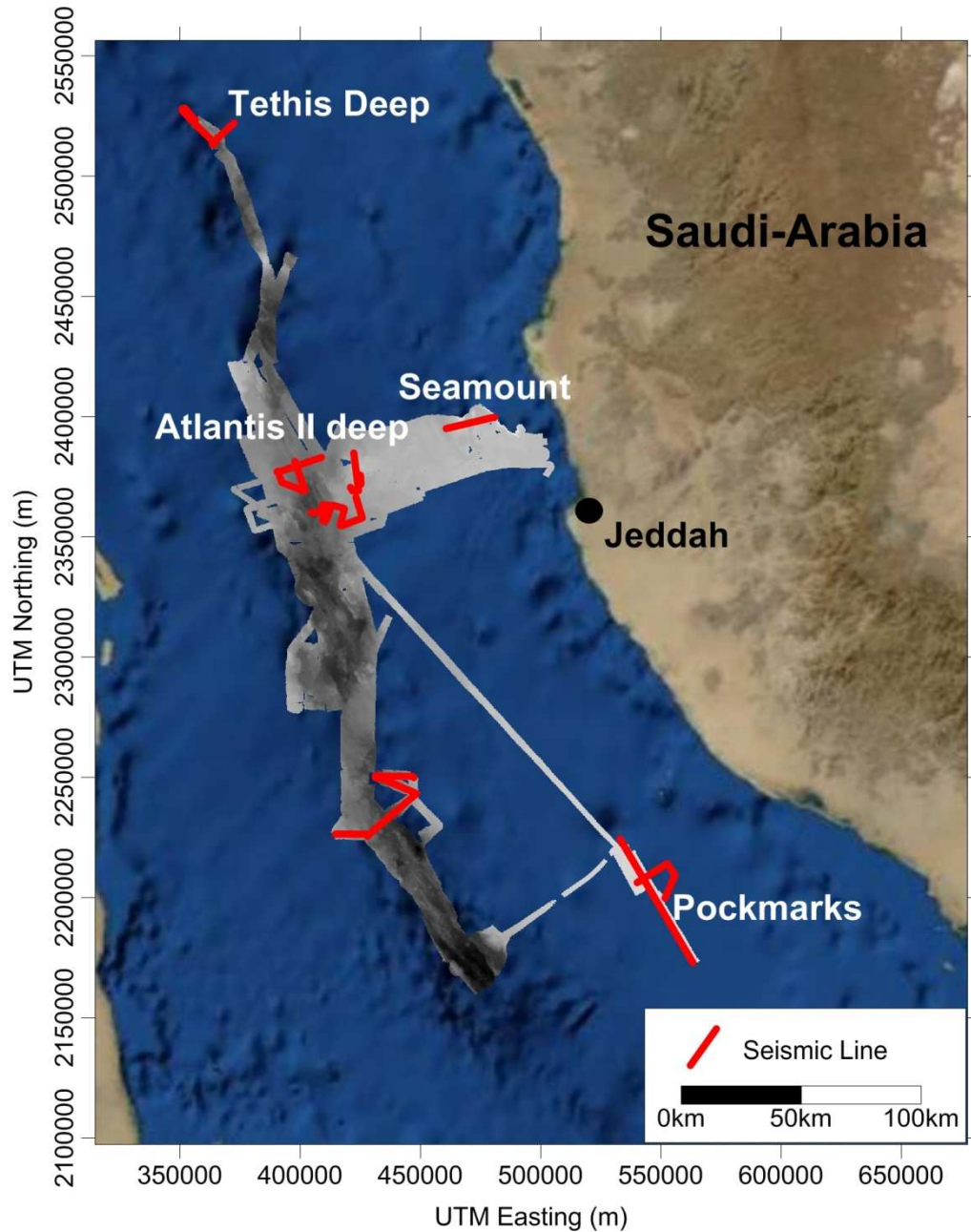


Figure A-4.3.2: Overview of seismic profile lines recorded during 64PE350.

During the cruise, 200 nautical miles of seismic data were recorded (Fig. A-4.3.2). Generally, no measurements were done during periods when the sea state reached or exceeded 6Bft.

Some examples of the resulting raw data are shown in Figs. A-4.3.3 and A-4.3.4.

Seismic profiles recorded over pockmarks in the SE part of the investigation area show that the pockmarks are spatially related to the synclines of folds observed in the evaporite surface. The evaporites can be recognized as a distinct reflector at a depth of a few hundred meters in large parts of the Red Sea (e.g., Mitchell et al. 2010).

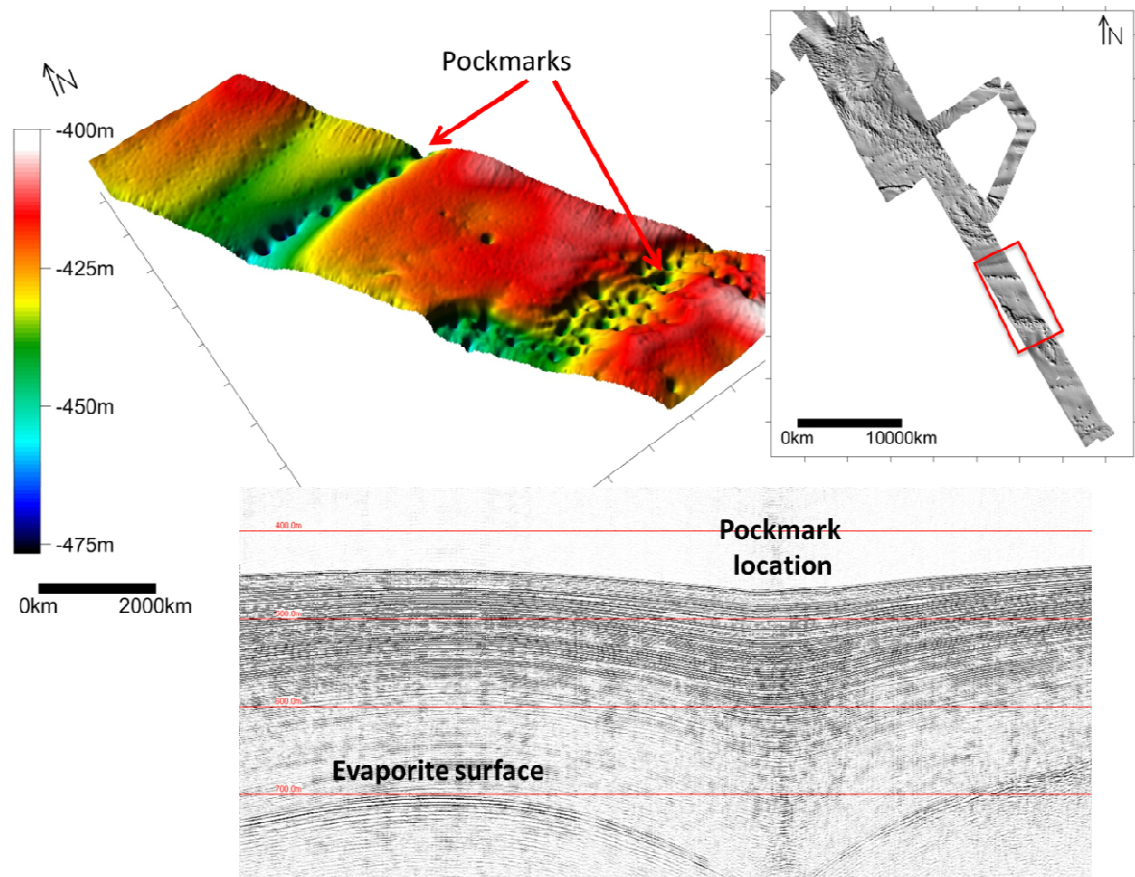


Figure A-4.3.3: A comparison of bathymetric and seismic data shows that pockmarks are spatially related to the morphology of the evaporite surface observed several hundred m beneath the seafloor.

Sparker measurements in deeper waters focused on the slope between the central deeps' floor and the surrounding shelf deposits. In these regions, wide-spread influence of submarine salt glaciers is assumed. Despite the reduced power discharge and limited data quality beneath a water depth of 1000 m, it is possible to trace the evaporite surface in the unprocessed raw data (Figs. A-4.3.3 and A-4.3.4). This will allow to establish the geometry of the salt glaciers and to estimate the stress field acting along the profiles. Sedimentary structures of larger scale, such as small basins acting as sediment depocenters, can be recognized in the raw data. To what extent smaller-scale features (e.g., faults) in the sedimentary layer overlying the evaporite can be resolved can only be assessed after further data processing and analysis.

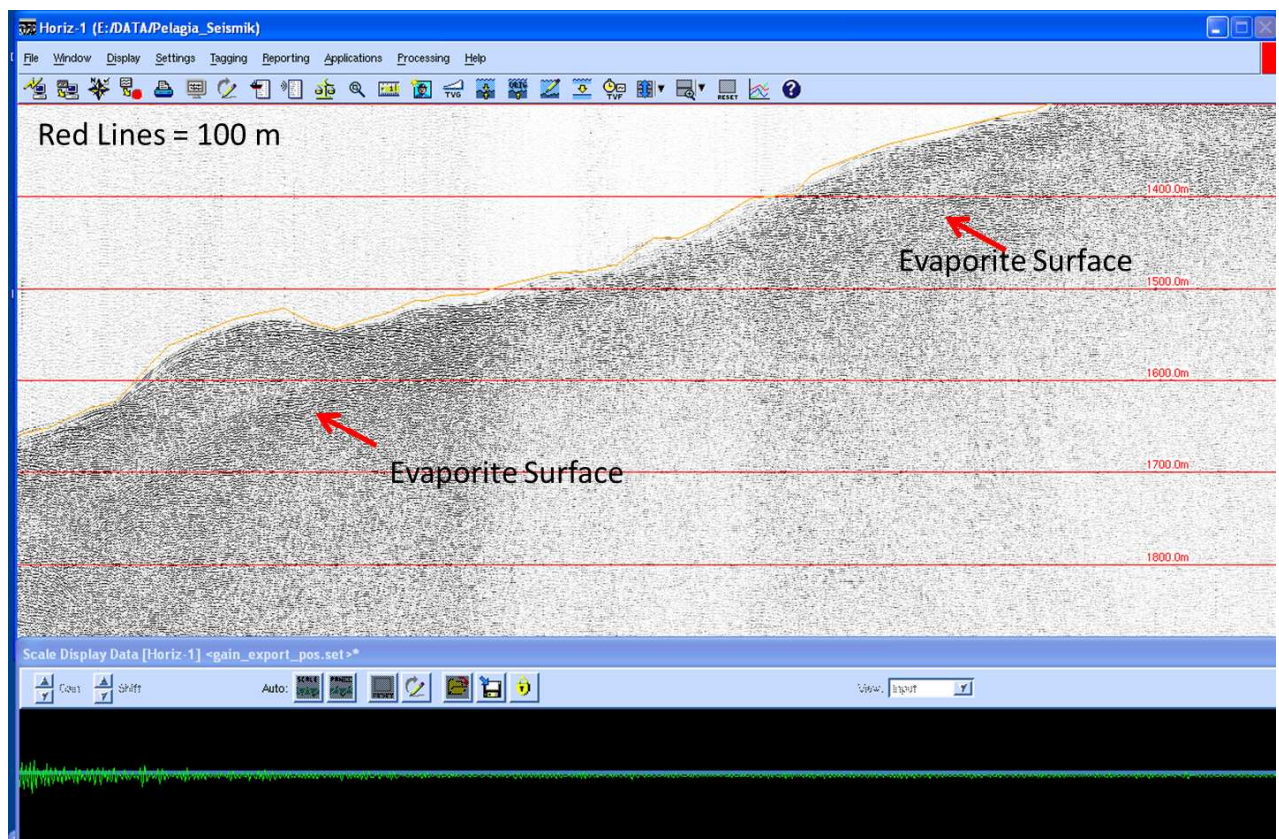
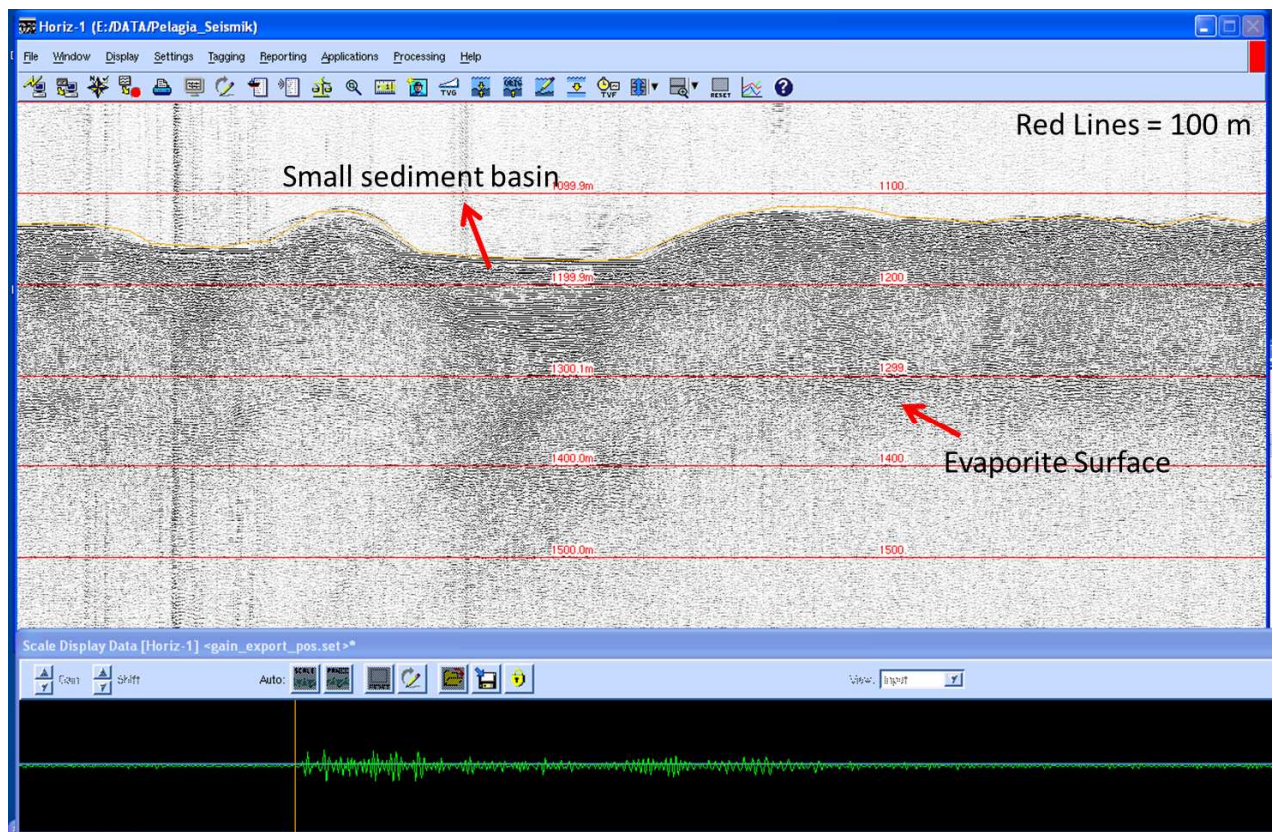


Figure A-4.3.4: Data quality in depth generally decreases below a water depth of 1000 m. Nevertheless, the evaporite surface and larger sedimentary structures can generally be recognized in the raw data.

References

- Baumann, A., Richter, H., & Schoell, M. (1973). Suakin Deep: Brines and hydrothermal sediments in the deepest part of the Red Sea. *Geologische Rundschau*, 62(3), 684–697. Springer.
- Mitchell, N.C., Ligi, M., Ferrante, V., Bonatti, E., and Rutter, E., 2010, Submarine salt flows in the central Red Sea: *Geological Society of America Bulletin*, v. 122, no. 5-6, p. 701-713.
- Montaggioni, L., Behairy, A., El-Sayed, M. K., & Yusuf, N. (1986). The modern reef complex, Jeddah area, Red Sea: a facies model for carbonate sedimentation on embryonic passive margins. *Coral Reefs*, 5(3), 127–150. Springer.
- Searle, R. C., & Ross, D. A. (1975). A Geophysical Study of the Red Sea Axial Trough between 20.5° and 22° N*. *Geophysical Journal of the Royal Astronomical Society*, 43(2), 555–572. Wiley Online Library.

4.4 Water column sampling: Gas and fluid geochemistry in Red Sea brine

Stefan Sommer, Peter Linke, Stefani Walther, Radwan Al-Farawati, Alaa Al-Barakati, Mohammed Orif, Thorsten Bauersachs, Mark Schmidt

In order to determine the gas exchange between the different density layers in brine-filled Red Sea deeps (i.e. Atlantis II, Port Sudan, Erba, Albatros, Suakin), the gas composition of brine/ Red Sea water was measured during several CTD casts. A gas profile of Hatiba Deep was measured as an example for a non-brine-filled Red Sea Deep. The measured deeps strongly differ with respect to hydrothermal activity and the degree of evaporite dissolution. In order to evaluate the degree of hydrothermal activity, brine/ fluid sources and secondary transport and reaction processes in brine-filled Red Sea deeps' standard biogeochemical parameters will be measured in all water/ brine samples.

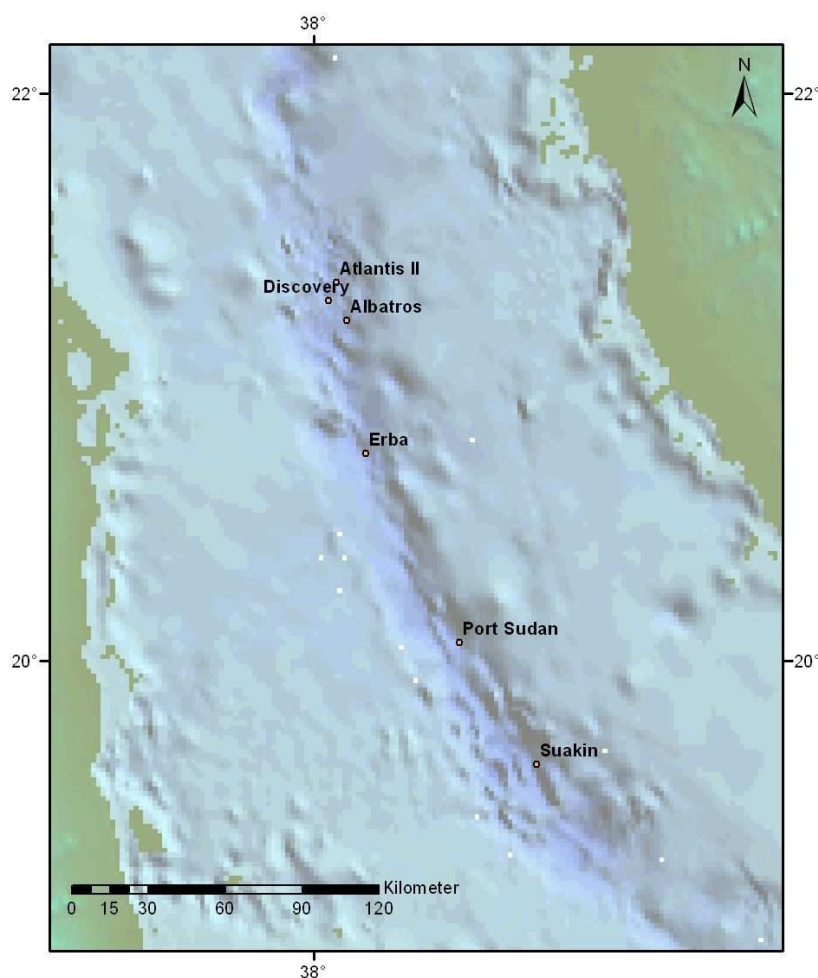


Figure A-4.4.1: General bathymetric map showing the locations of investigated brine-filled Red Sea deeps.

4.4.1 Methods

Water sampling

Water samples were taken by two different types of water sampling rosettes equipped with Niskin-bottles and CTD (Fig. A-4.4.2). The first one ("VCTD") was a small rosette equipped with 11 x 10-l Niskin-bottles, Sea and Sun Technology CTD, light and two cameras which made it possible to observe the sea floor during the sampling. The second type of water sampler rosette "Brine CTD" and "Huge CTD" had 24 x 10-l and 24 x 20-l bottles, respectively. This type of water sampling rosette was equipped with a Seabird 9plus CTD. The CTDs simultaneously measured temperature, conductivity and pressure. Ten CTD casts (Brine CTD, Huge CTD) and five CTD tracks (VCTD) were sampled during the 64PE350 cruises (Tab. A-4.1).

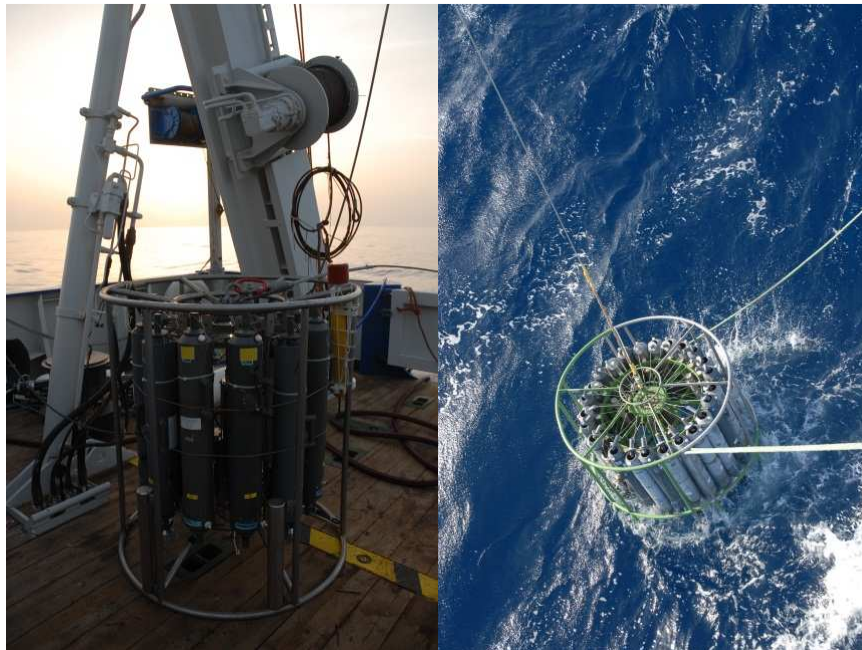


Figure A-4.4.2: (left) video-guided water sampling rosette (Sea and Sun Technology VCTD); (right) onboard Niskin rosette sampler (Seabird 9plus "Brine" CTD).

Gas analyses

Three different techniques of gas extraction and analysis were conducted onboard RV PELAGIA:

- (1) Head space gas extraction with gas chromatographic analysis
- (2) Vacuum gas extraction analysis with subsequent gas chromatographic analysis
- (3) Membrane inlet mass spectrometric analysis

Vacuum Extraction Device

The vacuum extraction device (Vakuum-Extraktions-Anlage, VEA) allows extraction of dissolved gas from a water sample (Keir et al. 2005). Pre-evacuated Schott glass bottles were filled with 1800 (900) ml of seawater or brine from a Niskin bottle immediately after the water sampler rosette was retrieved (Fig. A-4.4.3).



Figure A-4.4.3: Pre-evacuated Schott glass bottle is filled with brine.

Because of the vacuum in the bottles the gas is removed from the water phase and fills the free space at the top of the bottle. The VEA (Fig. A-4.4.4) makes it possible to remove the gas phase, measure its volume and transfer it to an evacuated vial.



Figure A-4.4.4: Assembly of the vacuum extraction device.

After the total volume of the extracted gas had been measured, 100 μ l of the gas sample were taken with a gas-tight syringe (SGE) and analyzed with a gas chromatograph (Shimadzu 2014). The residual gas was transferred into a pre-evacuated 21.6 ml head space vial. The vials were filled with 3 ml of saturated NaCl solution. Samples were stored at 4 $^{\circ}$ C for subsequent isotope analyses.

Head space extraction

The sampling for the head space analysis according to Kampbell 1989 was made right after the sampling for the VEA. 21.6-ml glass vials were filled bubble-free with water or brine from the Niskin-bottles and were closed with a butyl rubber septum and an aluminum crimp cap. The head space was created by removing 5 ml of the water (brine) sample with a plastic syringe while Argon from a gas bottle flowed through a hollow needle into the vial. A pressure control valve prevented gas pressure from rising above atmospheric level. The samples were equilibrated at laboratory temperatures for a few hours before the GC measurement was performed.

Gas chromatography

The onboard analysis of the gas samples was conducted with a Shimadzu 2014 gas chromatograph equipped with a flame ionization detector (FID) and a 4-m Porapak (mesh 50/ 80) column. An isotherm program was conducted at 50 °C for two minutes. Calibration gases of 10 ppm, 100 ppm, 1000 ppm, and 1% of CH₄ in Nitrogen (Air Liquide) were used.

Membrane inlet mass spectrometry

The gases were also determined by using a Membrane Inlet Mass Spectrometer (MIMS, GAM 200, IPI Bremen), which is suitable for simultaneous measurement of various volatiles dissolved in a fluid sample. Ar, CO₂, N₂, O₂ and CH₄ were determined in water and brine samples. Standards of dissolved gas concentrations were prepared by bubbling known concentrations of gas mixtures at constant temperatures into glass vials filled with (saline) water. Cross calibration was also conducted for methane by using onboard gas chromatography.

Water/ brine analyses

Alkalinity and pH-values were determined onboard immediately after retrieving the water/ brine samples according to <http://www.geomar.de/en/research/fb2/fb2-mg/benthic-biogeochemistry/mg-analytik/>.

Subsamples for further biogeochemical analyses have been sampled from the Niskin bottles. Anions and major and trace element composition will be measured by ion chromatography and ICP-OES/MS, respectively.

4.4.2 First results

Preliminary concentration-depth profiles show a variable increase of CH₄ concentration with depth at the brine-seawater interfaces of five investigated brine-filled Red Sea deeps (Fig. A-4.4.5). The graphs plotted below show the calculated methane concentration in nmol per liter brine or seawater at the depth (expressed in dbar) where the samples were taken. For better depth resolution only the concentration data from water depths below 2000 m is presented. In the water column above 2000 mbsl, CH₄ concentration is less than 25 nM.

Albatros Deep

Figure A-4.4.5 shows the methane concentration of the Albatros Deep plotted against depth. The Albatros Deep is about 2175 dbar deep and the interface of the seawater and the brine is at a depth of about 2100 dbar. Above the interface in the Red Sea Deep Water 25 nmol/l of dissolved methane were detected. In the brine methane concentrations of up to 300 – 400 nmol/l are measured. The maximum brine temperature of 23.8 °C is about 2.1 °C higher than the average temperature of the Red Sea deep water (21.7°C). Salinity (calculated by conductivity sensor measurements) shows values of up to 227 PSU.

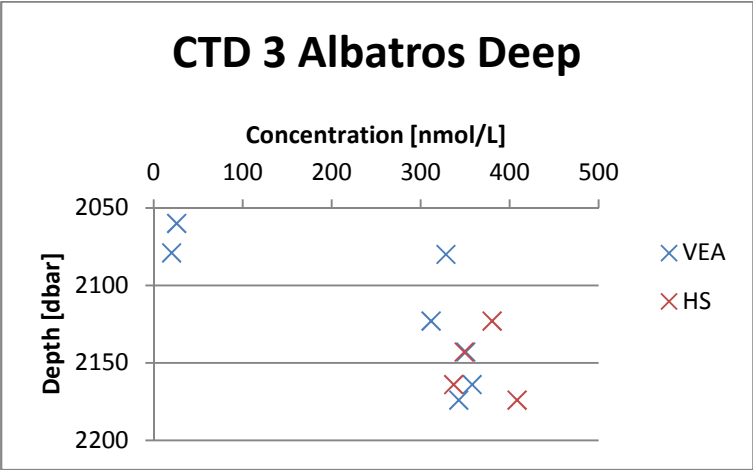


Figure A-4.4.5: Methane profile in the Albatros Deep.

Erba Deep

The plot of the Erba Deep in figure A-4.4.6 shows that the brine/ seawater interface occurs at a depth of 2412 dbar. The methane concentrations measured are at about 100 nmol/l close to the interface and went up to 600 nmol/l in the deepest headspace samples. The salinity rises from 40 PSU to 61 PSU at the interface and to 160 PSU at the seafloor. The headspace samples consistently show higher values than the VEA samples.

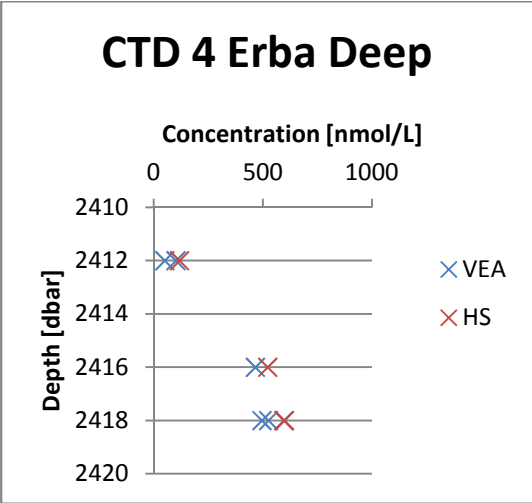


Figure A-4.4.6: Methane concentration profile of the Erba Deep

Port Sudan Deep

The plot (Fig. A-4.4.7) shows that at the interface (2550 dbar) methane concentration rises from atmospheric equilibrium concentrations (~ 2 nmol/l) to 400 nmol/l. The temperature goes from 21.5 °C to 35.8 °C. The samples from the greatest depth were taken in the Port Sudan Deep.

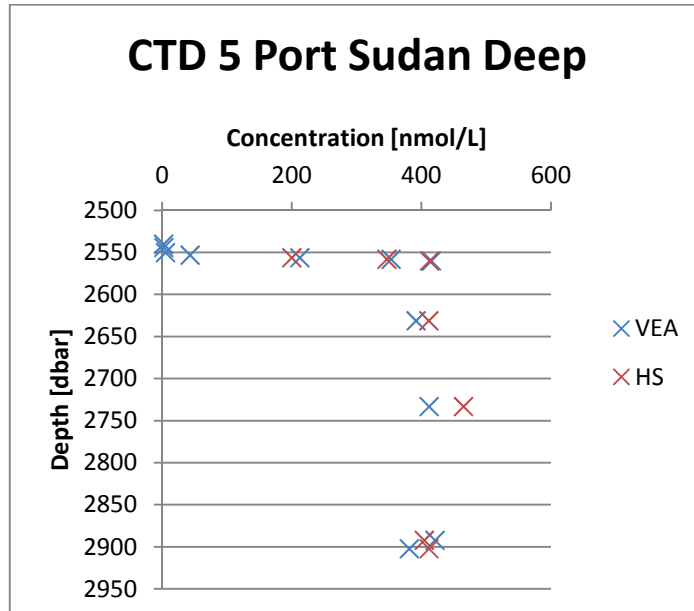


Figure A-4.4.7: Methane concentration profile in the Port Sudan Deep

Suakin Deep

Figure A-4.4.8 shows the methane concentrations of the Suakin Deep. The methane concentration in the brine is up to 300 nmol/l. At 23°C, the temperature of the brine is just 1.3 °C higher than that of average Red Sea deep water. The salinity of brine is about 152 PSU.

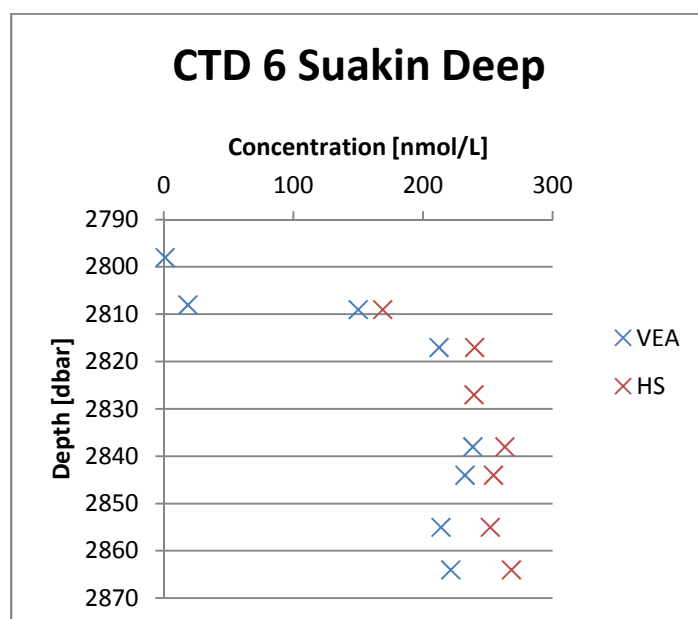


Figure A-4.4.8: Methane concentration profile of the Suakin Deep

Atlantis II Deep

In figures A-4.4.8-11, CH₄-concentration data of different parts of the Atlantis II Deep is presented. The Atlantis II Deep shows the highest methane concentrations (and the highest temperatures) in brine of all investigated brine-filled deeps (Fig. A-4.4.1). The maximum methane concentrations are around 7000 nmol/l. The temperature reaches values of 68.2°C. A summary of gas concentrations measured by membrane inlet mass spectrometry is presented in figure A-4.4.12.

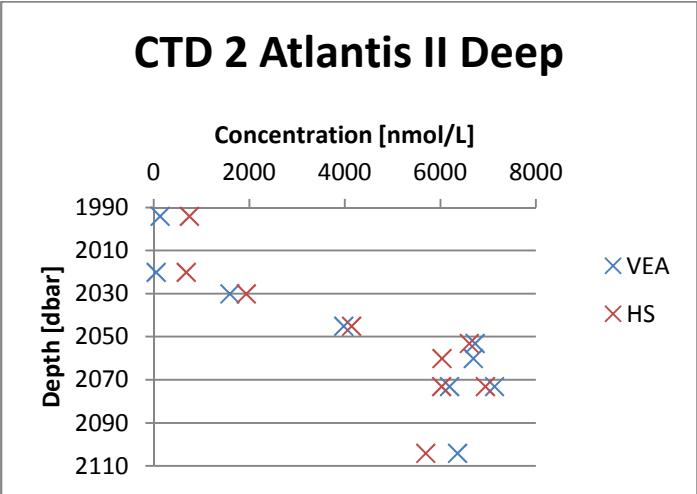


Figure A-4.4.8: Methane profile of the Atlantis II Deep.

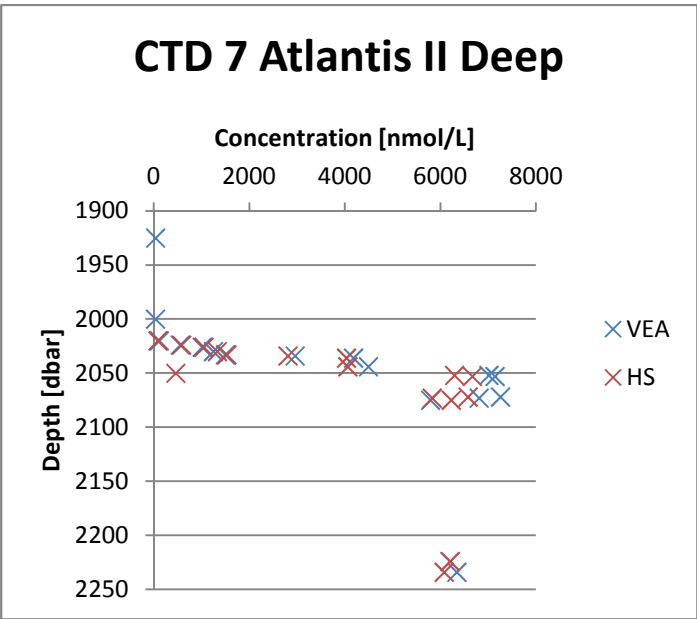


Figure A-4.4.9: Methane profile of the Atlantis II Deep.

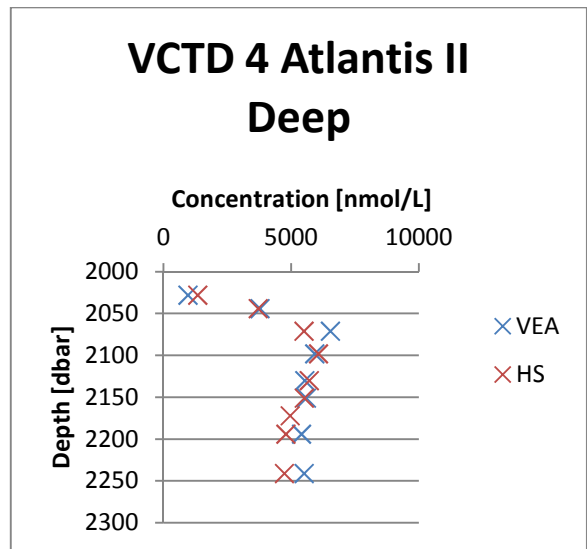
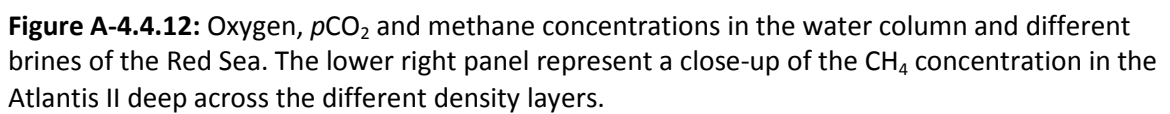


Figure A-4.4.11: Methane profile of the Atlantis II Deep.



Outlook

Particularly in the Atlantis II deep, a distinct vertical zonation of the gas distribution across the different density layers within the brine was discerned. Using diffusivity rates determined by McGinnis et al. (pers. comm.), gas fluxes between the different convective brine layers (e.g. Schmidt et al., 2003) and the overlying water column will be re-calculated. Furthermore, the data allows an assessment of methane source strength and potential methane sinks including anaerobic but also aerobic methane oxidation in the oxic transition zone (time series compared with Faber et al., 1998 and Schmidt et al., 2003). Microbial biomarkers which are currently determined in filtrates from water/ brine samples of selected water depths will help to resolve major microbiologically active water masses (e.g. photic zone, transition zone, brine/ seawater interface). Moreover, all hydrocarbon gas samples (C1-C4) will be measured by stable isotope ratio mass spectrometry to determine hydrocarbon sources and secondary degradation processes in brine-filled Red Sea Deep areas.

References

- Faber E., Botz R., Poggenburg J., Schmidt M., Stoffers P., and Hartmann M. (1998) Methane in Red Sea brine waters. *Org. Geochemistry* 29(1-3), 363-379.
- Kampbell D. H., Wilson J. T. and Vandegrift S. A. (1989): Dissolved Oxygen and Methane in Water by a GC Headspace Equilibration Technique, *International Journal of Environmental Analytical Chemistry*, 36:4, 249-257.
- Keir R., Greinert J., Rhein M., Petrick G., Sültenfuß J., Fürhaupter K. (2005): Methane and methane carbon isotope ratios in the Northeast Atlantic including the Mid-Atlantic Ridge (50°N). *Deep-Sea Research* 50, 1043-1070.
- Schmidt M., Botz R., Faber E., Schmitt M., Poggenburg J., Garbe-Schönberg D., Stoffers P. (2003) High-resolution methane profiles across anoxic brine-seawater boundaries in the Atlantis-II, Discovery, and Kebrit deeps (Red Sea). *Chemical Geology* 200, 359-376.

4.5 Seafloor observations (Diving with submersible JAGO)

Karen Hissmann, Jürgen Schauer, Tom Kwasnitschka, Alaa Barakati

The manned research submersible JAGO of GEOMAR, Kiel, was on board to be used for visual exploration and selective sampling at the pockmark sites which were discovered and mapped in detail during the first weeks of 64PE350.

JAGO has a maximum operating depth of 400 m and is therefore a very suitable tool for working within the twilight zone along the shelf break of the Red Sea. JAGO can accommodate two persons, the pilot and a scientist/ observer. The highly maneuverable vehicle has two large acrylic dome ports, one at the front (diameter 70 cm) and one at the top (45 cm). It is electrically driven and moves autonomously within the reach of the navigation and communication systems on board of the support vessel. The submersible is equipped with an USBL underwater positioning system, an electronic compass, vertical and horizontal sonar, underwater telephone for communication, digital video (HDV) and digital still cameras, CTD and a manipulator arm for collecting and handling sampling devices. The compact size (3 x 2 x 2.5 m LWH) and relatively small weight of 3 tons allow launch and recovery from a wide variety of ships with sufficient crane capacity (min. 5 tons SWL at 3 m outboard reach). The entire equipment including the submersible fits into a single 20' ISO container. The supporting team consists of three persons: the chief pilot/ senior technician, the operational manager in charge of the communication and navigation on board of the support vessel, and a technician assistant/ swimmer for support during launch and recovery.

JAGO operates worldwide and is regularly used from international research and support vessels. 64PE350 was the first cruise with JAGO on board of RV PELAGIA. The vessel has a hydraulically powered stern A-frame with a maximum vertical clearance of 8 m, an inside horizontal clearance of 8 m and a maximum outboard reach of 3 m making it suitable for safe handling of the submersible. Two towing winches, capable for lifting 5 tons SWL, are mounted on both of the frame legs. The free board of the vessel is 2.8 m.

The submersible was transferred on board of PELAGIA in Malta in a 20' sea freight container and then mobilized by the submersible team in the port of Jeddah on 27 March. First lifting and out-boarding tests with JAGO hanging at the stern A-frame were performed while the vessel was still in port. The PELAGIA work boat (6 m TL inflatable with rigid hull and 60 HP outboard engine) was used to tow JAGO away from the ship's stern after deployment and back under crane position for recovery.

Voice communication between JAGO and PELAGIA during dives was maintained by acoustic underwater telephone (ORCATRON) and a hydrophone/ transducer that was attached to the end of an outrigger pole lowered over the ship's port side to a water depth below sea surface of ca. 4 m.

While submerged, JAGO was tracked and guided by a HiPAP100 USBL underwater positioning and navigation system by Kongsberg, part of the ship's equipment. The Kongsberg transponder (70 cm long, 8.5 cm \varnothing , 11.5 kg in air), powered by internal lithium batteries, was mounted on the stern of the submersible. To display and follow both JAGO and PELAGIA tracks geographically and in real time on a computer monitor, the positioning data (ship and sub) were integrated into OFOP software (<http://ofop.texel.com>) and displayed upon GIS-based bathymetric maps produced prior to the dives.

All JAGO dive tracks are presented in Fig. A-4.5.1. The positions of sampling sites are available to be plotted on 3-D bathymetric maps, combined with individual dive logs, video sea floor observations and CTD records (Tables A-4.5.1, A-4.5.2). Time codes were all set and synchronised to GMT.

It was planned to use JAGO for visual exploration and selective sampling at the pockmark sites that had been discovered and mapped in detail during the weeks before. Unfortunately, strong winds prevented training of the crew in deployment and recovery of JAGO with the stern A-frame during the entire last week of 64PE350. On 01 April, the weather conditions finally allowed for operations, which started with a handling drill of the crew (Fig. A-4.5.2). Due to the very limited time remaining, dive sites had to be re-selected at locations closer to Jeddah port.

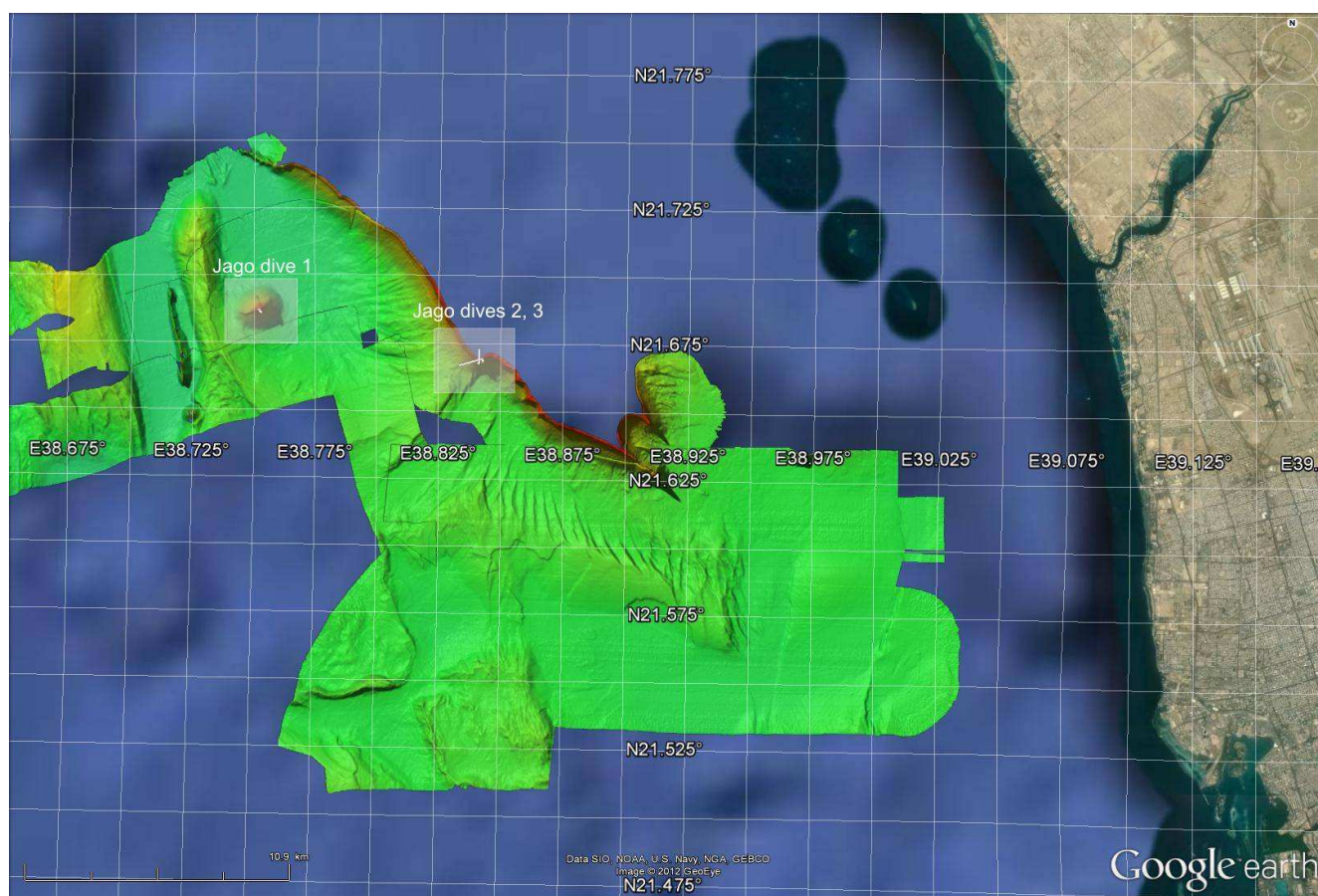


Figure A-4.5.1: Jago dive map showing the Seamount dive 1 and the dives 2 and 3 at the reef edge (Shi'b Al Kabir), northwest of Jeddah.

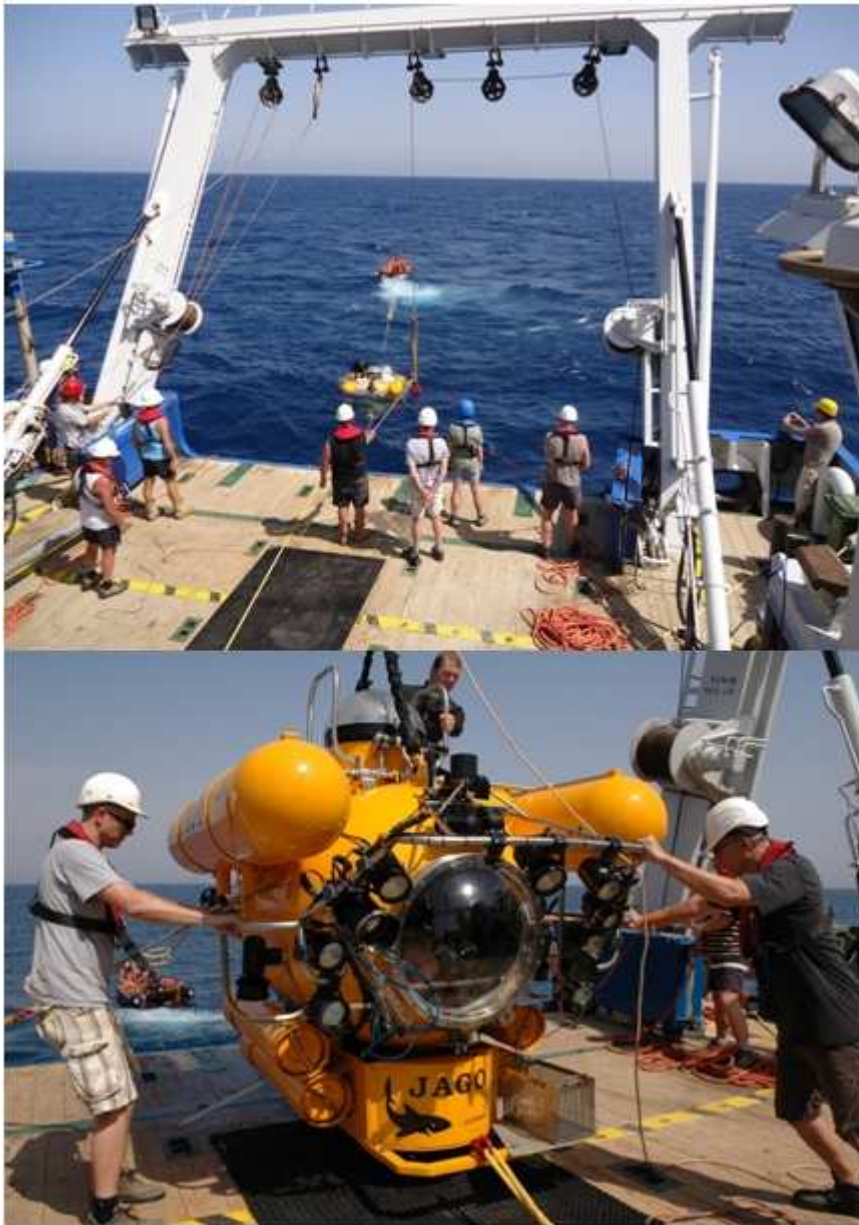


Figure A-4.5.2:
Submersible JAGO
recovery on board of
RV PELAGIA during
64PE350.

JAGO Dive 1178-1 was performed on the southern flank of an isolated seamount that had been located by multibeam earlier during the cruise. Dr Alaa Albarakati (KAU) participated in this dive as scientific observer.

The submersible landed at the southern flank of the sea peak at a water depth of 307 m and slowly followed the contours of a very steep slope on a vertical transect. Locally, vertical grooves cut deeply into the carbonate rock wall. They are caused by bypassing sediment that first carves out vertical furrows which then gradually develop into deep grooves (Fig. A-4.5.3). The surfaces of the near-vertical walls are not plain but covered by a flaky black crust that accumulates bright carbonate sediment. Video and photo close-ups revealed that small white tubes and other carbonate macro/ microstructures are embedded in these crusts. The tubes are probably secreted by polychaete worms. Parts of these crusts might be or might have been formed by calcifying bacteria which also bind sediment particles. The black coating of the crusts is most likely caused by (manganese-) iron oxidation.

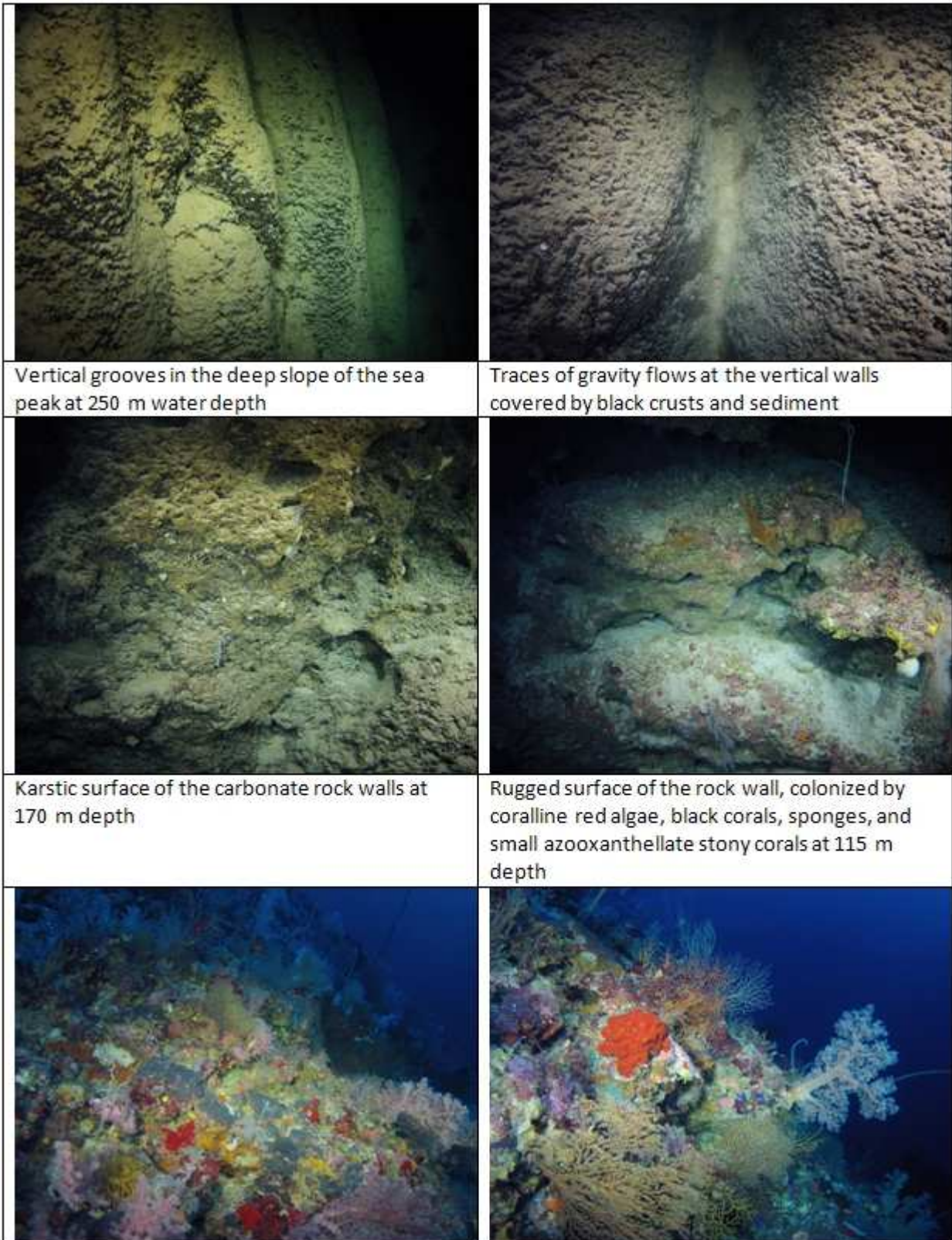


Figure A-4.5.3: Top of the sea peak at a depth of 75 m. Benthic community of encrusting sponges, soft and small stony corals, gorgonians, black corals.

Community at the top of the sea peak.

The vertical walls are extremely barren between water depths of 300 and 160 m. Sessile macrofauna is very rare and restricted to few specimens of a white-opaque sponge (glass sponge?), single individuals of deep-water solitary cup corals (genus *Desmophyllum*?) and, very scattered, small fragile gorgonians. There were no encrusting sponges at these walls, and no fish was encountered. The first living calcareous red algae (performing photosynthesis) occurred at a water depth of around 170 m, a proof for the remarkably clear water with a vertical visibility of almost 200 m. The surface of the walls slowly changed from a depth of 140 m upwards; it became more irregular and rugged, fragmented by small niches, caves and undercuttings. It is assumed that these structures were formed by karstification during the last glacial lowstand of the sea level. The benthic community now consists of red coralline algae, small yellow and red encrusting sponges, a few azooxanthellate (non-symbiotic) stony corals and small gorgonians. Fish are still almost absent. First black corals (antipatharians, white whip corals and red bushy black corals) occurred at 116 m. The slope angle slowly decreased from 106 m upwards. First zooxanthellate corals, probably of the genus *Leptoseris*, and coral fish (*Chaetodon* etc) were encountered at 105 m. The density of red coralline algae and encrusting sponges again increased from 102 m upwards. At 90 m a current set on and visibility decreased due to more particles in the water column. The benthic community at 74 m included big fan corals, soft corals, whip and bushy-shaped black corals, encrusting and vase-shaped sponges and flat-growing stony corals. The top of the sea peak was reached at a depth of 62 m.

The sea peak dive was followed by two dives at the steep cliffs of Shi'b Al Kabir Reef northwest of Jeddah. The texture of the near-vertical walls that were faced at this cliff during **JAGO Dive 1179-2** (Fig. A-4.5.4) was very similar to the facies found at depths between 300 m and 200 m during the previous dive at the sea peak. The black rocky walls, covered with bright sediment, were as barren as those at the sea peak, except that white and yellow gorgonians were encountered more regularly. Dive 1179-2 started at a water depth of 312 m and followed the slope up to the shelf break at around 90 m. Below the photic zone at around 200 m the surface of the cliff was more rugged, resulting from ledges which protruded more horizontally from the walls. These ledges are shingle-like structures that grow on the surface of steep rocky walls. Similar but slightly more pronounced ledge structures were described by Dullo et al. (1990) and Brachert and Dullo (1991) as slow-growing laminar micrite crusts which occur below the lower limit of coralline algae growth. Their formation is most likely due to biogenic processes unrelated to the photic zone. In the Red Sea and other locations these ledges are always associated to vertical walls, documented by submersible off Sudan (Brachert and Dullo 1991), Southern Sinai (Fricke 1996) and Moorea, French Polynesia (Dullo et al., unpublished).

The rounded edge of the shelf break at a depth of 88 m was found to be covered by a dense bed of rhodoliths, coralline red algae that do not encrust rocky substrate but grow as nodules unattached to the rocky seabed. They can be overturned due to water motion (during storms) or biogenic activities. Some rhodoliths at Shi'b Al Kabir Reef were colonized by encrusting sponges, whip and stony corals. Several specimens of the zooxanthellate stony coral *Leptoseris fragilis*, attached to rhodoliths, were collected during this dive for incubation experiments during 64PE351.










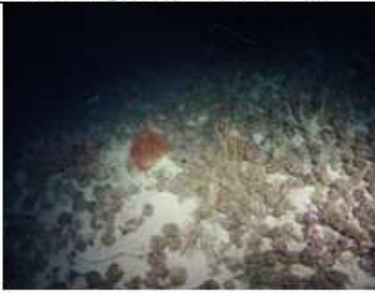
			
Surface of the vertical wall at 300 m depth		Gorgonians (living and dead specimens) at the edge of an overhang	
			
Structures of the wall at 200 m depth		Furrow in the ledge structure at vertical wall	
			
Karstic features, red algae and black corals		Increasing density of coralline red algae encrusting the carbonate rock	
			
Rhodoliths and black corals at the upper edge of the reef cliff		Dense bed of rhodoliths on the shelf above the cliff edge, colonized by black corals and the stony coral <i>Leptoseris</i>	

Figure A-4.5.4: Submersible dives at the Shi'b Al-Kabir Reef.

JAGO Dive 1180-3 was also performed at Shi'b Al Kabir Reef. It started at a steep rocky slope at a water depth of 324 m, covered with a thick layer of white sediment and single large rocks that have broken off from the upper part of the slope (Fig. A-4.5.5). The slope angle increases to an almost vertical cliff at around 250 m with a crust texture similar to that found on the walls followed during dive 1179-2. Gullies, cutting deeply into the rock wall, probably caused by a continuously downward movement of sediments along the cliffs, are dominant geomorphological features on these walls between 250 and 190 m. The upper side of the crust ledges on this steep cliff was densely covered with soft carbonate sediment. The hard substrate of the ledges was only visible on their underside. Hardly any sessile organisms colonize these rocky walls. The dominant species are white-opaque sponges and long thin tubes of probably polychaete worms that are attached like whiskers or kemps to the lower edge of the ledges. The ledges become bigger and more pronounced at a water depth of 200 m, strongly resembling the so-called "christmas tree structures" described by Brachert and Dullo 1990 on the steep forereef cliffs off Sudan. At 190 m the wall is partly overhanging, with distinct caves and niches. At 180 m the entire surface of the wall seems to be more "eroded" and "karstic", the black colour due to iron oxidation is now absent. First calcareous red algae occur on the exposed carbonate rock from 150 m upwards, in addition there are a few small gorgonians and small individuals of a zooxanthellate orange stony coral (genus *Dendrophyllia* or *Solenosmilia*?). The slope angle slightly decreased at 102 m where also the first specimens of *Leptoseris* corals occurred. The dive ended on the shelf plateau at a depth of 75 m. The exposed outcrop on the plateau was shallower, with white sediment patches accumulated in between rock structures. Dominant sessile macroorganisms were again encrusting red algae, encrusting sponges and zooxanthellate stony corals of the genus *Leptoseris*, a few specimens of which were collected for experiments.

The steep deep slopes that were visited during 64PE350 are clearly vertically differentiated into a lower zone with black crusts and ledge structures on almost vertical carbonate rock walls, and an upper zone with karstic features. These features might be interpreted as indicators for a sea level lowstand during the last glacial maximum. Karstification (dissolution of carbonate rock caused by mildly acidic water, e.g. rain water) only occurs above sea level. In all three dives the first karst features occurred at around 160 m, indicating that this zone might have been a surf zone in ancient times. Coralline red algae occurred down to a depth of 170 m which is not untypical for the Red Sea.

References

- T. Brachert and W.-Ch. Dullo (1991) Laminar micrite crusts and associated forslope processes, Red Sea. *Journal of Sedimentary Petrology* 61, 354-363.
- W.-Ch. Dullo, E. Moussavian, T.C. Brachert (1990) The foralgal crust facies of the deeper fore reefs in the Red Sea: a deep diving survey by submersible. *Geobios*, 261-281.
- H. Fricke (1996) Deep-water exploration of the Red Sea by submersible. In: F. Uiblein, J. Ott, M. Stachowitsch (eds): Deep-sea and extreme shallow-water habitats: affinities and adaptations. *Biosystematics and Ecology Series* 11: 67-89.

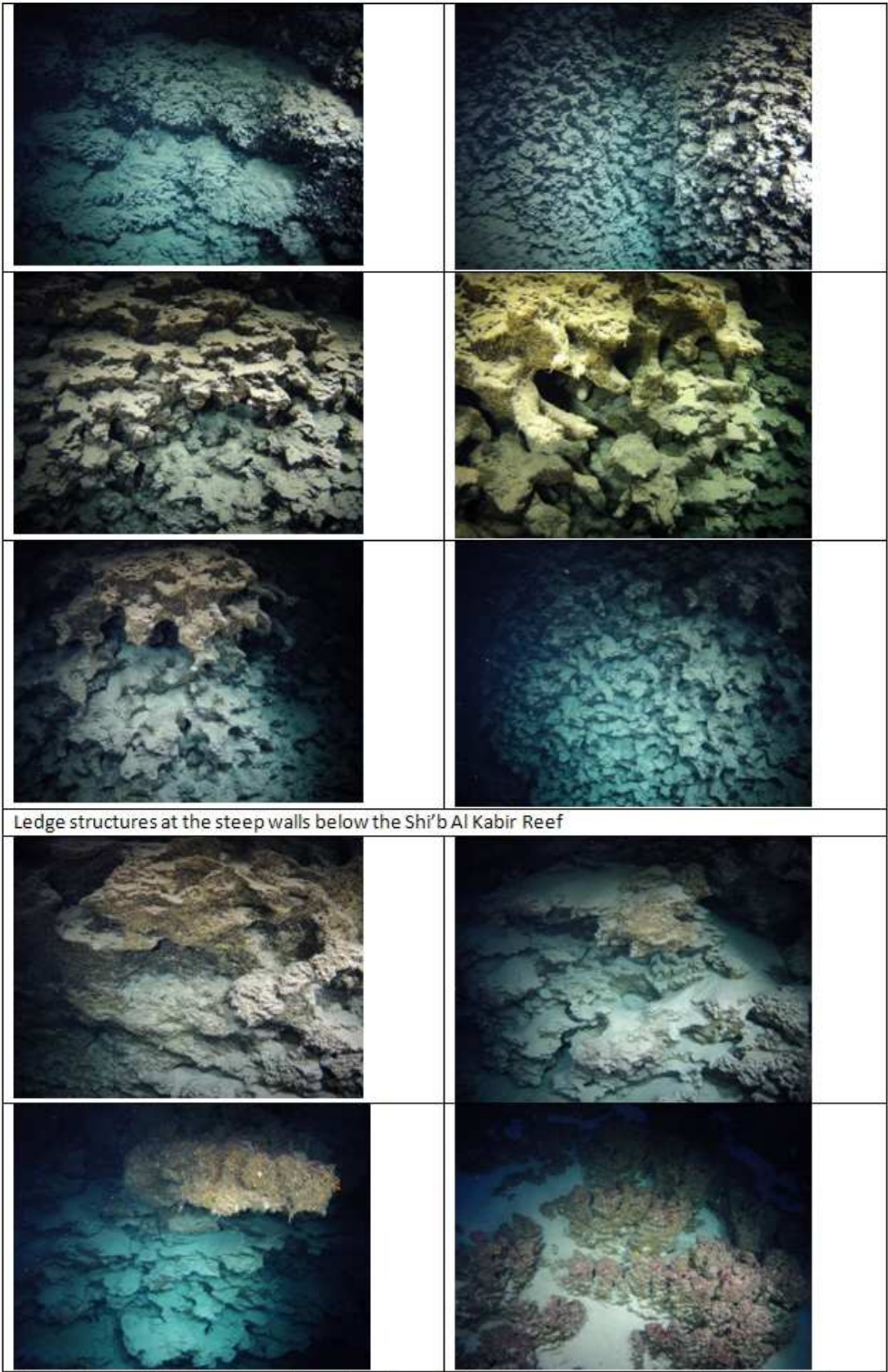


Figure A-4.5.5: Karstic structures on the carbonate walls from 180 m upwards and the edge of the cliff at a depth of 100 m with coralline red algae.

Table A-4.5.1: Jago dive track data (64PE350b, Station 1)

JAGO Dive 1178 (1) 01.04.2012			J.Schauer, Alaa Albarakati		Seamount	
					north-west of Jeddah	
Time (UTC)	Depth (m)	North	East	Comments		
08:47	0	21°41.135	38°45.28	submerged at ship's position	above 305 m depth	
09:08	295	21°41.136	38°45.289	at the bottom, very steep	, no current	
09:14	304	21°41.131	38°45.289	vertical wall (carbonate rock)		
09:22	307	21°41.129	38°45.284			
09:33	306	21°41.124	38°45.264			
09:40	290	21°41.130	38°45.261	still moving upslope		
09:49	264	21°41.140	38°45.258			
09:53	257	21°41.144	38°45.255			
09:56	250	21°41.148	38°45.255			
10:00	240	21°41.148	38°45.252	vertical wall with deep gullies (erosion gullies?)		
10:08	214	21°41.150	38°45.251			
10:16	195	21°41.153	38°45.245			
10:18	190	21°41.155	38°45.244			
10:26	160	21°41.160	38°45.245			
10:30	145	21°41.162	38°45.243			
10:35	130	21°41.163	38°45.248	more benthic life, antipatharians, sponges, red algae		
10:40	115	21°41.165	38°45.252			
10:46	101	21°41.168	38°45.245			
10:49	95	21°41.170	38°45.242			
10:51	88	21°41.171	38°45.237	slope shallower, closer to top		
10:53	74	21°41.179	38°45.226	increasing current		
10:58	58	21°41.199	38°45.213			
10:59	57	21°41.206	38°45.215			
11:00	60	21°41.206	38°45.215	on plateau		
11:13	60	21°41.206	38°45.215	lift off bottom		
11:19	0	-	-	surfaced		

Table A-4.5.2: Jago dive track data (64PE350b, Station 2)

JAGO Dive 1179 (2) 05.04.2012			J.Schauer, Jürgen Mlynec (HGF)		Jeddah	
					Shi'b Al Kabir Reef	
Time (UTC)	Depth (m)	North	East	Comments		
04:12	0	-	-	submerged		
04:21		21°40.368	38°50.485	descending		
04:50	280	21°40.058	38°50.488	still descending		
05:01	300	21°40.04	38°50.486	at steep wall, deep gullies		
05:05	306	21°40.045	38°50.477			
05:16	312	21°40.049	38°50.466	took sample		
05:23	302	21°40.051	38°50.463			
05:28	277	21°40.060	38°50.455	moving upslope along the wall		
05:37	250	21°40.073	38°50.454			
05:49	190	21°40.068	38°50.469			
05:55	164	21°40.071	38°50.472			
06:00	150	21°40.071	38°50.478			
06:09	110	21°40.081	38°50.476			
06:28	100	21°40.085	38°50.473	sampled rhodoliths with <i>Leptoseris</i> corals		
06:33	86	21°40.088	38°50.471	very steep, partly overhanging wall		
06:42	89	21°40.088	38°50.471	field of rhodoliths, with <i>Leptoseris</i> corals attached to it		
06:49	88	21°40.088	38°50.473	start ascent		
06:52	80	21°40.090	38°50.471	ascending		
06:58	0	-	-	surfaced		

Table A-4.5.3: Jago dive track data (64PE350b, Station 3)

JAGO Dive 1180 (3) 05.04.2012			J.Schauer, Georg Teutsch (UFZ/HGF)		Jeddah	
					Shi'b Al Kabir Reef	
Time (UTC)	Depth (m)	North	East	Comments		
08:54	0			submerged		
09:00		21°40.11	38°50.61	descending		
09:14	233	21°40.117	38°50.588	at the bottom, at steep w all		
09:24	320	21°40.088	38°50.578			
09:29	324	21°40.088	38°50.575	start moving up along wal l		
09:39	280	21°40.114	38°50.570	butterflyfish <i>Chaetodon jayakari</i>		
09:47	250	21°40.119	38°50.571			
09:55	230	21°40.123	38°50.575			
09:59	219	21°40.129	38°50.577			
10:02	210	21°40.129	38°50.575			
10:03	200	21°40.129	38°50.574			
10:17	166	21°40.129	38°50.576			
10:25	140	21°40.129	38°50.571			
10:33	111	21°40.133	38°50.570			
10:41	90	21°40.143	38°50.566			
10:51	85	21°40.148	38°50.569			
10:58	89	21°40.150	38°50.561			
11:00	75	21°40.158	38°50.562			
11:05	76	21°40.157	38°50.562	collected <i>Leptoseris</i> corals		
11:15	75	21°40.157	38°50.560			
11:22	0	21°40.	38°50.	surfaced		

Table A-4.5.4: Station data summary of Jago dives performed during 64PE350 legs a and b (UTC time = Local Time – 3h)

JAGO Dive #	Dive	Date	Location	Time submerged	Time surfacing	Total dive time	Touch down Position	Lift off position	Min-Max Depth	Pilot	Observer/ guest	Video tapes #	Remarks
				(UTC)	(UTC)	(min)			(m)				
1178	1	01.04.12	Seamount NW of Jeddah	08:47	11:19	152	21°41.14'N 38°45.29'E	21°41.21'N 38°45.22'E	59-312	J.Schauer	Alaa Al-Barakati	1, 2	exploration southern flank of sea peak
1179	2	05.04.12	Shi'b Al Kabir Reef	04:12	06:58	166	21°40.05'N 38°50.48'E	21°40.09'N 38°50.47'E	88-315	J.Schauer	Jürgen Mlynek	3, 4	vertical survey along steep wall up to reef edge, coral sampling
1180	3	05.04.12	Shi'b Al Kabir	08:54	11:22	148	21°40.12'N 38°50.59'E	21°40.16'N 38°50.56'E	76-326	J.Schauer	Georg Deutsch	5, 6	vertical survey along steep wall

4.6 Petrology and seafloor rock sampling

Froukje van der Zwan, Nico Augustin

Basaltic rock samples are required for (ongoing) Chlorine investigations of basaltic samples that are performed within the Jeddah Transect Project (JTP) Subproject 2, in order to trace seawater infiltration and hydrothermal processes in the crust. In the Red Sea, special interest is paid to the presence of brine deeps, and how deep in the oceanic crust these highly saline waters can be traced due to hydrothermal circulation. Therefore, samples from various locations are required, particularly from different deeps, since the deeps are tectonically slightly different, with increasing maturity from north to south. Furthermore, not all of them are filled with brine. In addition, studying basalts from the Red Sea can be important for the relation of the magmatism and the tectonics of the deeps, i.e. different styles of deeps may have a higher degree of melting or a magma chamber at different depths/ temperatures/ compositions. Of particular interest are the transitional deeps (changeover from continental discrete rift centers to fully matured oceanic spreading); from Thetis Deep up to Suakin Deep.

Basalts from the Red Sea deeps are known to occur in all major deeps South of Shaban Deep (25°15' N). However, outcrops of basaltic rock are patchy due to the high sedimentation rate in the Red Sea, which results in large sediment packs covering the surface. Therefore it is generally not easy to recover basalts, and mainly fresher basalt flows from recent eruptions can be recovered.

Basalt recoveries described in earlier studies are mainly from the Atlantis II Deep area, since studies performed in the 1970s – 1980's mainly concentrated on the brine-filled deeps, mostly the Atlantis II Deep. Other samples studied were mainly from Mabahiss Deep, Suakin Deep and the Red Sea rift at 18°N. More recently, programs were carried out at Shaban and Thetis Deep, including the recovery of basalt samples. Single samples are known from Port Sudan, Erba, Shagara, Hadarba and Nereus. However, the availability of those samples is poor, and only a few basaltic glasses from Shaban- and Atlantis II Deep were available for studies within the JTP. In addition, during the JTP RV Poseidon expedition P408/1 in January 2011, good basalt samples could be recovered from the Hatiba Deep. Due to the limited extension of the 2011 working area, it was not possible to recover more basalts during cruise P408/1.

Therefore, from the petrological point of view the aim for expedition 64PE350 was to collect basalts over a large variety of deeps, from north to south along the Red Sea Rift, mainly by dredging.

On cruise P408/1 it was found out that older volcanoes are often covered by sediment or carbonate crusts. Therefore, dredge locations could not be selected merely based on bathymetric data, but were to be chosen more carefully. During this cruise, in addition to the interpretation of multibeam topography, very important information was provided by multibeam backscatter imaging (see Multibeam chapter), which was not fully available during P408/1. Areas with bright backscatter signals are mainly interpreted as hard bottom (e.g. from basaltic rocks) and therefore preferentially chosen as dredge targets for sampling basaltic rocks. Furthermore, the locations of basalt samples given in the literature were used during 64PE350/1 to aid in finding suitable places for dredging. Not only do they indicate actual locations where basalt is present, but they also mark structures of volcanic origin. Although rocks could not be recovered

everywhere, this new targeting strategy resulted in a very good success rate and high diversity of dredged samples compared to the previous year's sampling program (Table A-4.6.1).

First results

A total of 33 individual basaltic samples (rocks and glass) from 6 different deeps (Hadarba, Atlantis II, Shagara, Erba, Port Sudan and Suakin Deep) were collected and described. Together with the samples collected from Hatiba Deep last year they provide a continuous set of volcanic samples from all major deeps between 22°23' and 19°35' N (Fig. A-4.6.1). In addition to the dredged samples, two samples were collected from Port Sudan Deep by gravity corer, where a basaltic surface was hit instead of the expected sediments. Apart from volcanic basalts (with glass), various sedimentary rocks and crusts as well as a variety of crusts with hydrothermal origin (Atlantis II Deep) were recovered. An overview and description of all samples is given in Fig. A-4.6.2 and table A-4.6.2.

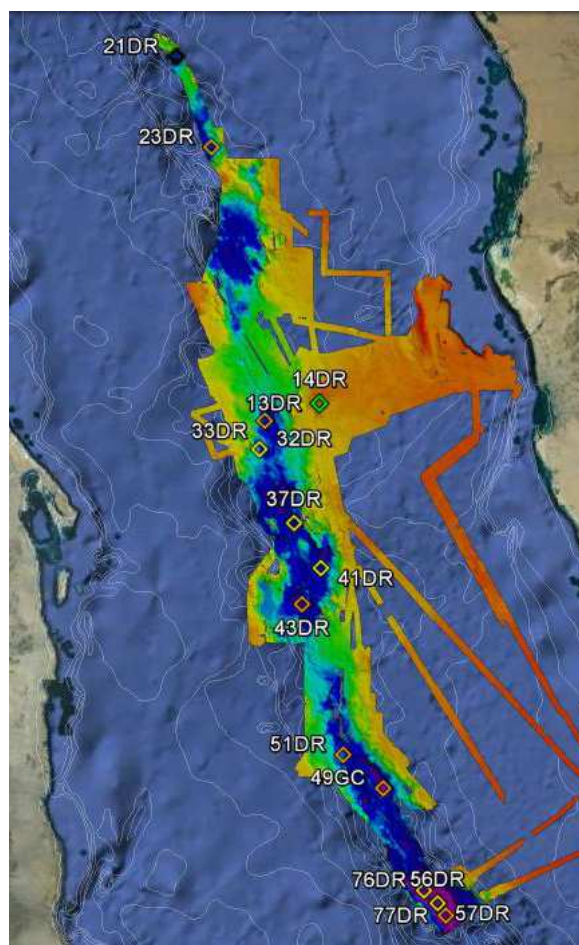
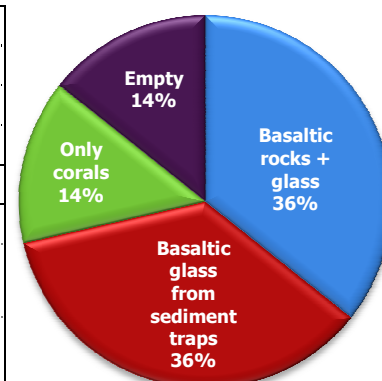
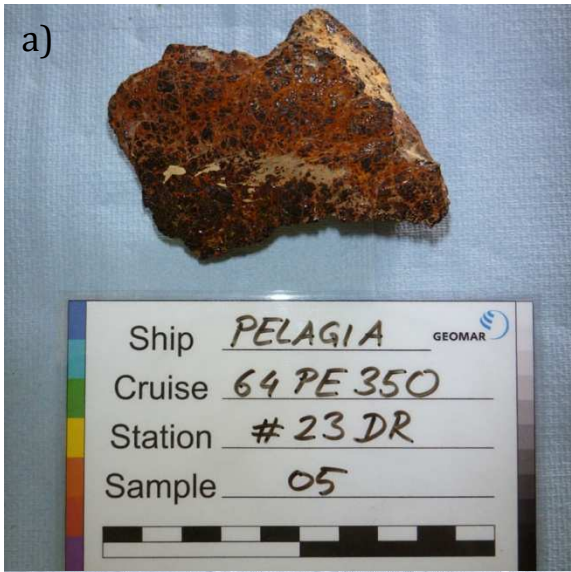


Figure A-4.6.1: Overview map (based on actual bathymetry) with dredge locations. Orange diamond represents basaltic rocks. Yellow: basaltic glass. Green: Ancient corals. Black: Empty

Table A-4.6.1 - Dredge sampling statistics

Total amount of dredges	14 dredges	
Total dredge time	32 hours 12 min.	
Average dredge time	2 hours 18 min.	
Total dredged length	~6.6 km	
Success rates	In dredges	Percent
Basalt rock recovery (incl. glass fragments)	5	35.7%
Basaltic glass recovery from sediment traps (no rock recovery)	5	35.7%
Sedimentary rock/ carbonate crust/ coral recovery	5	35.7%
No rock or glass recovery	2	14.3%





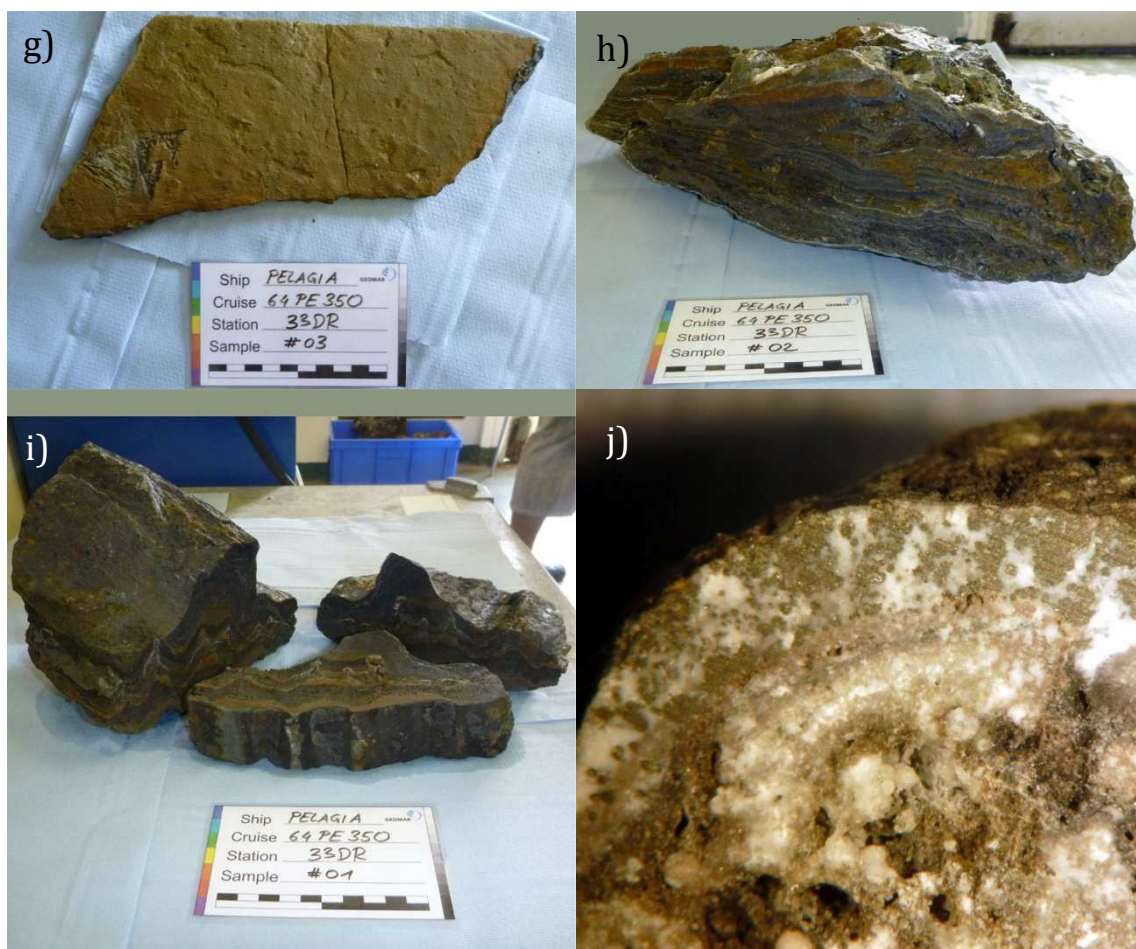


Figure A-4.6.2: Examples of rock samples. a) Palagonite altered basaltic sheet flow from Hadarba Deep. b) Heavily altered blocky basalt from Atlantis II. c) Fresh pillow basalt; Erba Deep. d) Section of layered carbonate crust from Suakin Deep. e) Ancient corals from east of Atlantis II. f) Silicate sponge and carbonate pinnacles on ancient corals. g) Silicate crust from Atlantis II. h) Section of finely layered hydrothermal crust from Atlantis II. i) Section of thick layered hydrothermal crust from Atlantis II. j) Close-up of pyrite rim in hydrothermal crust.

Basalt samples

The samples recovered during 64PE350 have different outer appearances, ranging from sheet lavas (e.g. from Hadarba, Fig. A-4.6.2a) to blocky basalts (e.g. from Atlantis II, Fig. A-4.6.2b) and pillows (e.g. from Erba, Fig. 4.6.1c), though mixed appearances occur as well in a single dredge (e.g. from Hadarba). Therefore, the outer appearance does not seem to be directly related to the location of the samples. The samples generally consist of basalts with a glassy rim, which varies from a few millimeters to centimeters in thickness. Cutoffs of the samples are generally fresh and alteration seems restricted to the outer surfaces, mainly in the form of palagonite rims (Fig. A-4.6.2a) or carbonate encrustations. An exception are samples dredged from the brine of Atlantis II (33DR; Fig A-4.6.1b); these are heavily altered and the least fresh of the sampled basaltic rocks. Samples from Erba Deep (43DR; Fig 1c) appear freshest and display no visible alteration. Hence they seem to come from a relatively recently active volcanic area within the shallow Erba brine pool. All basaltic samples show little vesicularity with a maximum of 20%, but mostly less than 5%. Minerals' occurrence in the basalts is maximally 5%, and mostly plagioclase, apart from the Port Sudan samples (49GC, 51DR), which also contain olivine crystals.

Ancient corals and carbonate crusts

Manganese-coated corals were recovered W from Atlantis II from a (potentially) old volcanic edifice (Fig. A-4.6.2e, f). These are old, solitary rudimentary corals, though fresher parts of organisms growing on the corals were also recovered (Fig. A-4.6.2f). Carbonate crusts were found in dredges from several deeps (Hadarba, Port Sudan, Suakin) and seem to be a common feature on older (inactive) volcanoes (Fig. A-4.6.2d). Foraminifera, Pteropoda and Gastropoda shells, which are omnipresent in/ on these crusts, are also common in all the (pelagic) sediments collected by sediment traps (mounted in the dredge).

Hydrothermal crusts

From the Atlantis II Deep, hydrothermal crusts were recovered, which are most likely to come either from the brine, or from the brine-seawater interface. The crusts were connected to the top of basalt boulders and show a layering of various colours (white to green to (dark) brown; Fig. A-4.6.2h, i). In contrast to the regular sedimentation, they do not consist of carbonates (i.e. no reaction with HCl), but rather of silicates, sulfates and sulfides. Sulfides are visible in the top layer as small (<2 mm) pyrite concretions (Fig. A-4.6.2j), while the lower layers potentially contain sphalerite. Hard shards of (potentially) siliceous crusts, without any visible hydrothermal mineralization, are associated with these crusts (Fig. A-4.6.2g).

Table A-4.6.2: Dredge station list with sample descriptions

Station abbreviations: DR = Chainbag dredge (Kettensackdredge); GC = Sedimentary Gravity Core (Schwerelot); BS = backscatter image from multibeam.

Station Area	Latitude (°N)/ Longitude (°E)	Date/ Time (UTC)	Depth (m)	Sample descriptions and samples taken (TS = thin section/microprobe slide; Gl = Glass; Mn = manganese; Qtz = quartz; Pl = Plagioclase; Ol = Olivine)
13 DR (Volcanic?) Cone W of Atlantis II, SW flank. Hard rocks observed in VCTD	21°27.713'/38°15.723' to 21°27.791'/38°15.667'	11.03.12 10:59 - 12:56	841 - 810	5 dm pieces; >10 cm pieces of carbonate crust with (solitaire) corals. Partially covered by black Mn crust and pteropoda shells. Carbonate crust displays some layering and minor bioturbation. In addition, 2 fresh (living?) silicate sponges and fresher carbonate pinnacles are on the crusts; those are put into ethanol. 15 samples bagged. One piece frozen at 80°.
14 DR Same as 13 DR	21°27.716'/38°15.727' to 21°27.896'/38°15.794'	11.03.12 13:40 - 14:46	839 - ~700	6 dm sized pieces; carbonate crusts with (solitaire) corals, similar to 13 DR. 6 pieces bagged. 2 ethanol-filled sample pots with fresh (living?) material.
21 DR E Thetis Deep, steep deep basin (bright BS)	22°43.646'/37°41.770' to 22°43.892'/37°41.848'	13.03.12 04:50 - 06:45	2007 - 1980	Empty dredge. Sediment traps filled with dark, almost black (metalliferous) sediment. Sieved for >0.5 mm and collected for <0.5 mm.
23 DR Volcanic cone at E edge of S basin of Hadarba Deep.	22°23.567'/37°50.371' to 22°23.946'/37°50.222'	13.03.12 12:22 - 15:10	2098 – 1980	11 dm sized pieces + many smaller: basalt pillows, lobate basalts and sheet flows. Covered by carbonate crusts. 1: 30x15x13 cm: Massive block basalt with a thin 2-3 mm glass crust at several sides (top uncertain: hang/side of volcano). Altered with pinkish + palagonite mud/minerals and white bands of aragonite/carbonate. Some carbonate crust. Basalt grey altered + some layering which does not extend to inner side rock. Glass semifresh. Basalt: <1% vesicles (up to 1 mm), irregularly distributed. No obvious minerals. Gl. 2: 22x14x10 cm: Lobate basalt with small pillow edges (<5 cm), half covered with mms sized glass crust. Altered with palagonite + pinkish/white weathering. Covered partially by carbonate crust, incl. cm sized sed. grains. Basalt half altered. Glass (semi-)fresh. Basalt: <1% vesicularity, but locally (following the outer pillow rims) up to 5% (up to 3 mm). 1% Pl. Gl, TS. 3: 12x10x9 cm: Basalt block with at top mms thick glass crust. White/pinkish alteration + small aragonite needles and palagonite. Bottom grainy pockmark weathered. Basalt: ~2% vesicular, irregularly distributed, some connected (up to 1 ½ mm). ~2% Pl minerals of <1 mm. Gl. 4: 18x13x10 cm: Corner of pillow basalt (round edge) with mms glass crust. Palagonite alteration and carbonate crusts. ~2% vesicularity, irregularly distributed; zoned along the surface (up to 2 mm). ~1% Pl. Gl, TS. 5: 8x5x4 cm: Basalt glass sheet flow. 1-2 cm bent layer. Cracked at the top, smooth bottom. Fresh, palagonite alteration (mainly) at the top. No vesicularity. Gl. 6: 4½x4x½ cm (A), 4½x3x½ cm (B): Basalt glass sheet flows/layers. Fresh, covered with palagonite. Flowing structures on top, imprints on bottom. Gl (A) 7: 13x9x2 cm: Basaltic glass layer (9x6x1) with carbonate crust (as 10) partially on both sides. Fresh glass covered by palagonite. Flow + rounded imprints on bottom. Gl. 8: 6½x5x2 ½ cm (A), 4½x4x2½ cm (B): Thin basaltic crust with (continued on page A 50)

Continued from page A-49:

				<p>alteration mineralization. Very altered, porous basalt from which grow white/pinkish hard <1 mm thick layered alteration minerals. No reaction with HCl. 1 round white secondary mineral on A.</p> <p>9: 13x5x<1 cm: Carbonate crust (as 10) with palagonite altered glass fragments on bottom. GI.</p> <p>10: 8x8x<1 cm (A), 4x3x2 cm (B): Hard carbonate crust. Reaction with HCl. Grey brown to orange-grey-brown. Porous (up to 2 mm) holes to massive. B has a cm hole. Fragments of gastropoda and pteropoda shells and forams.</p> <p>Extra rocks:</p> <p>1 lobate basalt with mini-pillows (extra 1)</p> <p>1 (altered) basalt block (extra 2)</p> <p>1 sheet basalt (extra 3)</p> <p>1 carbonate crust with basalt (extra 4)</p> <p>7 pieces of carbonate crust (bagged together)</p> <p>Station glass</p>
32 DR W most steep ridge of Atlantis II, up to plateau. Bright BS.	21°17.945'/38°01.771' to 21°17.855'/38°01.843'	16.03.12 08:49 - 12:00	1860 – 1820(?)	Empty. Basalt and glass fragments in sediment traps. Sieved for >1 mm and > 0.5 mm.
33 DR N edge of ridge W of Atlantis II, from small basin, 200 m up, dredging to N. Start dredge in the brine.	21°24.009'/38°03.037' to 21°24.297'/38°03.034'	16.03.12 13:57 - 16:10	2132 – 2011	<p>>25 of layered dark crust, dms sized. ~13 basalt pieces with glass, dms sized. 11 glass pieces, cm sized. ~16 basalt pieces with no glass, dms sized. >10 shards of hard yellowish crust.</p> <p>1: 30x20x15 cm: Layered dark crust. >10 discrete (<1 mm up to 5 cm) different coloured layers (reddish-brown to grey-green to black to white (those <½ mm)), semiparallel and wavy. Crust has low density and ~25-30% vesicularity (up to mms sized pores). No reaction with HCl: cemented by silica? White, soft, shiny mineral on surface. 1 slide to Kiel (Augustin), 1 to KAU (Bantan).</p> <p>2: 45x20x15 cm: Layered dark crust (as 1) with numerous cm sized glass crust fragments/layers on bottom, partially in the coating. Glass is fresh. In addition, greenish + whitish coating on the rock. GI.</p> <p>2B: Layered dark crust (as 2). Thin mm sized coating on top, containing small portions of sulphite: pyrite. Inside layering, other sulphites (sphalerite?).</p> <p>2C: Layered dark crust (as 2). Many thin white layers. Thin mm sized coating on top, containing small portions of sulphite: pyrite. Inside layering, other sulphites (sphalerite?).</p> <p>3: 25x10x1 cm: Sedimentary, yellowish-grey-brown crust. No reaction with HCl and hard: silica? Internal parallel mm layering. Inside + on surface many pteropoda (carrying component?). Dense, ~1% vesicular. Greenish + white coating.</p> <p>4: 30x18x15 cm: Pillow basalt with up to 1 cm thick glass crust. Semifresh to altered with green/yellow coating and covered with white mineral. ~5% vesicularity (up to 1 mm; some filled with alteration coating). <1% Pl. Cracks inside filled with brown/yellow sedimentation/alteration. GI.</p> <p>(continued on page A-51)</p>

Continued from page A-50:

				<p>5: 30x26x7 cm: Sheet basalt with patches of glass up to 1½ cm. Both sides covered by sedimentary crust (3) and some white mineral. Glass partially in the sedimentary crust and in the rough surface. ~20% vesicles (up to 2 mm; minor of them filled by alteration coating). ~1% Pl (up to 2 mm). GI</p> <p>6: 20x18x18 cm: Basalt block with <1 cm glass crust on top. Weathered surface: palagonite, white mineral, green coating, bluish coating. ~10% vesicularity (up to 1 mm). 2% Pl (<1 mm). GI</p> <p>7: 18x14x8 cm: Basalt block with <1 cm glass crust on top. White + green weathering, less altered than 6. Dense, >1% vesicularity. ~1% (up to 2 mm) minerals: Pl? GI.</p> <p>8: 19x6x6 cm: Basalt block with glass rim. Grey, green, white weathering coating, slightly fresher than 7. 2-5% vesicles (up to 1 mm; some filled with secondary mineral coating), lower % close to glass rim. <1% Pl (up to 1 mm). GI</p> <p>9: 16x10x8: Basalt block, no glass. White mineral coating. Greenish weathering. 10% vesicles (up to 2 mm; partially filled with green/white coating). <1% Pl.</p> <p>10: 12x7x2 cm: Basaltic glass layer. Strongly altered with palagonite + green alteration. Inside glass is fresh. Some cracks. ~2% vesicularity (up to 1 mm; some filled). GI</p> <p>11: 9x6x2 cm: irregular basaltic glass fragment. No clear layering. White + brown altered. Semi-fresh GI.</p> <p>12: 6x5x2 cm: Basaltic glass layer. Thin alteration coating (brown/ green/ yellow/ grey). Glass fresher than 10. GI.</p> <p>13: 4½x4x1 cm: Basaltic glass layer. Similar to 12, but thinner/flatter. GI.</p> <p>14: White mineral from sediment traps.</p> <p>Extra rocks:</p> <p>1 layered crust with glass and green-white coating (extra 1)</p> <p>1 sedimentary crust (extra 2)</p> <p>1 basalt + glass (extra 3)</p> <p>3 glass crusts (extra 4 – 6)</p> <p>Unsorted layered and sedimentary crusts.</p> <p>Unsorted basalts with and without glass.</p>
37 DR Shagara Deep, N of middle basin. Volcanic flat area. Bright BS	21°01.826'/38°09.869' to 21°01.958'/38°09.875'	17.03.12 13:06 - 16:20	2288 – 2270	Empty. Glass fragments in sediment traps. Sieved for >1 mm and > 0.5 mm.
41 DR NE of Erba Deep. (S end of Shagara). Small valley between hummocky volcanics. Bright BS	20°52.021'/38°16.126' to 20°52.226'/38°16.133'	18.03.12 13:54 - 15:45	2281 – 2246	Empty. Glass fragments in sediment traps. Sieved for >1 mm and > 0.5 mm.

43 DR Erba Deep. Small hill in eastern basin (close to literature sample). Start dredge in brine.	20°44.048'/38°11.728' to 20°44.406'/38°11.727'	19.03.12 05:06 - 07:46	2378 - 2283	<p>~40 (1-50 cm) basaltic pillows and blocks. Very fresh.</p> <p>1: 25x20x17 cm: Basalt block (part of huge pillow?) + glass crust <1 cm thick. Very fresh, minor yellowish/white cover (salt from inside the rock after drying). ~5% vesicularity (up to 2 mm), irregularly spaced; on 1 cm scale 1-20%. No macroscopic minerals visible. (¼ of original rock that was dredged). GI.</p> <p>2: 25x20x18 cm: Lobate/flat pillow basalt with <1 cm glass crust over ¾ of the rock. Glass crust 2% vesicular, fresh. Basalt fresh apart from salt layer. 5% vesicular (up to 2 mm; some filled?). GI</p> <p>3: Small pillow basalt with up to ½ cm glass crust on half of the sample. Round/wavy surface. Fresh, apart from salt. 3% vesicular (up to 3 mm; some filled?). No obvious minerals. GI.</p> <p>Extra rocks:</p> <p>1 basalt block (extra 1).</p> <p>1 basalt pillow large (extra 2).</p> <p>2 basalt pillows small (extra 3, 4).</p> <p>1 Basalt with edge between two pillows, thin glass crust (extra 5).</p>
49 GC In Port Sudan Deep, in the brine.	20°04.227'/38°30.598'	20.03.12 08:01 - 09:12	2701	<p>Carbonate crust, basaltic glass and basalt caught in the core catcher.</p> <p>1: 8x6x½ cm: Hard yellow-grey sedimentary crust. <1%-2% vesicularity from top to bottom. Some patterns on surface of uncertain origin. No distinctive features/grains. Little reaction with HCl (= light carbonatic), sulfur smell after reaction. (also bagged 11 smaller fragments).</p> <p>2: <2 cm sized (total ~20 cm³) basaltic glass fragments. No vesicularity. <1 mm Pl crystals. Slightly weathered. GI</p> <p>3: 8x6x6 cm: Basalt block with sharp edge. No glass. Fresh, slightly altered at surface + on minerals. < ½ mm black (Mn) + white coating at surface. 1% vesicular (up to 2 mm). ~5% minerals: Ol, some Pl, up to 2 mm, slightly weathered. TS</p>
51 DR NW Port Sudan Deep, volcanic area, upslope larger volcano. Bright BS	20°11.460'/38°21.367' to 20°11.586'/38°21.306'	20.03.12 13:16 - 15:15	1941 - 1890	<p>4 basaltic rocks.</p> <p>1: 18x10x10 cm: Basalt pillow with up to 1½ cm glass rim all around its length. Outer side palagonite altered (on glass and basalt), inside fresh. Basalt: 1% vesicular (up to 1 mm). 2% minerals: Ol + Pl, up to 2 mm, partially altered on outside rock. GI.</p> <p>2: 15x9x5 cm: Basaltic glass layer/sheet with on 3 sides mm – ½ cm glass rim. Rectangular block. Palagonite on outside + some carbonate crust. Strong cuts in the glass. Some (cm sized) layering with glass top, not continuous inside the rock: pillow edges. <1% vesicles (up to 1 mm). ~2% minerals: Ol + Pl (up to 3 mm). GI</p> <p>3: 13x8x6: Basalt block with 2 (~3 mm thick) layers of glass (5 and 3 cm). Glass not continuous inside: pillow edges. Some palagonite + carbonate crust. Glass semifresh. <1% vesicle (up to 1 mm). 3% minerals: Ol + Pl (up to 3 mm; Pl smaller). GI.</p> <p>Extra rocks:</p> <p>1 basalt as 2 (extra 1).</p> <p>Station glass (up to 2 cm²).</p>

56 DR Middle of Suakin Deep, small hummocky structures/flows close to volcano, bright BS.	19°38.765'/38.43.256' to 19°38.996'/38°43.258'	21.03.12 10:10 - 12:30	2648 - 2625	Empty. Sieved for >1 mm and > 0.5 mm.
57 DR Suakin Deep, as 56 DR, 50 m E	19°38.793'/38.43.296' to 19°38.966'/38°43.269'	21.03.12 12:56 - 15:12	2674 - 2626	Empty. Glass fragments in sediment traps. Sieved for >1 mm and > 0.5 mm.
76 DR N Suakin Deep, volcanic flows between 2 (dark) cones. Bright BS	19°41.432'/38.40.066' to 19°41.791'/38°40.212'	29.03.12 06:29 - 08:44	2504 - 2451	Empty. Glass fragments in sediment traps. Sieved for >1 mm and > 0.5 mm.
77 DR Middle of S Suakin Deep, hummocky volcanic area	19°36.061'/38.45.188' to 19°36.276'/38°45.180'	29.03.12 10:24 - 12:51	2596 - 2477	<p>1 Basaltic glass rock with carbonate/Mn coating. + ~10 dm pieces + >20 cm pieces of carbonate crust with Mn coating in various forms.</p> <p>1: 7x7x4 cm: Basaltic glass 'finger'+ carbonate crust (4 cm glass, 3 cm crust). Fresh glass, centric cracked, no porosity, with <1 mm palagonite rim. Covered by 2-3 mm carbonate/Mn crust (dark brown). Rough pointy surface. Carbonate crust as 3, mostly dark porous; partially yellow carbonate in some sort of pocket. GI</p> <p>2: 30x21x13 cm: Layered carbonate crust of individual shards. Shards individually stick out of the rock. Up to 2 cm thick layers are nonparallel to each other. Irregular and diffuse boundaries. Cemented together. Some are broken and cemented again, or cracks filled up with different (darker) carbonate. Yellowish white to brown layers, fine to coarse grained with forams, pteropoda and gastropoda shells. Dense to 5% of ~2 mm holes. Covered with brown-black Mn coating; irregular, rough surface. 1 half to KAU (Basaham). 1 slice + 1 part to Kiel</p> <p>3: 23x17x5 cm: Porous dark brown carbonate crust. ~25% (1-5 mm) ~round holes, long: bioturbation (?). <10% forams, pteropoda and gastropoda remains (<1 mm – 1 cm long). Appears softer than type 2 and 4: less cemented. Massive layer with mixed dark and lighter brown. 1 half to KAU. 1 slice + 1 part to Kiel</p> <p>4: 12x10x2 cm: Hard yellow carbonate crust. Many < ½ mm holes (~50%) at one surface. Small fragments of pteropoda and forams (up to 1 cm long). (On comparable crusts up to 20% of pteropoda). Dendritic black patches: start of Mn encrustations. ~smooth surface. 1 similar crust (B) to KAU.</p> <p>Extra rocks: 11 unsorted carbonate crusts to Kiel 5 unsorted carbonate crusts to KAU</p>
85 Jago South flank of 'Sea Peak' for the coast of Jeddah.	21°41.136'/38.45.289' to 21°41.199'/38°45.215'	01.04.12 8:30 - 11:45	295 - 60	1 to 3: 3 dms sized yellow carbonate crusts. Smooth edges, organic forms. Silicate sponges, 'fresh' carbonate pinnacles, small crab embedded in ethanol.

4.7 Sediment sampling and pore water geochemistry

Ali Basaham, Rashad Bantan, Salim Al Nomani, Mohamed Orif, Elgasim Elgarafi, Radwan Al-Farawati, Mark Schmidt

Sediment sampling

A gravity corer with a tube length of 3.7 m (stainless steel tube with inner plastic liner) and a weight of 1 ton was used to obtain sediment samples from various seafloor environments of the Red Sea ranging in water depths between 450 m and 2774 m. A total of 12 sediment cores were obtained from 15 stations with core lengths usually ranging between 3.2 m and 3.7 m. Sediment samples from three stations could not be recovered either because the seabed was too hard and compact to be penetrated or the corer did not land on the seabed vertically.

After core recovery the inner plastic liner filled with sediment was cut into 1-m sections and split into archive and working halves. The sediment segments were photographed, described and sediment and pore water were sub-sampled from the working halves for various sedimentological, geochemical and microbiological analyses. The archive halves were stored in D-tubes and shipped to GEOMAR, whereas the working halves were transferred to the KAU laboratory for further sampling. A preliminary description of the core samples is presented in Table A-4.7.1.

Table A-4.7.1: List of Gravity Cores obtained during *R/V PELAGIA* Cruise 64PE350

Station No.	Gear No.	Station Name	Date	Time (UTC)	Latitude (N)	Longitude (E)	Sample Equipment	Water Depth (m)	Core Length (cm)	Number of Sections	Remarks
64PE350/1-16	G.C.1	Gas Site	12-03-2012	05:35	21° 27.517	38° 15.812	Gravity Core	834	15	0	Sample obtained from catcher (15 cm), some broken crust.
64PE350/1-17	G.C.2	Gas Site	12-03-2012	06:25	21° 27.214	38° 15.925	Gravity Core	840	35	1	
64PE350/1-22	G.C.3	Thetis Deep	13-03-2012	08:20	22° 48.205	37° 35.707	Gravity Core	1818	369	4	
64PE350/1-29	G.C.4	Atlantis // Deep North	15-03-2012	10:44	21° 26.475	38° 03.413	Gravity Core	2074	367	4	
64PE350/1-36	G.C.5	Atlantis // Deep South	15-03-2012	10:47	21° 09.621	38° 07.189	Gravity Core	2255	369	4	
64PE350/1-40	G.C.6	Erba Deep	18-03-2012	11:35	20° 47.983	38° 02.425	Gravity Core	1866	344	4	
64PE350/1-49	G.C.7	Port Sudan Deep	20-03-2012	08:35	20° 04.227	38° 30.598	Gravity Core	2650	0	0	No sediment; Basalt Rocks and Glass in core catcher
64PE350/1-50	G.C.8	Port Sudan Deep	20-03-2012	10:50	20° 04.585	38° 30.706	Gravity Core	2767	369	4	Some sediment from the top is lost in the weight barrel
64PE350/1-55	G.C.9	Suakin Deep	21-03-2012	08:42	19° 36.728	38° 43.170	Gravity Core	2774	369	4	
64PE350/1-63	G.C.10	Pockmark Central	23-03-2012	05:17	19° 57.754	39° 24.607	Gravity Core	483	344	4	
64PE350/1-70	G.C.11	Atlantis // Deep South East	25-03-2012	08:37	21° 20.267	38° 05.600	Gravity Core	2145	339	4	
64PE350/1-74	G.C.12	Sea Peak	28-03-2012	13:55	21° 40.854	38° 43.393	Gravity Core	839	320	4	
64PE350/1-79	G.C.13	Pockmark	30-03-2012	05:36	19° 59.544	39° 31.828	Gravity Core	465	363	4	
64PE350/1-80	G.C.14	Pockmark	30-03-2012	06:58	19° 55.121	39° 30.387	Gravity Core	450	365	4	
64PE350/1-81	G.C.15	Pockmark Reference	30-03-2012	08:06	19° 50.693	39° 29.796	Gravity Core	420	331	4	

Core descriptions and core photography

Cruise Number:	64 PE 350	Station Number:	16 (Gas site)
Latitude (N):	21° 27.518	Depth:	834 m
Longitude (E):	38° 15.812	Time (UTC):	05:35 hr
Core Number:	G.C. 1 (Gravity Core)	Core Length:	0 cm

Color (Munsell Soil Chart)

10YR, 5 / 4, Yellowish Brown.

2.5Y, 6 / 4, Light Yellowish Brown.

Remarks**Visual color:** Light Brown.**Visual texture class:** Sandy Mud.**Notes:**

- Sample obtained from the catcher only (0-15 cm).
- Sample contained some broken crust.
- Compact.
- Carbonate.



Cruise Number:	64 PE 350	Station Number:	17 (Gas site)
Latitude (N):	21° 27.214	Depth:	840 m
Longitude (E):	38° 15.925	Time (UTC):	06:25 hr
Core Number:	G.C. 2 (Gravity Core)	Core Length:	35 cm

Color (Munsell Soil Chart)
10YR, 5 / 4, Yellowish Brown.
10YR, 6 / 3, Pale Brown
10YR, 7 / 8, Yellow

Remarks	
Visual color:	Light Brown.
Visual texture class:	Sandy Mud.
Notes:	<ul style="list-style-type: none">• Dark at the top and shades to lighter at the bottom.• Sample length 0 – 28 cm.• Compact.• Carbonate.• Some yellow spots at the bottom (26 – 28 cm).



Cruise Number:	64 PE 350	Station Number:	22 (Thetis Deep)
Latitude (N):	22° 48.205	Depth:	1818 m
Longitude (E):	37° 35.707	Time (UTC):	08:20 hr
Core Number:	G.C. 3 (Gravity Core)	Core Length:	369 cm

Section 4 of 4	
Segment (cm)	Munsell Soil Color
0 - 69	5YR 2.5/1 Black



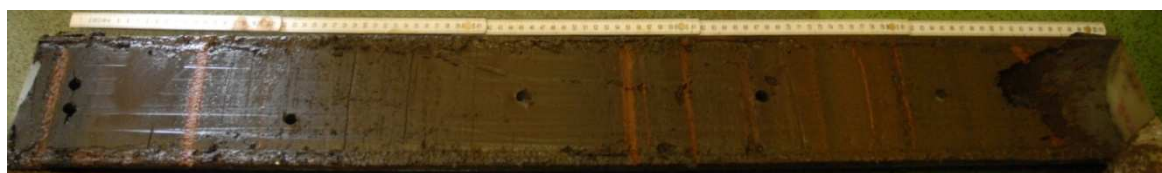
Section 3 of 4		
Segment (cm)	Core Length (cm)	Munsell Soil Color
69 – 71	0 – 2	2.5Y 3/3/3 Dark Olive Brown
71 – 136	2 – 67	7.5YR 3/4/4 Dark Brown
136 – 142	67 – 73	7.5YR 4/6/6 Strong Brown
142 – 146	73 – 77	2.5YR 4/8/8 Red
146 – 147	77 – 78	7.5YR 2.5/2/2 Very Dark Brown
147 – 149	78 – 80	2.5YR 4/8/8 Red
149 – 153	80 – 84	7.5YR 2.5/2/2 Very Dark Brown
153 – 157	84 – 88	7.5YR 4/6/6 Strong Brown
157 – 158	88 – 89	7.5YR 2.5/1/1 Black
158 – 162	89 – 93	2.5YR 4/8/8 Red
162 – 163	93 – 94	7.5YR 2.5/1/1 Black
163 – 167	94 – 98	2.5Y 4/3/3 Olive Brown
167 – 169	98 – 100	2.5YR 4/8/8 Red



Section 2 of 4		
Segment (cm)	Core Length (cm)	Munsell Soil Color
169 – 177	0 – 8	5YR 3/3/3 Dark Reddish Brown
177 – 185	8 – 16	2.5YR 3/6/6 Dark Red
185 – 186	16 – 17	Gley1 8/1/ 10Y Light Greenish Gray
186 – 189	17 – 20	Gley1 3/1/ 10Y Very Dark Greenish Gray
189 - 203	20 – 34	2.5Y 5/6/6 Light Olive Brown
		7.5YR 2.5/2/2 Very Dark Brown
203 – 204	34 – 35	10YR 4/4/4 Dark Yellowish Brown
204 – 205	35 – 36	Gley1 3/1/ 10Y Very Dark Greenish Gray
205 – 206	36 – 37	10R 4/6/6 Red
206 – 207	37 – 38	10YR 4/4/4 Dark Yellowish Brown
207 – 213	38 – 44	10R 3/4/4 Dusky Red
213 – 220	44 – 51	10R 3/6/6 Dark Red
220 – 224	51 – 55	10R 3/4/4 Dusky Red
224 – 224.5	55 – 55.5	Gley1 8/1/ 10Y Light Greenish Gray
224.5 – 225	55.5 – 56	Gley1 3/1/ 10Y Very Dark Greenish Gray
225 – 225.5	56 – 56.5	2.5YR 3/6/6 Dark Red
225.5 – 235	56.5 – 66	2.5YR 2.5/1/1 Reddish Black
235 – 238	66 – 69	10R 3/6/6 Dark Red
238 – 269	69 – 100	2.5YR 2.5/1/1 Reddish Black



Section 1 of 4		
Segment (cm)	Core Length (cm)	Munsell Soil Color
269 – 271.5	0 – 2.5	Gley1 2.5/N Black
271.5 – 272	2.5 – 3	5YR 3/3/3 Dark Reddish Brown
272 – 276	3 – 7	Gley1 2.5/N Black
276 – 285	7 – 16	Gley2 2.5/1/ 5PB Bluish Black
285 – 286	16 – 17	5YR 3/3/3 Dark Reddish Brown
286 – 291.5	16 – 22.5	Gley2 2.5/1/ 5PB Bluish Black
291.5 – 292	22.5 – 23	5YR 3/3/3 Dark Reddish Brown
292 – 323	23 – 54	Gley2 2.5/1/ 5PB Bluish Black
323 – 324	54 – 55	5YR 3/3/3 Dark Reddish Brown
324 – 328	55 – 59	Gley2 2.5/1/ 5PB Bluish Black
328 – 329	59 – 60	5YR 3/3/3 Dark Reddish Brown
329 – 333	60 – 64	Gley2 2.5/1/ 5PB Bluish Black
333 – 334	64 – 65	5YR 3/3/3 Dark Reddish Brown
334 – 340	65 – 71	5YR 2.5/1/1 Black
340 – 342	71 – 73	Gley1 2.5/N Black
342 – 344	73 – 75	5YR 2.5/1/1 Black
344 – 344.5	75 – 75.5	5YR 3/3/3 Dark Reddish Brown
344.5 – 348	75.5 – 79	5YR 2.5/1/1 Black
348 – 349	79 – 80	5YR 3/3/3 Dark Reddish Brown
349 – 360	80 – 91	10YR 2/1/1 Black
360 – 361	91 – 92	5YR 3/3/3 Dark Reddish Brown
361 – 363	92 – 94	10YR 2/1/1 Black
363 – 369	94 – 100	CATCHER



Cruise Number:	64 PE 350	Station Number:	29 (Atlantis // Deep North)
Latitude (N):	21° 26.475	Depth:	2074 m
Longitude (E):	38° 03.413	Time (UTC):	10:44 hr
Core Number:	G.C. 4 (Gravity Core)	Core Length:	367 cm

Section 4 of 4		
Segment	Munsell Soil Color	Remarks
0 – 2	Gley1 2.5/N Black	Black to dark olive marl, water content very high, oily.
2 – 3	10R 3/6/6 Dark Red	Dark brown to orange, not carbonate.
3 – 6	Gley1 2.5/N Black	Black to dark olive marl, oily, not carbonate.
6 – 7	10R 3/6/6 Dark Red	Dark brown to orange (Silicate + Sulfate)?
7 – 9	Gley1 2.5/N Black	Black to dark olive marl, oily, not carbonate.
9 – 10	10R 3/6/6 Dark Red	Dark brown to orange marl (Silicate + Sulfate)?
10 – 30	Gley1 2.5/N Black	Black to dark olive marl, oily, not carbonate.
30 – 32	10R 3/6/6 Dark Red	Layering repeated from dark brown to orange marl, (Silicate + Sulfate)?, interbedded with dark gray marl and light brown marl.
32 – 33	Gley1 2.5/N Black	
33 – 34	10R 3/6/6 Dark Red	
34 – 34.5	Gley1 2.5/N Black	
34.5 – 36	10YR 4/6/6 Dark Yellowish Brown	
36 – 58	Gley1 2.5/N Black	Black to olive black, oily, sporadically with manganite, distributed crust.
58 – 59	10R 3/6/6 Dark Red	Dark brown to orange marl.
59 - 67	Gley1 2.5/N Black	Black, olive black marl, oily, not carbonate.



Section 3 of 4		
Segment	Munsell Soil Color	Remarks
67 – 69	10YR 4/4/4 Dark Yellowish Brown	Interbedding of different thin layers, light brown marl, high carbonate, interlayered with strong gray detrital strong carbonate layers, fossiliferous particles, also interbedded with strong dark carbonatic marl with carbonate crust. The lower part is disturbed (Slided).
69 – 71	5Y 5/1/1 Gray	
71 – 75	10YR 4/4/4 Dark Yellowish Brown	
75 – 76	5Y 5/1/1 Gray	
76 – 81	10YR 4/4/4 Dark Yellowish Brown	
81 – 82	5Y 5/1/1 Gray	
82 – 85	5YR 3/3/3 Dark Reddish Brown	
85 – 86	5Y 5/1/1 Gray	
86 – 90	10YR 4/4/4 Dark Yellowish Brown	
90 – 91	7.5YR 4/4/4 Brown	
91 – 91.5	5Y 5/1/1 Gray	
91.5 – 92	10YR 4/4/4 Dark Yellowish Brown	
92 – 93	5Y 5/1/1 Gray	
93 – 94	10YR 2/2/2 Very Dark Brown	
94 – 95	10YR 5/4/4 Yellowish Brown	
95 – 96	10YR 4/4/4 Dark Yellowish Brown	
96 – 96.5	10YR 5/4/4 Yellowish Brown	
96.5 – 97	10YR 4/4/4 Dark Yellowish Brown	
97 – 98.5	10YR 5/4/4 Yellowish Brown	
98.5 – 102	5Y 5/1/1 Gray	
102 – 102.5	10YR 4/4/4 Dark Yellowish Brown	
102.5 – 103	10YR 5/4/4 Yellowish Brown	
103 – 104	5YR 3/3/3 Dark Reddish Brown	
	10YR 3/6/6 Dark Yellowish Brown	
104 – 105	10YR 5/4/4 Yellowish Brown	
105 – 115	5Y 5/1/1 Gray	
115 – 117	10YR 5/4/4 Yellowish Brown	
117 – 119	2.5Y 4/2/2 Dark Greenish Brown	
119 – 124	5Y 5/1/1 Gray	
124 – 126	10YR 4/4/4 Dark Yellowish Brown	
126 – 128	10YR 2/2/2 Very Dark Brown	
128 – 129	10YR 4/4/4 Dark Yellowish Brown	
129 – 130	5Y 5/1/1 Gray	
130 – 133	5Y 3/2/2 Dark Olive Gray	
133 – 135	5Y 5/1/1 Gray	
135 – 136	5Y 3/2/2 Dark Olive Gray	
136 – 140	5Y 2.5/2/2 Black	Light gray brown clay, oily, not carbonatic.
140 – 142	5Y 2.5/2/2 Black	
142 – 144	10YR 2/2/2 Very Dark Brown	
144 – 146	5Y 2.5/2/2 Black	
146 – 147	10YR 2/2/2 Very Dark Brown	
147 – 149	5Y 2.5/2/2 Black	
149 – 150	Gley2 2.5/1/5BG Greenish Black	

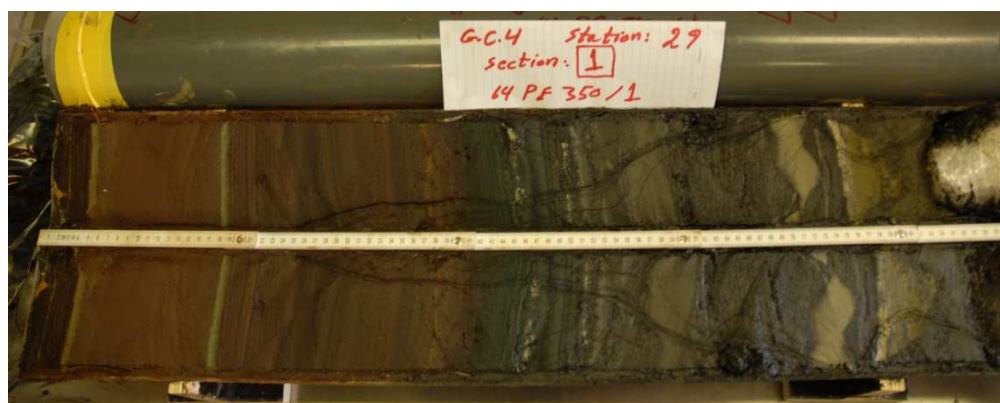
Continue Section 3 of 4		
Segment	Munsell Soil Color	Remarks
150 – 151	5Y 2.5/2/2 Black	Fine lamination, gray to brown, fine layering in mm, not carbonatic.
151 – 156	Gley2 2.5/1/5BG Greenish Black	
156 – 157	5Y 5/1/1 Gray	
157 – 160	Gley1 2.5/N Black	Gray with fine lamination marl, oily, strong carbonate reaction. Until the depth of 170 cm.
160 – 160.5	5Y 5/1/1 Gray	
160.5 – 162	Gley1 2.5/N Black	
162 – 163	5Y 5/1/1 Gray	
163 – 163.5	Gley1 2.5/N Black	
163.5 – 164	5Y 3/2/2 Dark Olive Grey	
164 – 167	Gley1 2.5/N Black	



Section 2 of 4		
Segment	Munsell Soil Color	Remarks
168 – 170	Gley1 2.5/N Black	Same as above
170 – 200	10R 2.5/2/2 Very Dusky Red	Dark red to dark brown, oily, light carbonate.
200 – 225	5Y 4/2/2 Olive Green	Greenish gray marl, strong carbonate, interlayered with detrital layer of 6 cm from 219 – 225.
225 – 235	2.5Y 4/4/4 Olive Brown	
235 – 248	10R 2.5/2/2 Very Dusky Red	Dark brown homogenous marl, oily, strong carbonate. (Iron, Manganese)?
248 – 263	2.5Y 2.5/1/1 Black	
263 – 265	10R 2.5/2/2 Very Dusky Red	
265 – 267	5Y 4/2/2 Olive Green	Yellow distributed marl, carbonatic.
	2.5Y 5/6/6 Light Olive Brown	



Section 1 of 4		
Segment	Munsell Soil Color	Remarks
267 – 270	10R 2.5/2/2 Very Dusky Red	Brown red marl intercalated with detrital thin layer, strong carbonate.
270 – 271	5Y 4/2/2 Olive Gray	
271 – 285	7.5YR 2.5/2/2 Very Dark Brown	
285 – 286	5Y 4/2/2 Olive Gray	
286 – 310	10R 2.5/2/2 Very Dusky Red	
310 – 313	Gley1 3/1/10Y Very Dark Greenish Gray	Black marl with a green layer, marl with fine sand, light carbonate.
313 – 313.5	Gley1 2.5/N Black	
313.5 - 315	Gley1 3/1/10Y Very Dark Greenish Gray	
315 – 315.5	Gley1 2.5/N Black	
315.5 - 318	Gley1 3/1/10Y Very Dark Greenish Gray	
318 – 339	Gley1 2.5/N Black	The former layer black marl with disturbed sliding gray non-layered parts which are very carbonatic.
339 – 341	5Y 4/2/2 Olive Gray	
341 – 344	Gley1 2.5/N Black	
344 – 349	5Y 4/2/2 Olive Gray	
349 – 354	5Y 2.5/1/1 Black	
354 – 367	CATCHER	

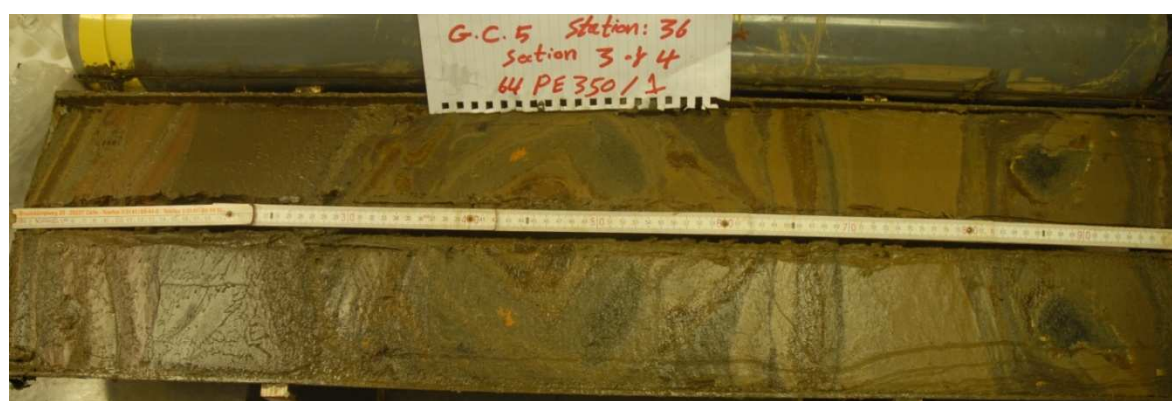


Cruise Number:	64 PE 350	Station Number:	36 (Atlantis // Deep South)
Latitude (N):	21° 09.621	Depth:	2255 m
Longitude (E):	38° 07.189	Time (UTC):	10:47 hr
Core Number:	G.C. 5 (Gravity Core)	Core Length:	369 cm

Section 4 of 4		
Segment	Munsell Soil Color	Remarks
0 – 20	2.5Y 5/4/4 Light Olive Brown	Marl brown to gray brown, watered to the extent that it slid on the top of the core within the core, homogenous, with high water content.
20 – 25	2.5Y 4/4/4 Olive Brown	
25 – 28.5	5Y 4/3/3 Olive	Detritus gray brown, finer than below, Nano fossiliferous, strong carbonate.
28.5 – 33	5Y 5/2/2 Olive Gray	Detritus, high brown, coarser than above, Nano fossiliferous.
33 – 67	2.5Y 3/2/2 Dark Olive Gray	Marl dark gray to black, very thin layers, maximum of 2 cm, often in mm thickness, interbedded with light gray to very thin olive layers. These dark gray to black layers are strongly carbonatic. The light gray layers are less carbonatic.
67 – 69	5Y 3/2/2 Dark Olive Gray	



Section 3 of 4		
Segment	Munsell Soil Color	Remarks
69 – 71	5Y 3/2/2 Dark Olive Gray	Marl dark brown layer, not horizontal (25°) light carbonatic, lined with 2 mm thin micro coquina layers on both sides.
71 – 71.5	2.5Y 5/4/4 Light Olive Brown	
71.5 – 72.5	2.5Y 3/3/3 Dark Olive Brown	
72.5 – 74	2.5Y 4/3/3 Olive Brown	Marl brown to red brown, strongly carbonatic, interbedded with 3 layers of about 2 – 3 mm micro coquina layers.
64 – 76	10YR 4/3/3 Brown	
76 – 77.5	5Y 3/2/2 Dark Olive Gray	
77.5 – 80	10YR 4/3/3 Brown	
80 – 81.5	2.5Y 3/3/3 dark Olive Brown	
81.5 – 83	7.5YR 3/4/4 Dark Brown	Marl dark brown, oily, strong carbonatic.
83 – 96	2.5Y 3/2/2 Very Dark Greenish Brown	
96 – 128	7.5YR 5/8/8 Strong Brown	Marl, no layering, totally disturbed, small tectonic faulting, red brown to gray, all slided disturbed layers, strong carbonate.
	2.5Y 4/3/3 Olive Brown	
	10YR 4/3/3 Brown	
	2.5Y 3/2/2 Very Dark Greenish Brown	
128 – 131.5	2.5Y 4/3/3 Olive Brown	
131.5 – 132	2.5Y 3/2/2 Very Dark Greenish Brown	
132 – 133.5	2.5Y 4/3/3 Olive Brown	
133.5 – 136	10YR 3/3/3 Dark Brown	
136 – 137	5Y 3/2/2 Dark Olive Gray	
137 – 137.5	2.5Y 2.5/1/1 Black	
137.5 – 149	2.5Y 4/4/4 Olive Brown	Marl, light brown, compact, strong carbonate.
149 – 169	2.5Y 6/8/8 Olive Yellow	Similar to 96 – 137.5 with a lens of 7cm long x 4cm, very black surrounded by a yellow ring. This ring is strongly carbonatic with a clear smell.
	2.5Y 4/3/3 Olive Brown	
	10YR 4/3/3 Brown	
	2.5Y 3/2/2 Very Dark Greenish Brown	



Section 2 of 4		
Segment	Munsell Soil Color	Remarks
169 – 189	2.5Y 3/2/2 Very Dark Greenish Brown	Marl high brown to dark brown, strongly disturbed, strong carbonate
	2.5Y 6/8/8 Olive Yellow	
	2.5Y 3/3/3 Dark Olive Brown	
189 – 200	2.5Y 3/2/2 Very Dark Greenish Brown	
	2.5Y 4/4/4 Olive Brown	
200 – 221	2.5Y 3/3/3 Dark Olive Brown	Marl light brown, 50% compact, homogenous, strongly carbonatic.
221 – 228	2.5Y 3/2/2 Very Dark Greenish Brown	
228 – 264	2.5Y 4/4/4 Olive Brown	
264 – 265	10YR 3/2/2 Very Dark Greenish Brown	Disturbed light brown to black marl, strong carbonate.
265 – 269	2.5Y 4/3/3 Olive Brown	
	2.5Y 3/1/1 Very Dark Gray	
	2.5Y 3/2/2 Very Dark Greenish Gray	



Section 1 of 4		
Segment	Munsell Soil Color	Remarks
269 - 290	2.5Y 3/3/3 Dark Olive Brown	Light brown marl, 70% compact, homogenous, strong carbonate.
290 – 294	2.5Y 4/4/4 Olive Brown	Light brown marl, disturbed fossiliferous.
294 – 294.5	10YR 3/2/2 Very Dark Greenish Brown	Light brown to brown, strongly fossiliferous, sandy marl.
294.5 – 299	2.5Y 5/2/2 Greenish Brown	
299 – 330	2.5Y 3/3/3 Dark Olive Brown	Brown homogenous marl, 70% compact, carbonatic.
	2.5Y 5/2/2 Greenish Brown	
	7.5YR 5/6/6 Strong Brown	
330 – 349	2.5Y 3/3/3 Dark Olive Brown	Marl, disturbed light brown to black with two large layers, sandy and all fossiliferous, dark black with strong HCl (3%) reaction with a strong smell.
	Gley2 2.5/1/PB Blueish Black	
349 – 359	2.5Y 3/3/3 Dark Olive Brown	
359 – 361	Gley2 2.5/1/PB Blueish Black	
361 - 369	CATCHER	



Cruise Number:	64 PE 350	Station Number:	40 (Erba Deep)
Latitude (N):	20° 47.983	Depth:	1866 m
Longitude (E):	38° 02.425	Time (UTC):	11:35 hr
Core Number:	G.C. 6 (Gravity Core)	Core Length:	344 cm

Section 4 of 4		
Segment	Munsell Soil Color	Remarks
0 – 35	10YR 6/4/4 Light Yellowish Brown	Marl, strongly carbonatic, very sticky, light brown, homogenous, H ₂ O > 70%.
35 – 44	2.5Y 5/3/3 Light Olive Brown	



Section 3 of 4		
Segment	Munsell Soil Color	Remarks
44 – 52	2.5Y 5/3/3 Light Olive Brown	Sandy marl, light brown, fossiliferous.
52 – 55	2.5Y 6/3/3 Light Yellowish Brown	Marl, brown, carbonatic, very sticky.
55 – 78	10YR 6/4/4 Light Yellowish Brown	
78 – 114	2.5Y 5/3/3 Light Olive Brown	Marl, brown to gray brown, 50% watered, disturbed carbonatic, gray brown fossiliferous.
114 – 135	2.5Y 5/6/6 Light Olive Brown	Disturbed marl, brown to reddish brown with needles fossils, compact carbonatic.
135 – 144	10YR 6/4/4 Light Yellowish Brown	Look below.



Section 2 of 4		
Segment	Munsell Soil Color	Remarks
144 – 148	10YR 6/4/4 Light Yellowish Brown	Marl, brown homogenous, carbonatic, sticky with 50% water content, intercalated at 148 and at 185 with 1 cm to 2 cm strong fossiliferous layers.
148 – 151	2.5Y 5/3/3 Light Olive Brown	
151 – 185	10YR 5/6/6 Yellowish Brown	
185 – 190	2.5Y 5/3/3 Light Olive Brown	
190 – 244	10YR 5/6/6 Yellowish Brown	



Section 1 of 4		
Segment	Munsell Soil Color	Remarks
244 - 344	10YR 5/6/6 Yellowish Brown	Same as above



Cruise Number:	64 PE 350	Station Number:	49 (Port Sudan Deep)
Latitude (N):	20° 04.227	Depth:	2650 m
Longitude (E):	38° 30.598	Time (UTC):	08:35
Core Number:	G.C. 7 (Gravity Core)	Core Length:	0 cm

Section 4 of 4		
Segment	Munsell Soil Color	Remarks
EMPTY		Some basalt rocks with broken glass.



Cruise Number:	64 PE 350	Station Number:	50 (Port Sudan Deep)
Latitude (N):	20° 04.585	Depth:	2767 m
Longitude (E):	38° 30.706	Time (UTC):	10:50 hr
Core Number:	G.C. 8 (Gravity Core)	Core Length:	369 cm

Section 4 of 4

Segment	Munsell Soil Color	Remarks
0 – 57	2.5Y 4/3/3 Olive Brown	Marl, brown, high water content approximately 60%, carbonatic.
57 – 69	5Y 3/2/2 Dark Olive Gray	Marl gray, homogenous, carbonatic.

**Section 3 of 4**

Segment	Munsell Soil Color	Remarks
69 – 86	5Y 3/2/2 Dark Olive Gray	Marl gray, homogenous, carbonatic.
86 – 87.5	5Y 5/2/2 Olive Gray	Light gray, sandy, micro coquina layer, fully fossiliferous, sponge carbonatic.
87.5 – 136	5Y 3/2/2 Dark Olive Gray	Dark gray, marl, circles bedded with white mm bands, carbonatic.
136 - 169	5Y 3/1/1 Very Dark Gray	Dark to dark olive marl, homogenous carbonatic.



Section 2 of 4			
Segment	Munsell Soil Color	Remarks	
169 – 173.5	5Y 5/2/2 Olive Gray	Micro coquina layers, sandy, strongly fossiliferous, strongly carbonatic.	
173.5 – 189	5Y 3/2/2 Dark Olive Gray	Dark gray marl, banded, carbonatic.	
189 – 211	5Y 4/1/1 Dark Gray	Marl, different colors, green, brown, light gray to brown. They go into each other gradually, carbonatic.	
	2.5Y 3/2/2 Very Dark Grayish Brown		
211 – 225	2.5Y 3/3/3 Dark Olive Brown	Marl, banded in mm. these bands are in different colors, red brown, gray to white gray, carbonate pieces.	
225 – 252	5Y 3/2/2 Dark Olive Gray	225 – 244	Marl gray to dark gray, water content about 30%, oily, slightly carbonatic.
		244 – 245	Marl, gray brown, slightly carbonatic.
		245 – 246	Marl, red brown, slightly carbonatic.
		246 – 252	Marl, light gray, water 30%, homogenous, oily, reacts to HCl (3%) with a strong smell.
252 - 269	5Y 3/1/1 Very Dark Gray	Marl, black to gray black, compact, less than 30% water, homogenous, slightly carbonatic.	



Section 1 of 4		
Segment	Munsell Soil Color	Remarks
269 – 286	2.5Y 2.5/1/1 Black	Marl, black to gray black, compact, less than 30% water, homogenous, slightly carbonatic.
286 – 307	5Y 2.5/2/2 Black	Marl, thinly laminated, compact, black gray, water < 30%.
307 – 325	2.5Y 2.5/1/1 Black	Sandy marl layer, strongly carbonatic, black to gray black, compact. Water content < 30%.
325 – 359	2.5Y 3/1/1 Very Dark Gray	Marl gray compact, homogenous layer part slided, oily, strong reaction with HCl (3%).
359 – 369	CATCHER	



Cruise Number:	64 PE 350	Station Number:	55 (Suakin Deep)
Latitude (N):	19° 36.728	Depth:	2774 m
Longitude (E):	38° 43.170	Time (UTC):	08:42 hr
Core Number:	G.C. 9 (Gravity Core)	Core Length:	369 cm

Section 4 of 4			
Segment	Munsell Soil Color	Remarks	
0 – 5	EMPTY		
5 – 17	10YR 2/1/1 Black	5 – 14.5	Marl gray to black, very fine lamination, H ₂ O content almost 50%, strong reaction with HCl (3%).
	10YR 2/2/2 Very Dark Brown		
	10YR 2/1/1 Black		
	5Y 5/3/3 Olive	14.5 – 15.5	Marl brown, 1 cm thin layer.
	2.5Y 3/3/3 Dark Olive Brown	15.5 – 17	Marl dark brown, 1 cm thin layer.
17 – 24	10YR 2/2/2 Very Dark Brown	Marl black, 50% H ₂ O content, reacts with HCl (3%) with a strong smell.	
24 – 25	5Y 5/3/3 Olive	Interbedding light brown marl and gray to black marl, 50% H ₂ O content, oily, strong reaction with HCl.	
25 – 26	10YR 2/2/2 Very Dark Brown		
26 – 27	5Y 5/3/3 Olive		
27 – 30	5Y 2.5/1/1 Black	Marl black, oily, 50% H ₂ O content.	
30 – 31	5Y 5/3/3 Olive		
31 – 33	5Y 2.5/1/1 Black		
33 – 37	5Y 5/3/3 Olive	50% homogenous, light reaction with HCl (3%)	
37 – 40	5Y 2.5/1/1 Black	Marl black, 50% H ₂ O content, oily, reacts with HCl.	
40 – 43	5Y 5/3/3 Olive	Marl olive green, 50% H ₂ O content, reacts with HCl.	
43 – 64	5Y 2.5/1/1 Black	Marl black to gray black, 50% H ₂ O content, oily, reacts slightly with HCl.	
64 – 66	5Y 5/3/3 Olive	Marl olive green, 50% H ₂ O content, reacts with HCl.	
66 – 69	5Y 2.5/1/1 Black	Marl black, 60% H ₂ O content, reacts strongly with HCl.	



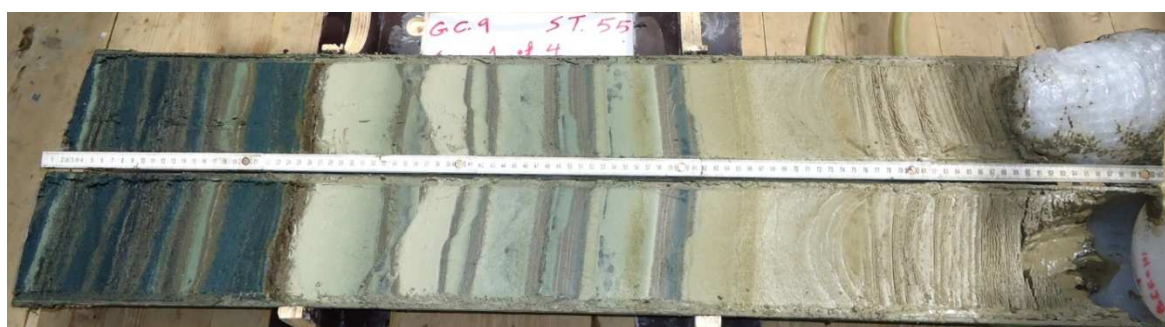
Section 3 of 4		
Segment	Munsell Soil Color	Remarks
69 – 72	5Y 2.5/1/1 Black	Marl black, 60% H ₂ O content, strong reaction with HCl (3%).
72 – 91	2.5Y 3/3/3 Dark Olive Brown	Marl brown, 50% H ₂ O content, oily, reacts with HCl.
91 - 98	5Y 2.5/1/1 Black	Marl black, thin layered, H ₂ O < 50%, reacts slightly with HCl.
98 – 102	2.5Y 3/3/3 Dark Olive Brown	Marl , interbedded light brown to gray brown to red brown, lamination in mm up to 4cm.
102 – 103	5Y 2.5/1/1 Black	
103 – 104.5	10YR 2/2/2 Very Dark Brown	
104.5 – 107	5Y 5/3/3 Olive	
107 – 108.5	10YR 2/2/2 Very Dark Brown	
108.5 – 111	5Y 5/3/3 Olive	
111 – 124	5Y 2.5/1/1 Black	Marl black, lamilated, spongy with H ₂ O < 50%
124 – 127.5	2.5Y 3/3/3 Dark Olive Brown	Marl, 50% H ₂ O content, oily, interbedded up to 4cm thick, different colors, dark gray to dark brown to dark olive green.
127.5 – 130.5	2.5Y 3/3/3 Dark Olive Brown	
130.5 – 132	5Y 5/3/3 Olive	
132 – 133	10YR 2/2/2 Very Dark Brown	
133 – 136	5Y 5/3/3 Olive	
136 – 137	5Y 2.5/1/1 Black	
137 – 140	2.5Y 3/3/3 Dark Olive Brown	Marl, interbedded between olive green to brown to dark brown layers up to 4 cm, < 40% H ₂ O, strong reaction with HCl.
140 – 146	5Y 2.5/1/1 Black	
146 – 151.5	5Y 3/2/2 Dark Olive Gray	
151.5 – 152.5	10YR 2/2/2 Very Dark Brown	
152.5 – 159	5Y 3/2/2 Dark Olive Gray	
159 – 164.5	5Y 2.5/1/1 Black	
164.5 – 165	2.5Y 2.5/1/1 Black	
165 – 168	5Y 3/2/2 Dark Olive Gray	
168 – 169	5Y 2.5/1/1 Black	



Section 2 of 4		
Segment	Munsell Soil Color	Remarks
169 – 205	5Y 3/2/2 Dark Olive Gray 10YR 4/3/3 Brown	Marl layered red brown, dark olive green, no reaction with HCl.
205 – 207	5Y 5/3/3 Olive	Marl, thin laminations in mm, black to gray brown to light brown to olive green with H ₂ O content < 50%, slight reaction with HCl.
207 – 213	5Y 3/2/2 Dark Olive Gray 10YR 4/3/3 Brown	
213- 220	2.5Y 3/3/3 Dark Olive Brown	
220 – 223	Gley2 2.5/1/5BG Greenish Black	Marl light brown interbedded by a 5 cm black layer, < 50% H ₂ O content, this black layer is oily and there is no reaction with HCl.
223 – 233	10YR 2/1/1 Black	
233 – 238	Gley2 2.5/1/5BG Greenish Black	
238- 245.5	5Y 3/2/2 Dark Olive Gray	Marl black laminated with brown mm bands, H ₂ O content < 50%, reacts with HCl, the lamination is in different colors, black to olive green to red brown in mm bands up to 3 cm in thickness.
245.5 – 246.5	5Y 3/1/1 Very Dark Gray	
246.5 – 248.5	5Y 3/2/2 Dark Olive Gray	
248.5 – 252	5Y 3/1/1 Very Dark Gray	
252 – 257	Gley2 2.5/1/5BG Greenish Black	
257 – 261	5Y 2.5/1/1 Black	
261 – 266	5Y 3/2/2 Dark Olive Gray	
266 – 267	Gley2 2.5/1/5BG Greenish Black	
267 – 269	5Y 2.5/1/1 Black	



Section 1 of 4		
Segment	Munsell Soil Color	Remarks
269 – 293	Gley2 2.5/1/5BG Greenish Black	Same as above.
	5Y 5/3/3 Olive	
	2.5Y 3/3/3 Dark Olive Brown	
293 – 295	10YR 2/2/2 Very Dark Brown	Marl light brown, disturbed, banded with green thin bands, oily green bands, < 30% water content, reacts strongly with HCl.
295 – 330	5Y 6/2/2 Light Olive Gray	
	5Y 3/2/2 Dark Olive Gray	
	5Y 5/3/3 Olive	
	Gley2 2.5/1/5BG Greenish Black	
330 – 356	5Y 4/3/3 Olive	Marl light brown < 30% H ₂ O content, consolidated oily, reacts strongly with HCl
356 – 369	CATCHER	



Cruise Number:	64 PE 350	Station Number:	63 (Pockmark Central)
Latitude (N):	19° 57.754	Depth:	483 m
Longitude (E):	39° 24.607	Time (UTC):	05:17 hr
Core Number:	G.C. 10 (Gravity Core)	Core Length:	344 cm

Section 4 of 4		
Segment	Munsell Soil Color	Remarks
0 – 29	5Y 4/2/2 Olive Gray	Marl, dark gray, H ₂ O content 50%, homogenous, strong reaction with HCl (3%).
29 – 35	5Y 5/2/2 Olive Gray	Marl, light gray, H ₂ O content 50%, homogenous, carbonatic.
35 – 44	5Y 3/2/2 Dark Olive Gray	Marl, very dark gray, 30% H ₂ O with compact white solid pieces that react strongly with HCl (3%).



Section 3 of 4		
Segment	Munsell Soil Color	Remarks
44 – 83	5Y 6/2/2 Light Olive Gray	Marl light gray, disturbed, high H ₂ O content > 50% with hard white precipitates, strongly carbonatic
83 – 86	5Y 5/2/2 Olive Gray	Like above but not disturbed.
86 – 97	5Y 6/2/2 Light Olive Gray	Marl gray, consolidated homogenous, H ₂ O 30%, carbonatic.
97 – 116	5Y 4/2/2 Olive Gray	Marl gray to brown, about to be layered, consolidated H ₂ O 40%, colors go into each other.
	5Y 5/2/2 Olive Gray	
116 – 144	5Y 6/2/2 Light Olive Gray	Marl light gray, homogenous H ₂ O < 40%, carbonatic.



Section 2 of 4		
Segment	Munsell Soil Color	Remarks
144 - 151	5Y 6/2/2 Light Olive Gray	Marl light gray, H ₂ O content 30%, carbonatic.
151 – 175	5Y 5/2/2 Olive Gray	
175 – 188	5Y 5/2/2 Olive Gray	Marl light gray, consolidated H ₂ O 30%, colors go into each other, reacts slightly with HCl (3%).
188 – 200	5Y 4/1/1 Dark Gray	
200 – 240	5Y 6/2/2 Light Olive Gray	Marl light gray, not layered, H ₂ O 50%, carbonatic.
240 - 244	5Y 5/2/2 Olive Gray	

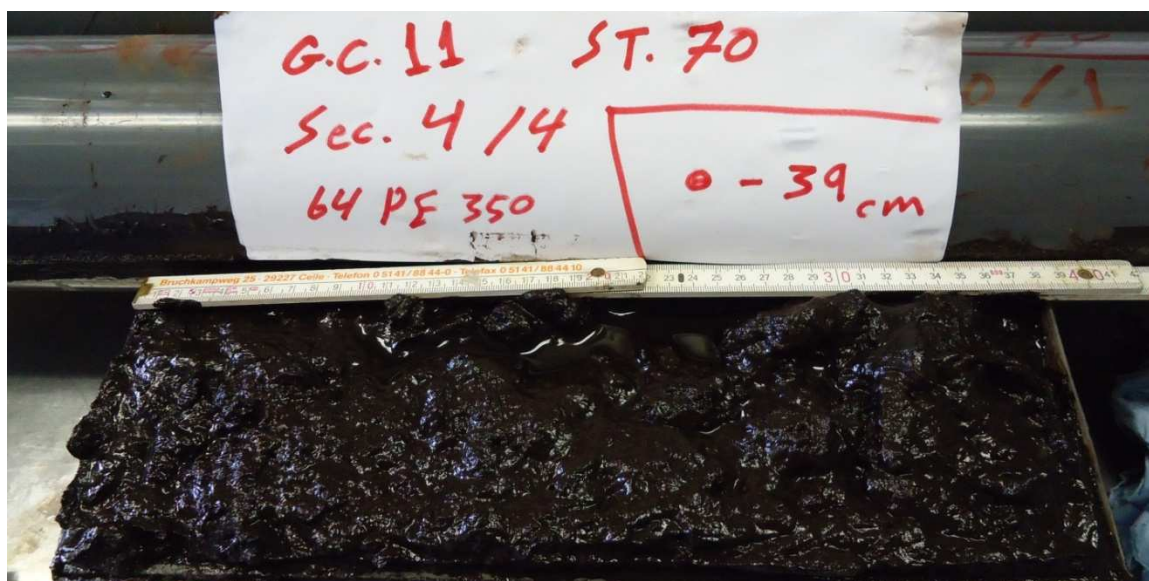


Section 1 of 4		
Segment	Munsell Soil Color	Remarks
244 – 265	5Y 5/2/2 Olive Gray	Marl gray, disturbed, colors go into each other, H ₂ O content 40%, reacts with HCl (3%).
265 - 331	5Y 6/2/2 Light Olive Gray	Marl light gray, consolidated H ₂ O 40%, homogenous, reacts with HCl (3%).
331 – 344	CATCHER	



Cruise Number:	64 PE 350	Station Number:	70 (Atlantis // Deep South East)
Latitude (N):	21° 20.267	Depth:	2144 m
Longitude (E):	38° 05.600	Time (UTC):	08:37 hr
Core Number:	G.C. 11 (Gravity Core)	Core Length:	339 cm

Section 4 of 4		
Segment	Munsell Soil Color	Remarks
0 – 39	5YR 2.5/1/1 Black	Marl, black, high water content, > 70%, lightly sandy, oily, disturbed.



Section 3 of 4		
Segment	Munsell Soil Color	Remarks
39 – 139	5YR 2.5/1/1 Black	Like above but not disturbed, water content 50% up to 90 cm and < 50% from 90 – 120 cm, oily, more consolidated.



Section 2 of 4		
Segment	Munsell Soil Color	Remarks
139 – 149	5YR 2.5/1/1 Black	Marl not well layered, changing layers, layers moving into each other from brown to red to gray to olive gray with metallic sparkling and small sulphide pieces, consolidated with a hard piece of marine sulfide at the depth of 150cm.
149 – 159	5YR 3/4/4 Dark Reddish Brown	
159 – 162	5YR 2.5/2/2 Dark Reddish Brown	
162 – 169	2.5YR 3/6/6 Dark Red	
169 – 177	7.5YR 4/1/1 Dark Gray	
177 – 182	2.5YR 3/6/6 Dark Red	
182 – 197	5YR 2.5/2/2 Dark Reddish Brown	
197 – 214	2.5YR 3/6/6 Dark Red	
	7.5YR 4/1/1 Dark Gray	
214 – 239	5YR 2.5/2/2 Dark Reddish Brown	
	5YR 3/4/4 Dark Reddish Brown	

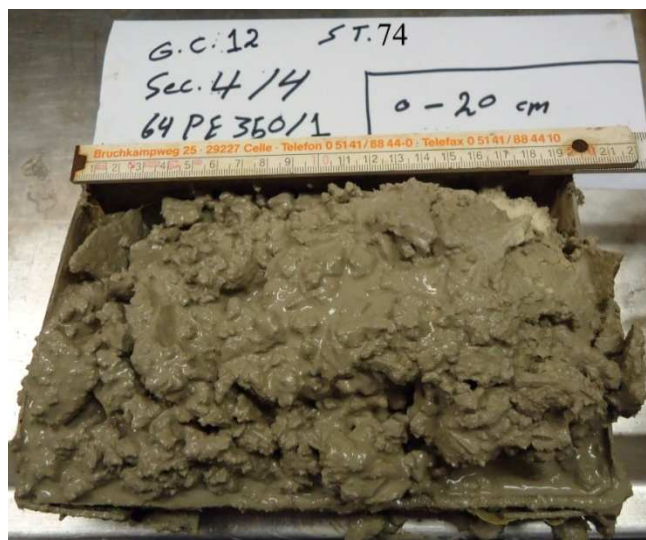
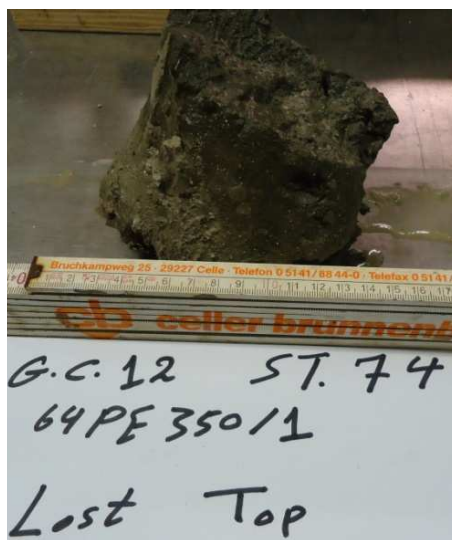


Section 1 of 4		
Segment	Munsell Soil Color	Remarks
239 – 325	2.5YR 3/4/4 Dark Reddish Brown	Like above
	7.5YR 4/1/1 Dark Gray	
325 – 339	CATCHER	



Cruise Number:	64 PE 350	Station Number:	74 (Sea Peak)
Latitude (N):	21° 40.854	Depth:	839 m
Longitude (E):	38° 43.393	Time (UTC):	13:55 hr
Core Number:	G.C. 12 (Gravity Core)	Core Length:	320 cm

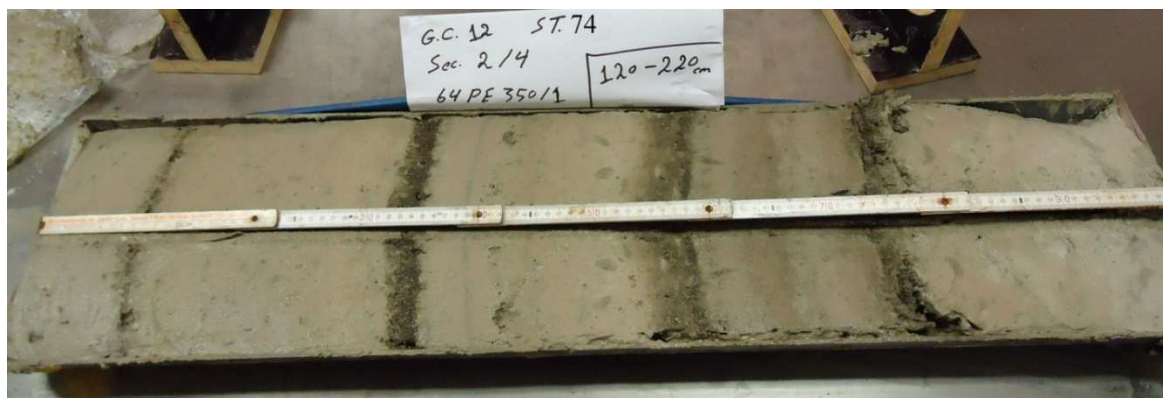
Section 4 of 4		
Segment	Munsell Soil Color	Remarks
0 – 2	5Y 7/2/2 Light Gray	Crust layer on top, very disturbed carbonate fractures and small poeces
2 – 20	5Y 6/2/2 Light Olive Gray	



Section 3 of 4		
Segment	Munsell Soil Color	Remarks
20 – 28	5Y 5/2/2 Olive Gray	Fractures of crust and pteropods with high H ₂ O content > 50%
28 – 35		Compact layer, silty clay, H ₂ O < 30%
35 – 50		Same as 20 – 28 with a small layer of yellow color (Mangan!!), disturbed.
50 – 62		Same as 28 – 35
62 – 68		Same as 20 – 28
68 - 83	5Y 6/2/2 Light Olive Gray	Compact, dissolution re precipitating carbonate layer with some organic deposits between 83 – 90
83 – 120		



Section 2 of 4		
Segment	Munsell Soil Color	Remarks
120 – 130.5	5Y 5/2/2 Olive Gray	Compact, water content 30%, with black layers of organic deposits, oily between 129.5 – 130, 153 – 155, 176 – 179, 195 – 197.
130.5 – 131	5Y 3/2/2 Dark Olive Gray	
131 – 153	5Y 5/2/2 Olive Gray	
153 – 155.5	5Y 3/2/2 Dark Olive Gray	
155.5 – 176	5Y 5/2/2 Olive Gray	
176 – 179	5Y 3/2/2 Dark Olive Gray	
179 – 195	5Y 5/2/2 Olive Gray	
195 – 198	5Y 3/2/2 Dark Olive Gray	
198 - 220	5Y 7/2/2 Light Gray	Very light gray, clayey



Section 1 of 4		
Segment	Munsell Soil Color	Remarks
220 – 310	5Y 7/2/2 Light Gray	Gray, H ₂ O content 40%, some corals between 292 – 294??!!
310 – 320	CATCHER	



Cruise Number:	64 PE 350	Station Number:	79 (Pockmark)
Latitude (N):	19° 59.544	Depth:	465 m
Longitude (E):	39° 31.828	Time (UTC):	05:36 hr
Core Number:	G.C. 13 (Gravity Core)	Core Length:	363 cm

Section 4 of 4		
Segment	Munsell Soil Color	Remarks
0 – 21	Gley1 4/1/10Y Dark Greenish Gray	Very thin laminated layer from dark olive green to greenish gray with pteropods
21 – 38	Gley1 5/1/10Y Greenish Gray	Disturbed light gray carbonate crust with pteropods, H ₂ O content more than 50%
38 – 53	Gley1 8/1/10Y Light Greenish Gray	Clayey, very light gray with carbonate crust, intercalated, disturbed, H ₂ O content more than 50%.
53 – 63		Compact, clayey, consolidated light gray with black spots



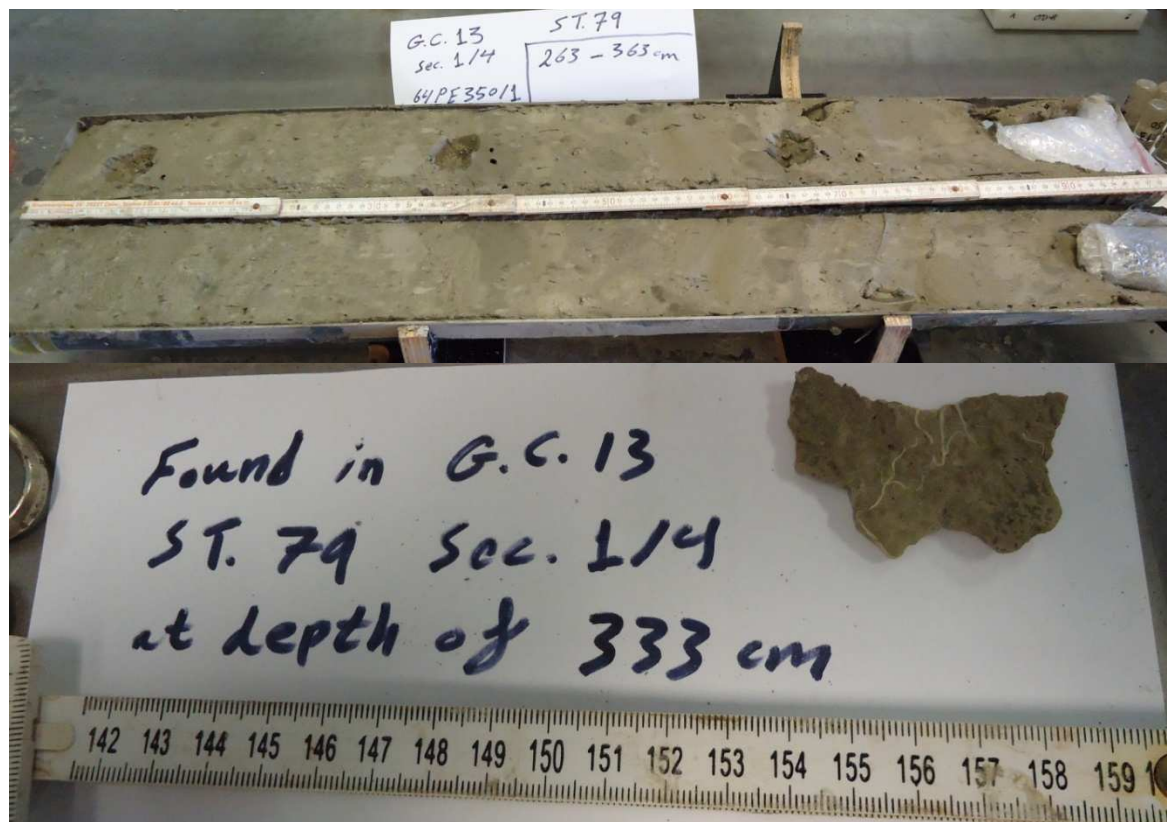
Section 3 of 4		
Segment	Munsell Soil Color	Remarks
63 – 66	Gley1 8/1/10Y Light Greenish Gray	Same as above
66 – 77	5Y 6/2/2 Light Olive Gray	Compact olive, H ₂ O content < 50%, consolidated.
77 – 134	5Y 4/2/2 Olive Gray	
134 – 163	5Y 3/2/2 Dark Olive Gray	Consolidated olive, clayey, H ₂ O < 40%
	5Y 6/2/2 Light Olive Gray	



Section 2 of 4		
Segment	Munsell Soil Color	Remarks
163 – 168	5Y 3/2/2 Dark Olive Gray	Same as above
168 – 263	5Y 5/1/1 Gray	Coarser marl with black spots, H ₂ O > 50%, compact.



Section 1 of 4		
Segment	Munsell Soil Color	Remarks
263 – 350	5Y 5/1/1 Gray	Clayey, H ₂ O content < 40% with broken carbonate shells intercalated with a carbonate crust showing some worms.
	5Y 6/1/1 Gray	
350 – 363	CATCHER	



Cruise Number:	64 PE 350 – 1	Station Number:	80 (Pockmark)
Latitude (N):	19° 55.121	Depth:	450 m
Longitude (E):	39° 30.387	Time (UTC):	06:58 hr
Core Number:	G.C. 14 (Gravity Core)	Core Length:	365 cm

Section 4 of 4		
Segment	Munsell Soil Color	Remarks
0 – 10	5Y 5/1/1 Gray	Dark olive hard carbonate crust, consolidated, couldn't cut with the cutter.
10 – 19	5Y 6/2/2 Light Olive Gray	Carbonate crust mixed with mud, not consolidated. The crust seems to be intercalated with pteropods and a thin gray layer. H ₂ O < 50%.
19 – 22		Consolidated marl, H ₂ O < 40%.
22 – 25		Repetition of segment (10 – 19)
25 – 28	5Y 4/1/1 Dark Gray	Repetition of segment (19 – 22)
28 – 38		Repetition of both (10 – 22) with a thin gray layer.
38 – 53		Darker in color, compact, muddy with carbonate fractures.
53 – 65	5Y 4/2/2 Olive Gray	



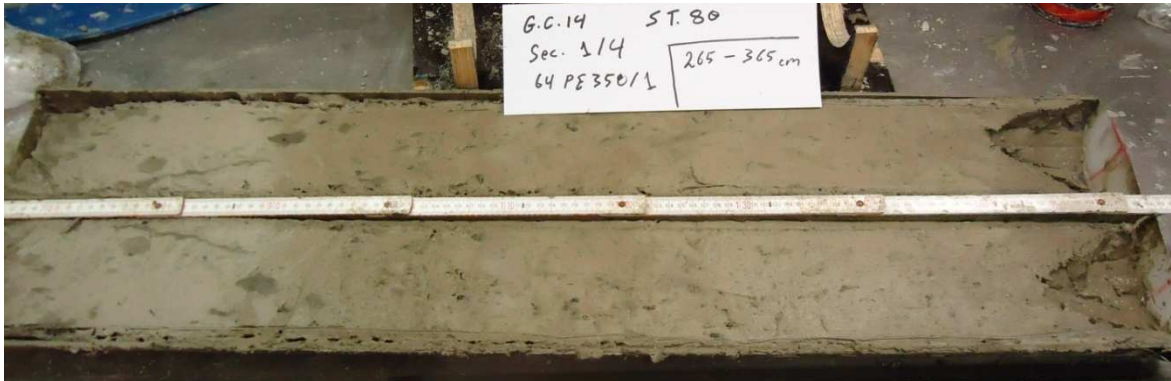
Section 3 of 4		
Segment	Munsell Soil Color	Remarks
56 – 73	5Y 6/2/2 Light Olive Gray	Compact, shading from dark olive gray to light olive gray, these shadings do not form a layer, they contain spots.
73 – 95	5Y 4/2/2 Olive Gray	
	5Y 4/2/2 Olive Gray	
95 – 116	5Y 6/2/2 Light Olive Gray	
	5Y 4/2/2 Olive Gray	
116 – 123	5Y 4/2/2 Olive Gray	
123 – 134	5Y 4/2/2 Olive Gray	Light gray, compact marl with some black spots, H ₂ O 30%.
134 – 144	5Y 4/2/2 Olive Gray	
144 – 165	5Y 6/2/2 Light Olive Gray	



Section 2 of 4		
Segment	Munsell Soil Color	Remarks
165 – 175	5Y 6/2/2 Light Olive Gray	Continued from above.
175 – 262	5Y 4/2/2 Olive Gray	Compact marl, dark olive intercalated with rounded light gray and mixtures of pteropods
262 – 265	5Y 6/2/2 Light Olive Gray	

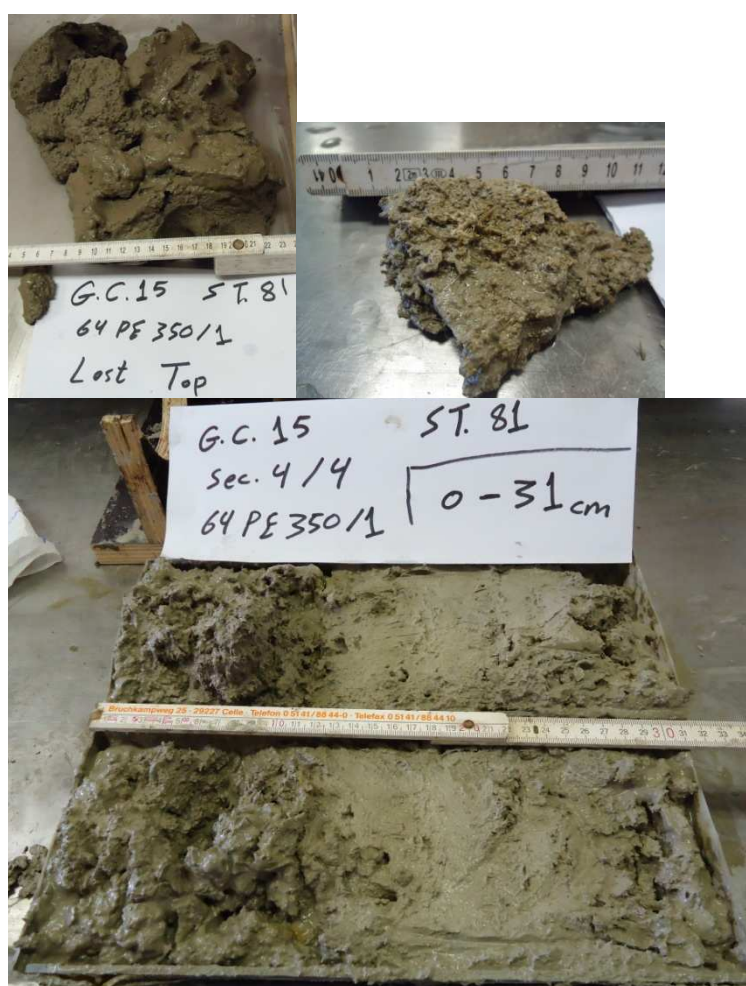


Section 1 of 4		
Segment	Munsell Soil Color	Remarks
265 – 269	5Y 5/2/2 Olive Gray	Compact marl, light gray intercalated with dark olive spots mixed with shells and black spots.
269 – 293	5Y 6/2/2 Light Olive Gray	
	5Y 5/2/2 Olive Gray	
293 – 322	5Y 4/2/2 Olive Gray	
	5Y 5/2/2 Olive Gray	
322 – 352	5Y 6/2/2 Light Olive Gray	
352 – 365	CATCHER	



Cruise Number:	64 PE 350	Station Number:	81 (Pock Mark Reference)
Latitude (N):	19° 50.693	Depth:	420 m
Longitude (E):	39° 29.796	Time (UTC):	08:06 hr
Core Number:	G.C. 15 (Gravity Core)	Core Length:	331 cm

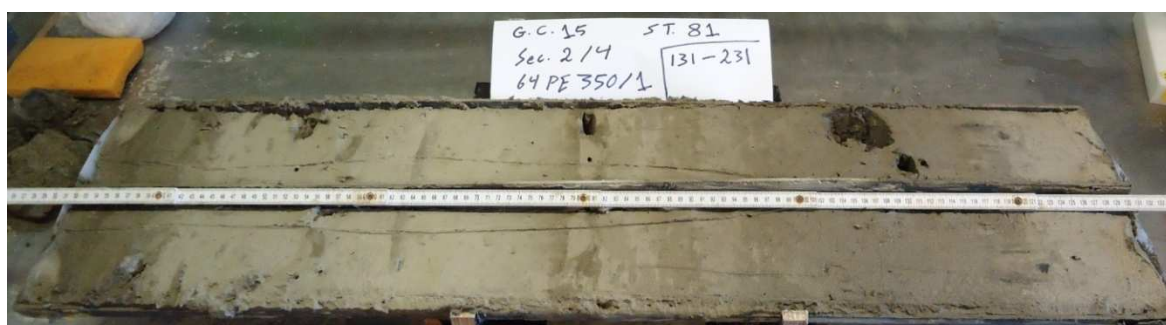
Section 4 of 4		
Segment	Munsell Soil Color	Remarks
0 – 13	5Y 5/2/2 Olive Gray	Dark olive gray fractures of carbonate crust intercalated with biogenic pteropods and some yellow dots ,probably indication of oxide with H ₂ O > 50%.
13 – 28	5Y 6/2/2 Light Olive Gray	Light gray marl, compact, intercalated with carbonate and pteropods, H ₂ O >50%.
28 – 31		Repetition of segment (0 – 13)



Section 3 of 4		
Segment	Munsell Soil Color	Remarks
31 – 40	5Y 6/2/2 Light Olive Gray	Continued from above
40 – 48		Light gray mixture of mud and carbonate crust with some shells interbedded into thin layers, H ₂ O 40%
48 – 59		Finer than above and darker in color with less H ₂ O content.
59 – 80	5Y 5/2/2 Olive Gray	Dark olive marl with black spots
80 – 87	5Y 6/2/2 Light Olive Gray	
87 – 102	5Y 5/2/2 Olive Gray	
102 – 110	5Y 6/2/2 Light Olive Gray	
110 - 131	5Y 5/2/2 Olive Gray	



Section 2 of 4		
Segment	Munsell Soil Color	Remarks
131 – 142	5Y 5/2/2 Olive Gray	Continued from above
142 – 197	2.5Y 6/2/2 Light Brownish Gray	Light gray marl intercalated with dark incomplete layers with a mixture of pteropods and sea shells.
197 – 222	5Y 5/2/2 Olive Gray	Dark olive marl with black spots
222 – 231	2.5Y 6/2/2 Light Brownish Gray	Repetition of segment (142 – 197) with black spots.



Section 1 of 4		
Segment	Munsell Soil Color	Remarks
231 – 238	2.5Y 6/2/2 Light Brownish Gray	Continued from above
238 – 273	5Y 6/2/2 Light Olive Gray	Olive marl with mixed shells
273 – 296	5Y 5/2/2 Olive Gray	Light olive marl, H ₂ O 40%, intercalated with darker olive incomplete layers and shells of 1 cm in diameter.
296 – 320	2.5Y 6/2/2 Light Brownish Gray	
320 – 331	CATCHER	



4.8 Organic-geochemical characterization of sediments from brine-filled Red Sea deeps

Thorsten Bauersachs, Jan-Peter Mayser, Lorenz Schwark

Introduction

The Red Sea is formed by the divergent movement of the Arabian and African continental plates, which is associated with the formation of new oceanic crust along a NW-SE striking axial graben (Altherr et al. 1988). This graben narrows north of 23°N and active seafloor spreading is replaced by a continental rift system (Martinez and Cochran 1988). As a consequence of the divergent movement, numerous tectonic depressions have formed along the axial graben, of which the Atlantis II Deep represents the largest and best studied example. About 25 of the Red Sea deeps are filled with anoxic brine waters having maximum temperatures of 70°C and salinities of up to 250 psu (Swift 2012) that originate from the dissolution of Miocene evaporates (Craig 1969). Due to the higher salinity in conjunction with higher temperatures and anoxic conditions, the Red Sea deeps are characterized by a depositional regime that is fundamentally different from the “normal” marine environment of the Red Sea. Previous studies have mainly addressed the inorganic properties of the brine-filled deeps and a wealth of information concerning their sedimentology, mineralogy and chemical composition is available. Only little is known, however, on the biogeochemical processes that occur in the hypersaline waters of the brine pools and the organic matter that is incorporated into the sedimentary sequence. Recent molecular investigations have shown that the brine-seawater interface layers of the Kebrit and the Shaban Deep harbour a myriad of previously undescribed extremophiles (Eder et al. 2001; Antunes et al. 2007, Siam et al. 2012). Detailed bulk geochemical and lipid biomarker analyses have been performed on sediments from the Kebrit and Shaban Deep located in the northern Red Sea (Michaelis et al. 1990; Botz et al. 2011) and the Atlantis II Deep (Simoneit et al. 1987). Here, we have extended our present knowledge on the organic geochemical properties of brine-filled deeps located in the central Red Sea. Special emphasis was placed on the GDGT distribution of the investigated brine systems in order to assess their potential as a proxy for the reconstruction of past oceanic sea surface temperatures of the Red Sea.

Materials and methods

Sediment samples

Sediment cores from several Red Sea Deep (Table A-4.8.1) were recovered using a gravity corer. All cores were split on board and 2-cm-thick sediment slices sampled at regular intervals were collected for the analysis of bulk geochemical and lipid biomarker properties. Samples were immediately stored frozen at -40 °C. After the cruise they were shipped to the organic geochemistry laboratory of the Christian-Albrechts-University (Kiel, Germany) on dry ice. Upon arrival, all sediments were washed with bidistilled water, freeze-dried and subsequently crushed to a homogenous powder using a rotary mill.

Elemental analyses

Total carbon (C_{tot}), total nitrogen (N_{tot}) and total sulfur (S_{tot}) contents were measured on powdered samples using a vario EL III elemental analyzer (Elementar, Germany). Total inorganic carbon (C_{carb}) contents were determined using a soliTIC module (Elementar, Germany) coupled to the above-mentioned elemental analyzer. The amount of total organic carbon (C_{org}) was calculated as the difference of C_{tot} and C_{carb} .

Extraction and separation

3-14 g of freeze-dried sediments were extracted with an accelerated solvent extractor (Dionex ASE 200) using a mixture of dichloromethane (DCM)/methanol (MeOH) (9:1, v/v) at a temperature of 75 °C and a pressure of $7.6 \cdot 10^6$ Pa. The obtained total lipid extracts were rotary evaporated, transferred to pre-weight vials and dried under a gentle stream of nitrogen. Elemental sulfur was removed by adding activated copper turnings to the total lipid extract. Aliquots of the total lipid extract were separated into apolar and polar fractions by Al_2O_3 column chromatography using hexane/DCM (9:1, v/v) and DCM/MeOH (1:1, v/v), respectively.

Table A-4.8.1. Geographical position, water depth, average sea surface temperatures of the investigated deeps.

Red Sea Deep	Latitude (°N)	Longitude (°E)	Depth (m)	SST (°C)
Northern Atlantis II Deep	21°26'28.50"	38°3'24.78"	2104	24.9
Southern Atlantis II Deep	21°09'37.26"	38°3'24.78"	2234	25.2
Erba Deep	20°47'58.98"	38°3'24.78"	2418	25.3
Port Sudan Deep	20°04'13.62"	38°3'24.78"	2902	25.8
Suakin Deep	19°36'43.68"	38°3'24.78"	2864	26.1
Thetis Deep	22°48'12.30"	38°3'24.78"	1710	26.5

GC-MS analysis

GC-MS was performed using an Agilent 7890A gas chromatograph interfaced to an Agilent 5975B mass spectrometer operated at 70 eV with a mass range of m/z 50-650. The gas chromatograph was equipped with a fused silica capillary column (30 m x 0.25 mm ID) coated with ZB-5HT (film thickness 0.25 μm). Helium was used as carrier gas at a constant flow of 1 ml/min. All samples were injected on column at 70°C and subsequently the oven was programmed to 140°C at 10°C/min and then at 3°C/min to 340°C at which the temperature was held isothermal for 13 min. Compound identification was achieved by comparison with published mass spectral data and the use of retention time indices.

HPLC analysis

Polar fractions were dissolved in hexane/isopropanol (99:1, v/v) with a concentration of 2 mg/ml and subjected to high performance liquid chromatography-mass spectrometry (HPLC-MS) with an Alliance 2690 (Waters, UK) HPLC coupled to a Quattro LC triple quadrupole mass spectrometer (Micromass, UK). Separation of GDGTs was achieved on a Prevail Cyano column (2.1 x 150 mm, 3 µm; Grace, US) at ambient temperature with a flow rate of 0.2 ml/min and the following gradient profile: 99% A and 1% B for 5 min, followed by a linear gradient to 1.8% B in 45 min, where A = hexane and B = 2-propanol. Detection was achieved using positive ion atmospheric pressure chemical ionization (APCI) on the eluent. HPLC-MS settings were as follows: corona 3 kV, cone 35 V, vaporizer temperature 450 °C, source temperature 150 °C and drying gas (N₂) flow 6 l/min. GDGTs were detected by selected ion recording (SIR) of their [M + H]⁺ ions (dwell time = 200 ms). TEX₈₆ values were calculated as:

$$\text{Tex}_{86} = \frac{[\text{GDGT2}] + [\text{GDGT3}] + [\text{Cren}']}{[\text{GDGT1}] + [\text{GDGT2}] + [\text{GDGT3}] + [\text{Cren}']}$$

The resulting Tex₈₆ values were employed to calculate sea surface temperatures of the Red Sea using the equation of Trommer et al. (2009):

$$\text{Tex}_{86} = 0.035 \cdot T - 0.09$$

The branched and isoprenoidal tetraether (BIT) index was calculated as a representation of the relative amounts of branched and isoprenoidal GDGTs in the sediments as a measure for the input of terrestrial organic matter to the brine systems:

$$\text{BIT} = \frac{[\text{I}] + [\text{II}] + [\text{III}]}{[\text{I}] + [\text{II}] + [\text{III}] + [\text{IV}]}$$

Results and discussion

Bulk geochemical parameters

Average TC values of the Red Sea Deep-sea are highly variable and range from 4.0% in the Thetis Deep to 8.2% in the Erba Deep (Table A-4.8.2). TIC measurements evidence that the majority of the total carbon is present in its inorganic form with TIC values ranging from 3.6% in the Suakin Deep to 8.1% in the Erba Deep. This indicates that about 30-70% of the sediments consist of carbonates, which agrees well with reports of the carbonate content of other Red Sea deep-seas (Michaelis et al. 1990). TOC contents on the contrary are comparatively low with average values ranging from 0.19% in the Thetis Deep to 1.4% in the Port Sudan Deep (Table A-4.8.2). TN contents show a strong positive correlation with TOC in all sediments ($r^2 = 0.96$), indicating that admixtures of inorganic nitrogen are only small and that the majority of nitrogen derives from an organic source. Sedimentary C_{org}/N_{tot} ratios can thus be employed to trace for the origin of organic matter. Average C_{org}/N_{tot} values of 8.1 to 12.3 indicate the dominance of bacterial and planktonic biomass in the brine systems with minor admixtures of organic matter of a terrestrial origin (Meyers 1997). Only in sediments deposited in the northern part of the Atlantis II Deep, C_{org}/N_{tot} ratios are unusually high with a maximum value of 32.6. Values of this magnitude are commonly considered to indicate a contribution of organic matter derived from terrestrial origin (Meyers 1997). In case of the Atlantis II Deep, however,

these values are likely to be derived from the impregnation of sediments with hydrothermally derived hydrocarbons, which agrees with the presence of an unresolved complex mixture in sediments with unusually high C_{org}/N_{tot} ratios. C_{org}/N_{tot} ratios of 40-90 have previously been reported from sediments of the Atlantis II Deep that were thermally altered by basaltic intrusions (Simoneit et al. 1987). Average S_{tot} -values range from 0.2% in the Erba Deep to 1.8% in the Suakin Deep. High S_{tot} values, likely related to the presence of pyrite and sphalerite (Michaelis et al. 1990), indicate that the depositional environment of the brine systems is permanently anoxic, which agrees with the reducing conditions currently prevailing in the studied brine systems.

Table A-4.8.2: Bulk geochemical properties of the Red Sea Deeps analyzed in this study

Depth	C_{tot}	C_{carb}	C_{org}	N_{tot}	S_{tot}	C_{org}/N_{tot}	C_{org}/S_{tot}
Northern Atlantis II Deep							
5	0.10	0.00	0.10	0.02	0.14	6.68	0.72
113	7.55	6.74	0.81	0.02	0.71	32.58	1.14
156	5.59	4.67	0.92	0.04	1.63	21.58	0.57
342	4.77	3.79	0.98	0.05	4.37	20.97	0.22
Southern Atlantis II Deep							
2	7.30	6.84	0.45	0.03	0.10	13.19	4.68
41	7.73	5.87	1.86	0.20	1.19	9.38	1.57
140	6.58	6.14	0.43	0.04	0.75	12.31	0.58
240	6.56	6.13	0.43	0.04	0.54	11.99	0.80
320	6.29	5.90	0.39	0.04	0.74	11.15	0.53
Thetis Deep							
11	3.00	2.75	0.26	0.02	0.31	10.90	0.83
91	5.42	5.32	0.11	0.04	0.54	2.89	0.20
141	4.42	4.28	0.13	0.02	0.11	5.44	1.14
187	3.31	3.04	0.27	0.02	0.36	13.44	0.74
Erba Deep							
1	8.18	7.84	0.34	0.06	0.61	5.93	0.57
75	7.83	7.40	0.43	0.03	0.09	17.10	4.70
223	8.35	8.00	0.35	0.02	0.10	18.43	3.36
305	8.34	8.01	0.33	0.02	0.08	15.52	4.31
Port Sudan Deep							
9	6.81	6.41	0.40	0.03	0.17	12.12	2.36
79	7.58	5.43	2.16	0.35	1.99	8.77	1.08
149	7.02	5.13	1.89	0.19	1.88	9.76	1.00
219	5.86	4.70	1.16	0.10	0.34	11.12	3.43
Suakin Deep							
6	7.26	5.43	1.84	0.17	1.71	10.51	1.07
76	6.74	5.79	0.94	0.09	0.30	10.49	3.16
116	0.59	0.13	0.46	0.03	6.46	16.44	0.07
146	5.43	4.20	1.23	0.10	0.38	11.76	3.20
221	3.16	2.18	0.98	0.08	0.36	12.25	2.71

Biomarker analysis

The apolar fractions from the investigated core top sediments are dominated by *n*-alkanes ranging from C₁₈ to C₃₅ with a bimodal distribution maximizing at C₂₁ and C₃₁ as shown for the Suakin Deep (Fig. A-4.8.1). The presence of long-chain homologues is typical for a contribution from vascular plant waxes (Eglinton and Hamilton 1967) and thus may reflect a terrestrial input to the marine sediments. The high-molecular weight homologues (>24) express a strong odd-over-even carbon number predominance in all investigated brine systems with carbon preference index (CPI) values usually ranging from 2.9 (Erba Deep) to 8.6 (southern Atlantis II Deep) and attest to the thermal immaturity of the sedimentary organic matter. Sediments of the northern Atlantis II Deep show particular low CPI values of 1.6, evidencing a higher thermal maturity of the organic matter. This agrees with the presence of an unresolved complex mixture (UCM), consisting of cyclic and branched hydrocarbons, which is typical for sediments impregnated by petroleum of hydrothermal origin. Similar impregnations have been reported from other Red Sea deeps (Michaelis et al. 1990).

Hop-17(21)-ene (1) and neohop-13(18)-ene (3) together with hopenes of unknown structure and homohopanes in their biological 17 β (H),21 β (H) configuration comprise the most dominant components observed in the m/z 191 traces. With increasing maturity the 17 β (H),21 β (H) configuration is gradually changed into the geological more stable 17 β (H),21 α (H)- or 17 α (H),21 β (H) configurations (Peters et al. 2007).

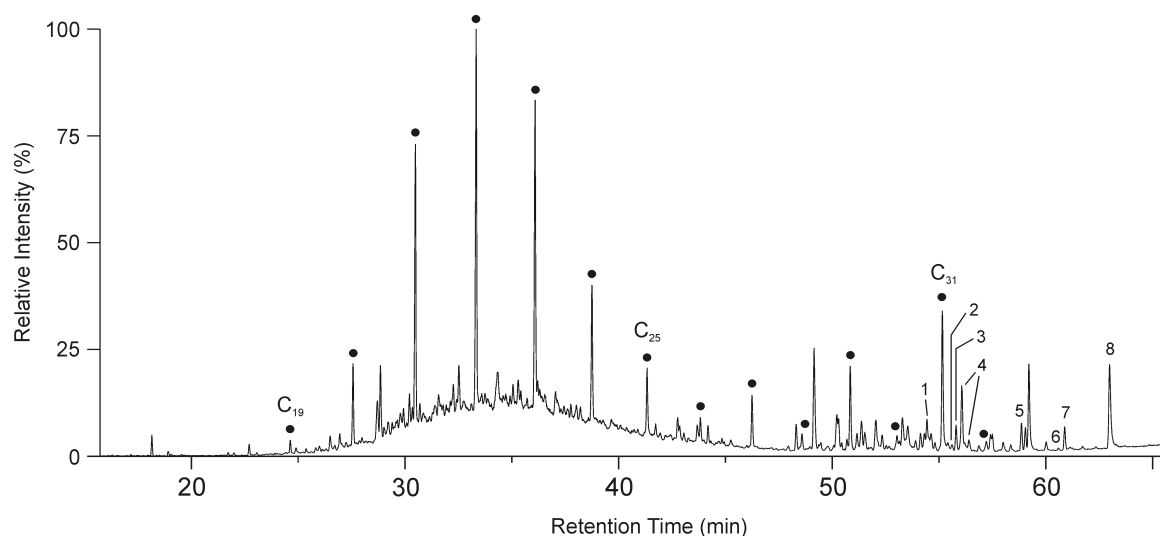


Figure A-4.8.1: Partial gas chromatogram of the apolar fraction from core top sediments of the Suakin Deep. *n*-Alkanes are indicated by black dots with the carbon number given for selected compounds. Identification of peaks marked by numbers is given in Table 3

Table A-4.8.3: Compounds identified in the apolar fraction of the Suakin Deep. Numbers refer to compounds displayed in Figure A-4.8.2.

1.	hop-17(21)-ene	2.	C ₃₀ αβ-hopane
3.	neohop-13(18)-ene	4.	unknown hopene structure
5.	hop-22(29)-ene (diploptene)	6.	homohop-30-ene
7.	17β(H)-21β(H)-homohopane	8.	lycopane

We observed the presence of the C₃₀αβ-hopane in only low concentrations in sediments of all Red Sea deeps. This component may derive from the thermal overprinting of freshly deposited hopanoids or from the impregnation of the organic matter with fossil hydrocarbons. Because the abundance of the C₃₀αβ-hopane is only low and other components of a higher thermal maturity are lacking, we suggest that this component derived from the thermal overprinting of the freshly deposited hopanoid structures. The dominance of hopenes in the investigated brine sediments is in agreement with the previously reported distribution of hopanoids in sediments of the Kebrit Deep (Michaelis et al. 1990) and provides additional evidence for the thermal immaturity of the preserved organic matter. In addition, the dominance of these components in the sediments of the Port Sudan Deep and the Suakin Deep suggest that aerobic bacteria are a significant source of the sedimentary organic matter.

Glycerol dialkyl glycerol tetraethers

The TEX₈₆ (TetraEther index of GDGTs with 86 carbons) proxy is commonly used to reconstruct past sea surface temperatures (SST) in marine settings (Menzel et al. 2006; Jenkyns et al. 2012). It is based on changes in the cell membrane lipid composition of marine planktonic Crenarchaeota that raise the number of cyclopentane moieties in the GDGT structure with increasing temperature (Schouten et al. 2002). Previous applications of the Tex₈₆ palaeothermometer on sediments of the Red Sea have shown that there is no simple linear relationship with SST as observed for other oceanic regions (Kim et al. 2008). Consequently, Tex₈₆ values significantly deviate from the global core top calibration and overestimate SST in the Red Sea (Kim et al. 2010). It was speculated that the Red Sea harbours an endemic population of marine Crenarchaeota that is adapted to the high salinity environment and evolved unique physiological responses to temperature changes (Trommer et al. 2009). The same authors established a regional calibration for the Tex₈₆ palaeothermometer to determine SST of the Red Sea that was used in the present study.

Isoprenoidal and branched glycerol dialkyl glycerol tetraethers (GDGTs) were present in similar distributions in the investigated core top sediments. A representative HPLC chromatogram showing the distribution of GDGTs in the northern Atlantis II Deep is shown in Fig. A-4.8.2. Tex₈₆ values of core top sediments recovered from the various Red Sea deeps ranged from 0.79 to 0.91, which is similar to those reported for other sediments of the Red Sea (Trommer et al. 2009). The Tex₈₆-derived water temperature ranged from 25.02°C in the Erba Deep to 28.51 °C in the Atlantis II Deep. These values show a strong positive correlation with measured sea surface temperatures, suggesting

that GDGTs accumulating in the Red Sea deeps are derived from mesophilic Crenarchaeota thriving in the upper water column and are not produced within the brine systems.

BIT values range from 0.03 to 0.19 with the latter being present in the northern Atlantis II Deep. Similar low values have been reported from oceanic regions without a significant supply of soil organic matter such as the Arabian Sea (Hopmans et al. 2004) and agree well with the lack of significant riverine discharge into the Red Sea. The comparatively high BIT values of the Atlantis II Deep agree well with the concomitant dominance of long-chain *n*-alkanes and suggest a higher loading of terrestrial-derived organic matter to the Atlantis II Deep.

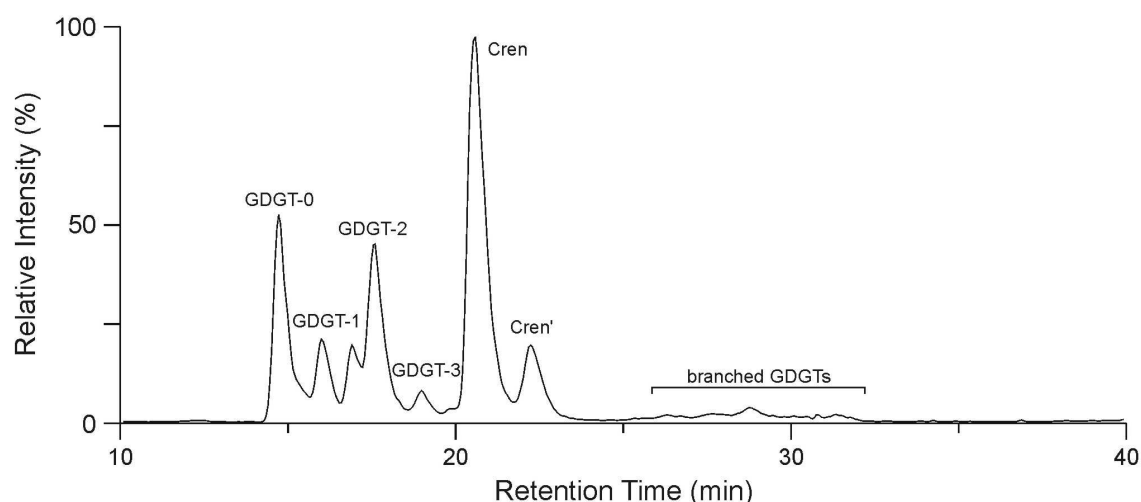


Figure A-4.8.2: HPLC/MS mass chromatogram showing the distribution of isoprenoidal and branched GDGTs in core top sediments (0-5 cm) collected from the northern part of the Atlantis II Deep. Numbers of the isoprenoidal GDGT refer to the number of pento rings in the GDGT structure.

References

- Altherr, R., Henjes-Kunst, F., Puchelt, H., Baumann, A. (1988) Volcanic activity in the Red Sea axial trough – evidence for a large mantle diapir? *Tectonophysics* 150, 121-133.
- Antunes, A., Franca, L., Rainey, F.A., Huber, R., Nobre, M.F., Edwards, K.J., da Costa, M.S. (2007) *Marinobacter salsuginis* sp. nov., isolated from the brine-seawater interface of the Shaban Deep, Red Sea. *International Journal of Systematic and Evolutionary Microbiology* 57: 1035-1040.
- Bonatti, E. (1985) Punctiform initiation of seafloor spreading in the Red Sea during transition from a continental to an oceanic rift. *Nature* 316: 33-37.
- Botz, R., Schmidt, M., Kus, J., Ostertag-Hennin, C., Ehrhardt, A., Olgun, N., Garbe-Schönberg, D., Scholten, J. (2011) Carbonate recrystallisation and organic matter maturation in heat-affected sediments from the Shaban Deep, Red Sea. *Chemical Geology* 280: 126-143.
- Craig, H. (1969) Geochemistry and origin of the Red Sea brines. In: Degens, E.T., Ross, D.A. (Eds.) *Hot brines and recent heavy metal deposits in the Red Sea*, pp. 208-242, Springer-Verlag.

- Eder, W., Jahnke, L.L., Schmidt, M., Huber, R. (2001) Microbial Diversity of the brine-seawater interface of the Kebrit Deep, Red Sea, studied via 16S rRNA gene sequences and cultivation methods. *Applied and Environmental Microbiology* 67: 3077-3085.
- Eglinton, G., Hamilton, R.J. (1967) Leaf epicuticular waxes. *Science* 156: 1322-1335.
- Jenkyns, H.C., Schouten-Huibers, L., Schouten, S., Sinninghe Damsté, J.S. (2012) Warm middle Jurassic-early Cretaceous high-latitude sea-surface temperatures from the Southern Ocean. *Climate of the Past* 8: 215-226.
- Kim, J.H., Schouten, S., Hopmans, E.C., Donner, B., Sinninghe Damsté, J.S. (2008) Global sediment core-top calibration of the TEX₈₆ paleothermometer in the ocean. *Geochimica et Cosmochimica Acta* 72: 1154-1173.
- Kim, J.H., van der Meer, J., Schouten, S., Helmke, P., Willmott, V., Sangiorgi, F., Koc, N., Hopmans, E.C., Sinninghe Damsté, J.S. (2010) New indices and calibrations derived from the distribution of crenarchaeal isoprenoid tetraether lipids: Implications for past sea surface temperature reconstructions. *Geochimica et Cosmochimica Acta* 74: 4639-4654.
- Martinez, F., Cochran, J.R. (1988) Structure and tectonics of the northern Red Sea: catching a continental margin between rifting and drifting. *Tectonophysics* 150: 1-32.
- Menzel, D., Hopmans, E.C., Schouten, S., Sinninghe Damsté, J.S. (2006) Membrane tetraether lipids of planktonic Crenarchaeota in Pliocene sapropels of the eastern Mediterranean Sea. *Palaeogeography, Palaeoclimatology, Palaeoecology* 239: 1-15.
- Meyers, P.A. (1997) Organic geochemical proxies of paleoceanographic, paleolimnologic, and paleoclimatic processes. *Organic Geochemistry* 27: 213-250
- Michaelis, W., Jenisch, A., Richnow, H.H. (1990) Hydrothermal petroleum generation in Red Sea sediments from the Kebrit and Shaban Deeps. *Appl. Geochemistry* 5: 103-114.
- Peters, K.E., Walters, C.C., Moldowan, J.M. (2007) *The biomarker guide*. 1155 p., Cambridge University Press, Cambridge.
- Schouten, S., Hopmans, E.C., Schefuß, E., Sinninghe Damsté, J.S. (2002) Distributional variations in marine crenarchaeotal membrane lipids: a new tool for reconstructing ancient sea water temperatures? *Earth and Planetary Science Letters* 204: 265-274.
- Siam, R., Mustafa, G.A., Sharaf, H., Moustafa, A., Ramadan, A.R., Antunes, A., Bajic, V.B., Stingl, U., Marsis N.G.R., Coolen, M.J.L., Sogin, M., Ferreira, A.J.S., El Dorry, H. (2012) Unique prokaryotic consortia in geochemically distinct sediments from the Red Sea Atlantis II and Discovery Deep brine pools. *Plos one* 7: 1-10.
- Simoneit, B.R.T., Grimalt, J.O., Hayes, J.M., Hartmann, H. (1987) Low temperature hydrothermal maturation of organic matter in sediments from the Atlantis II Deep, Red Sea. *Geochimica et Cosmochimica Acta* 51: 879-894.
- Swift, S.A., Bower, A.S., Schmitt, R.W. (2012) Vertical, horizontal, and temporal changes in temperature in the Atlantis II and Discovery hot brine pools, Red Sea. *Deep-Sea Research I* 64: 118-128.
- Trommer, G., Siccha, M., van der Meer, M.T.J., Schouten, S., Sinninghe Damsté, J.S., Schulz, H., Hemleben, C., Kucera, M. (2009) Distribution of Crenarchaeota tetraether membrane lipids in surface sediments from the Red Sea. *Organic Geochemistry* 40: 724-731.

4.8 Microbiological sampling

Mamdoh T Jamal

4.8.1 Introduction

Many studies have been seeking to discover natural microbiological life in the deep sea. It was previously expected that there was no life in depths of more than 600 m (Austin, 1988). This opinion was changed when some strains of bacteria were isolated from the sea by different researchers using different techniques, i.e. different cultivation methods, medium compositions, growth temperatures, pressure tolerances, and many other techniques (Austin, 1988).

The necessity and the lack of such studies become clear in view of their importance and benefits, i.e. uses of deep sea microbiological life as an indicator of certain conditions in different fields, for example the existence of natural gas and oil.

This study will focus on different goals like using new techniques and a variety of medium compositions to classify culturable bacteria. The resulting information will be used as a biological indicator for gases. On the other hand, bacteria could be important to be used as antimicrobial producing sources against human, animal and plant diseases if studied by using new cultivation methods (Yan, 2005; Jamal et al.; 2006).

4.8.2 Methods

In order to determine and survey the microbial life in sediments and water of the Red Sea deeps from some selected sites (i.e. Atlantis II, Port Sudan, Erba, Albatros, Suakin, Hatiba) and to detect the functions of the isolated bacteria and their relations to hydrocarbons in the sediment/ brine and brine/ seawater interfaces, 160 bacterial colonies from all the deeps separately were isolated to be studied.

On the other hand, this study focuses on discovery of a novel antimicrobial agent against some human bacterial pathogens.

Water sampling

As described in chapter A-4.4.1, water samples were taken by two different types of water sampling rosettes equipped with Niskin-bottles and CTD (Fig. A-4.4.2). 160 bacterial isolates from the different water, brine (and sediment) samples as summarized in table A-4.8.1 will be studied.

Moreover, additional brine samples were sampled into one liter Schott glass bottles for further microbiological investigations at GEOMAR (Tab. A-4.8.2).

Table A-4.8.1.: Samples and station data of microbial isolates.

Count of isolates	Station	Site	Longitude	Latitude
19	24	Hatiba Deep	37° 59.768'E	22°18.559'N
46	28	Atlantis II	38° 04.755'E	21° 20.565'N
19	39	Erba Deep	38° 02.471'E	20° 48.042'N
27	48	Port Sudan Deep	38° 30.639'E	20° 04.303'N
21	54	Suakin Deep	38° 43.169'E	19° 36.722'N
28	63	Pockmark area	39° 24.603'E	19° 57.748'N

Table A-4.8.2: Station data of brine samples for microbiological studies at GEOMAR.

Longitude	Latitude	Salinity	Temperature	Depth	Deep	Niskin No.	Station	Sample ID
38° 04.755'E	21°20.565'N	267.80	68.02	2191	Atlantis II	10	28	28/10
38° 04.755'E	21°20.565'N	267.80	67.90	2241	Atlantis II	11	28	28/11
38° 04.739'E	21°20.612'N	116.00	51.80	2021	Atlantis II	10	31	31/10
38° 04.739'E	21°20.612'N	94.70	46.20	2007	Atlantis II	11	31	31/11
38° 06.935'E	21°11.904'N	227.04	23.85	2174	Albatross	2	35	35/2
38° 02.471'E	20°48.042'N	162	26.70	2418	Erba	3	39	39/3
38° 30.639'E	20°04.303'N	211.75	35.80	2892	Port Sudan	2	48	48/2
38° 43.169'E	19°36.722'N	152.70	23.60	2864	Suakin	1	54	54/1
38° 05.603'E	21°20.249'N	----	48.80	2221	Atlantis II	1	69	69/1

Onboard cultivation and subsequent microbiological investigations

Gram staining and micromorphology

Overnight cultures were stained by the Gram staining method (Hucker and Conn, 1923) and examined with a Kyowa light microscope at x1000 magnification.

Catalase production

Drops of 5% (v/v) hydrogen peroxide were added to overnight cultures. The development of effervescence within 60 s was recorded as evidence of positivity.

Oxidase production

A piece of Whatman filter paper was saturated with 1% (w/v) N, N, N', N'-tetramethyl-*p*-phenylenediamine dihydrochloride (Sigma). A sterile wooden stick was used to transfer inoculum from overnight cultures, and a purple coloration, which developed within 30 s, was indicative as a positive result.

Identification by using 16s rRNA gene sequencing

- Extraction of DNA

A fresh 24-h culture in TSB, was harvested by centrifugation at 5000 x g for 10 min, the bacterial cells were lysed, and the DNA extracted using a DNeasy kit (Qiagen) following the protocol for isolation of total DNA from animal tissues.

- DNA amplification by PCR

A polymerase chain reaction (PCR) thermal cycler machine (Perkin Elmer) was used to amplify the DNA templates using universal primers, which amplified a 1500-bp region of 16s rRNA gene (9F: 5'-GAGTTTGATCCTGGCTCAG-3', 1492R: 5'-GGYTACCTTGTTAACGACTT-3') (Reysenbach *et al.*, 1994). The thermal cycling profile was as follows: 1 cycle of 95 °C for 5 min; 29 cycles consisting of 94 °C for 1 min, 36 °C for 1 min and 72 °C for 2 min; and a final cycle of 72 °C for 5 min.

- Sequencing of purified DNA

Sequencing was performed by the Wayne State Applied Genomics Technology Center for DNA sequencing. 16s rRNA gene sequencing was used to search for the nucleic acid sequence databases using the basic local alignment search tool (Blast) (Altschul *et al.*, 1990).

- Agarose gel electrophoresis

To amplify the DNA, agarose gel electrophoresis was carried out with a Bio-Rad mini cell. A mix of 1% (w/v) agarose (Integra Bio Science) dissolved in 200 ml of TAE buffer and 1.7 µl ethidium bromide (Sigma) was added to 0.5 µg/ml final concentration after heating in a microwave. Then, the gel was poured and a comb was positioned. After the gel had set, the comb was removed, and the samples and marker 1 kbp DNA Ladder (MBI Fermentas) were used to provide 11 and 14 discrete fragments (in base pairs 10000, 8000, 600, 5000, 4000, 3500, 3000, 2500, 2000, 1500, 1000, 750, 500 and 250) which were added to the different wells in 2-µl quantities. After mixing the sample or the marker with 6x gel loading buffer (Fermentas) on a ParafilmTM, the gel was covered with enough TAE buffer to a depth of ~1 mm, and the electricity connected and run for 1 h at 100 volts. Then, the gel was visualised under a U.V Transilluminator (300 nm; UV Products). A band of 50 ng of DNA could be clearly visualised on the ethidium bromide stained gel. Photographs were taken with Polaroid 665 film through a red filter (Wrattan) using a Polaroid MP-4 Land camera.

Screening the bacterial cultures for the presence of antimicrobial activity

- Primary screening for isolates producing antimicrobial compounds

Antimicrobial activity was assessed by the cross-streaking method (Fig. A-4.8.1) using marine 2216E agar, TNA, DST and the equi-mixture of marine 2216E agar and TSA against a range of Gram-positive and Gram-negative bacteria, i.e. methicillin resistant *S. aureus* (MRSA) 9551 and MRSA J2407 (supplied by Professor S.G.B. Amyes, University of Edinburgh), vancomycin resistant enterococci (VRE) 788 and VRE 1349 (supplied by Professor S.G.B. Amyes), *L. monocytogenes* (NCTC [National Collection of Type Cultures, Colindale, London] 10357 and NCTC 7973), *E. coli* (laboratory culture), *P. aeruginosa* (laboratory culture) and *Salmonella enteritidis* (laboratory culture). Briefly, the environmental cultures were streaked at right angles across lines of inocula of the named deep sea isolates with incubation at room temperature for up to 7 days.

Interruption in the growth of the named deep sea isolates was used as an indication of the presence of antimicrobial compounds. A second method involved use of sterilized (121°C/15 min) 6-mm diameter filter paper discs (Whatman) that were seeded with a fresh culture and inoculated onto lawns of the named Gram deep sea isolate cultures with incubation at room temperature for up to 7 days. A clear zone around the discs was interpreted as evidence for the production of antimicrobial compounds.

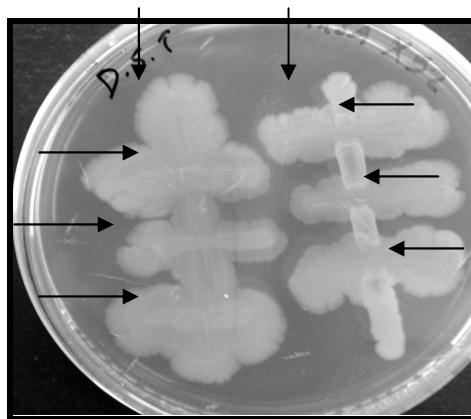


Fig. A-4.8.1: Inhibitory activity by using Cross-streaking method against Human pathogens (MRSA)

- Secondary screening of bacterial isolates which produced antimicrobial compounds

The environmental cultures were inoculated into 10-ml volumes of tryptone soya broth (TSB; Oxoid) supplemented with 1% (w/v) NaCl (= TNB) in universal bottles, and incubated on a rotary shaker at 200 rpm and 28°C for three days. The cultures were then centrifuged at 2500 rpm at 4°C for 15 minutes, and the supernatant filtered through 0.22-µm pore size porosity filters (Millipore) before being transferred to dialysis tubing of different molecular cut-off (3500, 7000, 20000 Da), and washed in three changes of distilled water over 24 h at 4°C. The supernatants were re-filtered through 0.22-µm filters before the antimicrobial activity was assessed using the paper disc method (Mearns-Spragg *et al.*, 1998). Briefly, sterile (121°C/15 min) 6-mm diameter filter paper discs were saturated with the supernatant and left to air dry. The process was then repeated until 90 µl of the supernatant had been applied to each disc. These discs were then applied to freshly prepared lawns of the named Gram-positive and Gram-negative pathogenic bacterial cultures with incubation at 37°C for 24 hours, whereupon the presence or absence and size of any zone of clearing were recorded (Fig. A-4.8.2).

Cultures were inoculated into 5-ml volumes of marine 2216E Broth (Difco) in universal bottles and incubated on a rotary shaker at 200 rpm and 28°C for 5 days. A 1.5 ml volume from each culture was then transferred aseptically to sterile (121°C/15 min) Eppendorf tubes, and centrifuged at 13,000 rpm for 10 minutes at room temperature. The antimicrobial activity of the extract was assessed using 6-mm filter paper discs and freshly seeded lawns, as before.

Finally, if any isolates confirm a significant inhibitory activity, the compound isolation and purification protocol will be used.



Figure A-4.8.2: Inhibitory activity by using well diffusion method from deeps bacterial supernatant against Human pathogens (MRSA, VRE)

Outlook

Of the bacterial organisms isolated from Atlantis II during the 2011 Poseidon cruise, many were identified as “hydrocarbon bacteria” (i.e. *Exiguobacterium* sp , *Marinobacter hydrocarbonoclasticus*), which showed that the bacteria in the deeps could be used as an indicator for hydrocarbon-rich fluid seepage and secondary degradation activities. In this study, more efforts focusing on the survey of microbial life in Red Sea deeps will yield more results by using advanced cultivation methods. Furthermore, 20 % of 160 isolates from the Red Sea deeps were found to be associated with inhibitory activity against two severe pathogens, i.e. MRSA and VRE.

References

- Altschul, S. F., Gish, W., Miller, W., Myers, E.W. and Lipman, D.J. (1990). Basic Local Alignment Search Tool. *J. Mol. Biol.* 215, 403-410.
- Austin, B. (1988). *Marine Microbiology*. Cambridge: Cambridge University Press.
- Hucker, G. J. and Conn, H. J. (1923). *Method of Gram Staining*: N.Y. St. Agric. Exp. Stn. Tech. Bull. No. 93.
- Mamdoh T. Jamal, Peter C. Morris, Rasmus Hansen, Derek J. Jamieson, J. Grant Burgess, Brian Austin (2006). Recovery and Characterization of a 30.7-kDa Protein from *Bacillus licheniformis* Associated with Inhibitory Activity Against Methicillin-Resistant *Staphylococcus aureus*, Vancomycin-Resistant Enterococci, and *Listeria monocytogenes*. *Marine Biotechnology*. 8, 587–592
- Mearns-Spragg, A., Bregu, M., and Boyd, K.G. and Burgess, J.G. (1998). Cross-species induction and enhancement of antimicrobial activity produced by epibiotic bacteria from marine algae and invertebrates, after exposure to terrestrial bacteria. *Appl. Microbiol.* 27, 142-146.
- Reysenbach, A. L., Wickham, G. and Pace, N. (1994). Phylogenetic analysis of the hyperthermophilic pink filament community in Octopus Spring, Yellowstone National Park. *Appl. Environ. Microbiol.* 60, 2113–2119.
- Yan, L., Boyd, K.G. and Burgess, J.G. (2002). The effect of a roller bottle tidal simulation cultivation method on the production of antimicrobial compounds by marine epibiotic bacteria. *Mar. Biotechnol.* 4, 356-366.

5. Acknowledgements

All scientists who participated in the cruise acknowledge the professional and friendly support by the RV PELAGIA crew and the NIOZ support team (thank you for the 19°). We also highly acknowledge the support by Saudi and Sudanese authorities during the work permission process.

RV PELAGIA cruise No. 64PE351

Dates, Ports: 6 April 2012, Jeddah, – 22 April 2012, Duba

Chief Scientists: Prof. Ali Al-Aidaros, KAU, Jeddah, Dr. Benjamin Kürten, GEOMAR, Kiel

Number of Scientists: 20

Project: The Jeddah Transect

1. Abstract

In the framework of the joint Saudi Arabian – German project “The Jeddah Transect” in the Red Sea, RV PELAGIA cruise 64PE351 focused on sampling and monitoring plankton diversity and trophic structure of the pelagic food web along a north-south transect and covered seven main sampling sites between the northern Red Sea (26°57'N, 35°05'E) and the Farasan Archipelago (16°28'N, 40°54'E). This transect corresponds to a natural nutrient gradient of low-nutrient water in the North and higher-nutrient water in the South. The scientific program was successfully accomplished by a sampling program for Red Sea nutrient dynamics, plankton and isotope composition. Further objectives of the cruise were to deploy a mooring and a met-Ocean buoy, continue high-resolution mapping of the Red Sea bathymetry, collect volcanic material at selected sites in the northern and southern Red Sea, and to facilitate the collection of mesophotic corals using the research submersible JAGO.

2. Cruise narrative

On the evening of Thursday, 5 April 2012, a group of 20 researchers, technicians and students from King Abdulaziz University (KAU Jeddah), the Helmholtz Centre for Ocean Research Kiel | GEOMAR, and Christian-Albrechts-University (Kiel) (see chapter B-3) embarked on RV PELAGIA (NIOZ, The Netherlands) at Jeddah Islamic Port, Kingdom of Saudi Arabia, for the second leg to the Red Sea. The nautical crew (see chapter B-3) welcomed the researchers aboard. Well past midnight, researchers of Project 4, together with a technician from the manufacturer of the Met-Ocean buoy, finished the assembly and installation of sensors on the buoy, tested the sensors' functionality, and established satellite communication. RV PELAGIA cruise 64PE251 started as scheduled at 8:40 in the morning of 6 April (in the following, all times are given as ship time = UTC+3 h) and the ship headed to the mooring site of the ‘wave rider’ for Project 4. Prior to the deployment, seafloor topography was mapped using the ship's multi-beam echo sounder. After successful deployment of the mooring weights, the ship sailed to the second mooring site. Prior to deployment of the Met-Ocean buoy at the southern Eliza Shoals Reef, Jeddah, the topography was mapped in order to decide for a safe mooring site. The successful deployment was completed at 13:45, and the southbound transit to the first sampling site in the Southern Red Sea started. During the passage, equipment and gear were set up for an instantaneous start of sample collection after the arrival at the first sampling site. In the early morning of 7 April 2012, RV PELAGIA reached the meeting point with the Royal Saudi Arabian Navy warship *Al-Riyadh*, which had been arranged and called for anti-piracy protection. Both vessels continued the track southwards without any delay.

On Sunday, 8 April 2012, RV PELAGIA reached the first of seven biological sampling sites, situated along the south-to-north oriented transect. Sampling sites for the collection of plankton and water for researchers of TP3 and TP4 during cruise 64PE351 on RV PELAGIA were located along the central rift axis of the Red Sea at almost equidistant positions. The collection at the seven sites followed the S-N oriented natural nutrient gradient featured by the Red Sea. The first offshore site, Farasan West, was located westwards of the Farasan Archipelago in the center of the inflow region from the Indian Ocean into the Red Sea.

Here, researchers of Project 3 and 4 started their 24-hour sampling scheme at 6:25. The 24-hour sampling scheme included an extensive collection of water and plankton samples and included several CTD casts for water sampling, RAMSES light measurements, 3 types of plankton nets (Apstein, IOS, WP2), and oblique collections of mesozooplankton using a multinet for vertical distribution. CTD casts collected water from ecologically relevant sites.

Mineralization and respiration were assessed in experiments, which exposed water samples from discrete depth to light in incubators on deck for 24 hours. Weather permitting, this sampling scheme was subsequently repeated at all main sampling sites along the central Red Sea axis with little changes which only concerned the temporal order of gear deployments and cast depth.

After station work was completed in the early morning hours, the transit to the inner Farasan Archipelago began, where the manned research submersible JAGO was deployed. As the topography of the proposed dive site was unclear and available chart material appeared inaccurate, bathymetric maps were created by multi-beam mapping to allow more detailed planning of the JAGO dive. JAGO-Dive 1181 explored the southern side of Ad Dissan Island, characterized by a gradually rising slope that was covered mainly with soft sediment, and showed low diversity and abundance of benthic organisms. Sessile epibenthic macrofauna was mostly restricted to sponges, and few hard and soft corals. Some corals were collected, but the prioritized scleractinian genus *Leptoseris* sp. was absent. Collection of water from the dive site for on-deck incubations by CTD rounded up the JAGO activities at this site. Weather conditions prohibited the exploration of a second dive site at the Farasan Archipelago.

To improve the understanding of ecohydrodynamics in the inflow region north of Bab-al-Mandab, an East-West transect was sampled from the shallows of the southern Farasan Archipelago towards the deep waters at the border of Saudi Arabia with Eritrea. ADCP measurements for currents and particle distribution over depth during the E-W passage, supported by CTD profiling/ water sampling and the collection of one phytoplankton and one zooplankton net tow for biodiversity assessments at the three sites, started in the evening of 9 April. Currents of the upper water layers and water movements at lower depths could be distinguished both in magnitude and direction by ADCP (preliminary results). Information from CTD casts, such as salinity and temperature, clearly indicated the inflow of water masses from the Indian Ocean, with increased fluorescence at a depth of approx. 45 m. Information on plankton diversity and nutrients will be linked with this data.

In the morning of the 10 April, RV PELAGIA left the southern area and headed northwards following the central rift axis towards the next sampling site, the Red Sea

Rift. Shortly after leaving this site, researchers of Project 2 used a deep digging dredge to collect basaltic rock material at 16°47'N. The collection of plankton and water samples commenced at the Red Sea Rift at 23:00 the same day and continued until 2:08 on 11 April after the multinet had been heaved on deck. Additionally, another dredge was used to collect rock material during the night, but it got stuck. After successful retrieval of the dredge, only sediment could be collected from the gear.

According to schedule, the ship arrived at the Suakin deep on 12 April at 16:11, and at the Atlantis II deep on 14 April at 5:48, to facilitate repetitive collection of water and plankton for around 24 h at each site.

With the bathymetric knowledge obtained on the Atlantis II deep by TP2, on 15 April it was attempted to sample the zooplankton community above the brine layer in the western basin. Unfortunately, the collection was not successful, as the nets got tangled and blocked the entrance area of the multinet. Due to time constraints, the collection was not repeated and RV PELAGIA left the site to head towards the Nereus deep, where station work commenced in the early morning hours on 16 April. The routine collections were only slightly interrupted in the morning due to a torn net bag of the IOS net, which nevertheless could easily be replaced so that the station could be repeated later that day. On 16 April before midnight, TP2 researchers successfully collected a dredge full of carbonate rock, basaltic rock and also carbonate crusts at the steep eastern flank of the Nereus deep.

During the transit to the next site, the Mabahiss deep, RV PELAGIA sailed into poor weather on 17 April, with northeasterly winds at force 8. To the relief of some cruise participants, the sea state eased off a few hours after arrival at the Mabahiss deep, and most researchers were able to get back to their work on 18 April.

The weather forecast, however, again indicated increasing winds for the upcoming days. As such conditions would have endangered the JAGO deployment at the northernmost dive site close to Al-Wajh, the routine plankton and water collections were interrupted after lunch time by request of the JAGO team, and the ship headed inshore towards the outer reefs of Al-Wajh. After 4 hours of transit and additional multibeam mapping, JAGO was deployed at Al-Wajh on 18 April and was used to collect numerous *Leptoseris* sp. corals from a huge reef boulder densely colonized by gorgonians and encrusting red algae at depths between 95 and 77 m. During the dive, a RED One digital cinema camera and hemispheric fisheye lens recorded photographic data that will be used to create three-dimensional models of the reef slopes and form a basis for habitat mapping and biodiversity studies in correlation to the rugosity of the reef. At dusk, JAGO was recovered and incubation of corals for ecophysiological measurements started immediately after water had been collected from the dive site using the CTD sampler.

In order to complete the plankton and water collection at the Mabahiss deep, the ship then sailed back in the direction of the original site. During this transit, Project 4 used the multibeam echosounder for extensive multibeam mapping. In the early morning of 19 April a deep digging dredge was deployed at the southern flank of a caldera-type volcano, described as Mabahiss Mons. Here, sheet lava, and lobate basalt were successfully recovered from the dredge. In the afternoon, plankton and water collection were finished and the transit to the northernmost site of RV PELAGIA cruise 64PE351 began.

The ship reached the site at 8:30 in the next morning, on 20 April, and for the last time, a full program of water and plankton collection took place until 8:55 on 21 April. Before heading towards Duba, where the port call was scheduled for 6:00 on 22 April, multi-beam mapping of the Mabahiss area was continued for several hours. Although time would have been sufficient, the deployment of another dredge on the transit line towards Duba was denied by the military observer, due to a danger of cutting communication sea cables. The transit time was used to finish experimental work, zooplankton microscopy, water filtrations, and packing of equipment into transport boxes and containers. During the cruise all participants (see chapter 3) were healthy and in a good mood. Only one minor incidence of injury was reported related to a student cutting his finger while using a knife. In the morning of 22 April, at 6:00, RV PELAGIA arrived at the pilot station of the port of Duba, KSA, and by 11:00 the scientific participants and two NIOZ technicians of leg 64PE351 had disembarked.

3. Crew lists

64PE351 scientific crew			
No.	Name	Function, research area	Home country
1	Dr. Al-Aidaroos, Ali	Chief scientist, zooplankton	Saudi Arabia
2	Dr. Kürten, Benjamin	Co-chief scientist, biological-oceanography	Germany
4	Let. Co. Al-Dhwyhan, Ibrahim	Military observer	Saudi Arabia
5	Dr. Khomayis, Hisham	Scientist, phytoplankton	Saudi Arabia
3	Dr. El-Sherbini, Mohsen	Scientist, zooplankton taxonomy	Saudi Arabia
6	Dr. Augustin, Nico	Scientist, bathymetry, geology	Germany
7	MSc. Kwasnitschka, Tom	Ph.D. candidate, video imaging	Germany
8	MSc. van der Zwan, Froukje	Ph.D. candidate, petrology, geology	The Netherlands
9	MSc. Bruss, Gerd	Ph.D. candidate, ADCP	Germany
10	MSc. Pena Garcia, David	Ph.D. candidate, nitrogen cycling	Colombia
11	Dr. Al-Sofyani, Abdulmohsin	Scientist, coral reef ecology	Saudi Arabia
12	Dr. Sawall, Yvonne	Scientist, coral ecophysiology	Germany
13	Dr. Hissmann, Karen	JAGO team	Germany
14	Schauer, Jürgen	JAGO team	Germany
15	Al-Kanbashi, Radi	Technician	Saudi Arabia
16	Audritz, Saskia	Technician	Germany
17	MSc. Devassy, Reny	Technician, phyto- and zooplankton	India
18	Al-Haj, Ahmed	Student	Jemen
19	Al-Nuwairah, Muaadh	Student	Jemen
20	Sas, Ahmed	Student	Jemen

64PE351 nautical crew			
No.	Name	Function	Home country
1	J.C. Ellen	Master	The Netherlands
2	J. van Haaren	Chief officer	The Netherlands
4	N.L.A. Rombout	2nd officer	The Netherlands
5	C.T. Stevens	Boatswain	The Netherlands
3	J. Seepma	Chief engineer	The Netherlands
6	M.D.M. de Kleine	2nd engineer	The Netherlands
7	I. den Breejen	Cook	The Netherlands
8	R. van der Heide	Ships technician	The Netherlands
9	J.A. Israël Vitoria	Deck hand	Portugal
10	M.J. de Vries	Deck hand	The Netherlands
11	Y. Witte	Technician	The Netherlands
12	M. Laan	Technician	The Netherlands



Fig. B-3.1 Scientific participants and nautical crew after successful completion of RV PELAGIA cruise 64PE351

4. List of stations

During the course of RV PELAGIA cruise 64PE251, 15 sampling sites were visited (Tab. B-4.1). For the biological-oceanographic sampling, seven sampling sites were selected along the central rift axis of the Red Sea (Fig. B-4.1). The southernmost and northernmost sites along the central rift axis were situated westwards of the Farasan Islands and southwest of Duba, respectively. The manned submersible JAGO was deployed in the southern Red Sea at the Farasan Archipelago (Fig. B-4.1, insert), and in the northern Red Sea at Al-Wajh, east of the Mabahiss deep. Starting in the shallow waters of the southern Farasan Archipelago, an East-West transect in the Indian Ocean inflow region was sampled for nutrient and plankton biodiversity and high-resolution ADCP data (Fig. B-4.1). A total of 164 activities were logged by the bridge (Tab. B-4.2).



Fig. B-4.1: Biological-oceanographic sampling sites along the central rift axis of the Red Sea. The insert shows the sampling sites included in the East-West transect from the shallows of the southern Farasan Archipelago towards the deep waters at the border of Saudi Arabia with Eritrea and the JAGO dive site at the Farasan Archipelago.

Table B-4.1: Consecutive station numbers as logged on bridge, positions and dates, for the 15 sampling sites of RV PELAGIA cruise 64PE351. EW0-2 refers to the East-West transect in the southern Red Sea.

Site	Lat [°N]	Long. [°E]	Date	Site name	Comments
1	21°27'24.59"	39°02'46.39"	6.4.	Jeddah	Wave rider mooring
2	21°39'15.01"	38°59'54.60"	6.4.	Jeddah	Met-Ocean buoy deployment
3	16°28'17.37"	40°54'50.63"	8.-9.4.	Farasan West	Full sampling site
4	16°53'30.26"	41°37'59.44"	9.4.	JAGO Farasan	
5	16°28'14.04"	41°40'29.56"	9.4.	EW0	Transect
6	16°28'15.32"	41°25'16.50"	9.4.	EW1	Transect
7	16°28'13.47"	41°10'07.90"	10.4.	EW2	Transect
8	16°28'17.37"	40°54'50.63"	10.4.	Farasan West	1 CTD, 1 WP2 150 µm net
9	16°46'54.80"	40°48'58.29"	10.4.	Dredge Farasan	
10	18°00'14.56"	40°07'08.57"	10.-11.4	Red Sea Rift	Full sampling site, dredge
11	19°36'29.15"	38°45'16.83"	12.-13.4	Suakin	Full sampling site
12	21°28'31.44"	38°01'00.66"	14.-15.4	Atlantis II	Full sampling site
13	23°13'50.42"	37°15'39.83"	16.4.	Nereus	Full sampling site, dredge
14	25°19'35.34"	36°09'23.85"	17.-19.4.	Mabahiss Al-Wajh	Full sampling site, dredge 1 JAGO dive
15	26°57'02.94"	35°05'24.97"	20.-21.4.	Duba	Full sampling site

Table B-4.2: Count of gear deployment per full sampling site for water and plankton collection. EW0-2 refers to the East-West transect in the southern Red Sea.

Site	Gear							
	Apstein	CTD	Dredge	IOS	Multinet	Ramses	WP2 - 150 µm	WP2 - 320 µm
Farasan West	2	4	1	2	1	2	10	1
EW0	1	1					1	
EW1	1	1					1	
EW2		1					1	
Red Sea Rift	2	2	1	3	2	2	10	2
Suakin	2	3		2	1	1	11	1
Atlantis II	2	2		2	2	3	10	2
Nereus	2	2	1	3		2	11	1
Mabahiss	2	2	1	2	1	full day	10	2
Duba	2	2		2	1	1	10	3

5. Individual reports of the Subprojects

5.1. Subproject 3.1

5.1.1. Nutrient gradients in the Red Sea - How do they correlate with plankton abundance and biodiversity

Benjamin Kürten, Ali Al-Aidaros, Hisham Khomayis, Ulrich Sommer

The ecosystem of the Red Sea features nutrient gradients at multiple temporal and spatial scales including a natural latitudinal and localized anthropogenic nutrient input – none of them well explored and some more expected than shown so far. To elucidate sources of nitrogen and potential responses of phytoplankton and zooplankton to different nutrient regimes, subproject 3.1 of the Jeddah Transect aims at exploring the effects of nutrient stoichiometry on plankton biodiversity and food web structure in the Red Sea. Primary producers, particularly phytoplankton, rapidly transform and incorporate inorganic elements into organic matter, causing biogeochemical changes including depletion of inorganic nutrients (N, P, Si), removal of CO₂, shifts in the isotopic composition (¹³C:¹²C, ¹⁵N:¹⁴N), changes in the composition of the suspended particulate organic matter (POM), and synthesis of lipids required for the reproduction and growth of heterotrophs, including bacteria, zooplankton and benthic consumers. Heterotrophic bacteria, Cyanophyceae, Bacillariophyceae and Dinophyceae are key pelagic functional groups with substantial influence on micro- and macronutrient fluxes, whereas zooplankton are the key link between primary producers and the herbivorous and microbial loop food web to higher trophic levels. The Red Sea is suited for the project because of its latitudinal, eutrophic-oligotrophic gradient (Acker et al. 2008) and because of its high functional diversity of zooplankton, from particle feeding microphageous Tunicata and Ostracoda to macrophageous Copepoda and predatory Amphipoda. It was also hypothesized that across the latitudinal gradient the importance of nitrogen derived from the utilization of aerosol nitrate by unicellular cyanobacteria as indicated by low $\delta^{15}\text{N}$ and its propagation onto higher trophic levels in the Gulf of Aqaba (Aberle et al. 2010) decreases towards the south, where the inflow of Indian Ocean water contributes nitrogen sources with higher $\delta^{15}\text{N}$. The study of plankton biodiversity uses taxonomic analysis via stereomicroscopes and complementary biogeochemical methods (flow cytometry, pigment fingerprinting, DNA barcoding), whereas trophodynamics are described by comparisons of natural abundances of carbon and nitrogen stable isotopes. These data are linked with biological oceanographic information and used to explain expected differences in food web structure and biodiversity. During cruise 64PE251 on RV PELAGIA an intensive sampling scheme was carried out at all seven sites (Tab. B-4.1) that included the collection of water and plankton samples.

Sample collection

The NIOZ general purpose CTD consists of a SBE9plus underwater unit, a SBE11plusV2 deck unit, a SBE32 carousel, a SBE3plus thermometer, a SBE4 conductivity sensor, a SBE5T underwater pump, a SBE43 dissolved oxygen sensor, a Chelsea Aquatracka MKIII fluorometer, a Wetlabs C-Star transmission meter (25 cm, deep, red), a Satlantic logarithmic PAR sensor for underwater PAR, and a Satlantic linear PAR sensor for deck reference. For water sampling 24 water samplers (12 l) manufactured by Ocean Test

Equipment were used.

At each site, one CTD cast was fixed in time to around 12:30 and measured the maximal PAR over depth when the sun crosses the meridian and is about at its highest elevation in the sky. Moreover, CTD casts were used to collect water from ecologically relevant depth, including the:

- Surface mixed layer (SML, 25 m)
- Deep chlorophyll maximum (DCM, 40-80 m)
- Below the fluorescence maximum (~100-120 m)
- Oxygen minimum zone (OMZ; 300-450 m)
- Mid-water (below OMZ; 600 m)
- Deep mid-water (900 m)
- Bottom (varying depth)

Preliminary observations from the CTD data indicated a decrease of depth of the DCM from approx. 40 m at the Farasan site in the south to approx. 80 m in the central Red Sea at the Atlantis II site. No change of depth of the DCM was observed towards the more northern sites.

On deck, seawater was tapped from the CTD/ water sampler for further treatment, e.g. filtrations, preservation and experimental works. Samples were collected for the determination of:

- Nutrients: NH_4^+ , NO_3^{2-} , NO_2^- , SiO_4^{3-} , PO_4^{3-} , Urea
- Total N and Total P
- DON, DOP
- DI^{13}C , alkalinity (carbonate chemistry)
- Respiration (O_2 , Winkler)
- Flow cytometry of nano- and picophytoplankton and bacteria
- EA-IRMS of particulate organic matter (POC, PN), $\delta^{13}\text{C}$ and $\delta^{15}\text{N}$
- Chlorophylls and accessory pigments
- Scanning electron microscopy of Coccolithophores (biogeography of *Emiliania* sp. and *Gephyrocapsa* sp.)
- Compound-specific stable isotope analysis of lipids

During the cruise plankton was collected vertically using three types of nets. The Apstein (20 μm mesh size; Fig. B-5.1.1) was used twice, at daytime, to collect net phytoplankton from a depth of 120 m to the surface for microscopic enumeration. Phytoplankton was preserved with Lugol's iodine and stored in the dark for microscopic enumeration. In total, 223 phytoplankton taxa were identified, 140 of which were related to the group Bacillariophyceae (diatoms) and 80 to the group Dinophyceae (dinoflagellates).

The Indian Ocean Net (IOS; 55 μm mesh size) was towed vertically from a depth of 1000 m to the surface twice at each sampling site, at daytime, for collection of micro-



Figure B-5.1.1: Apstein phytoplankton net with cowl (20 μm mesh size).

and mesozooplankton. Both samples were split for four analytical traits:

- Sample 1 a) biodiversity assessments of zooplankton (KAU, formalin preservation)
- Sample 1 b) biodiversity assessments of oncaeid Copepoda (Dr. R. Böttger-Schnack, formalin preservation)
- Sample 2 a) overall DNA barcoding, global biogeographic study of *Paracalanus* sp. (Dr. R. Böttger-Schnack, GEOMAR; Dr. A. Cornils, AWI, ethanol preservation)
- Sample 2 b) dot blot hybridization of plastid 16S rRNA gene amplicons (Dr. John Pearman, KAUST)

To assess biodiversity and zooplankton vertical migration pattern, a series of nets casts using the WP2 net (150 μ m mesh size) was collected at day and night from depths of 1000 m -, 800 m -, 500 m -, 300 m -, 200 m -, 100 m to the surface, respectively. These samples were preserved in formalin. One WP2 net (320 μ m mesh size) was deployed to a depth of 200 m to collect fresh zooplankton for life sorting and stable isotope analysis.

Zooplankton was also collected with a multinet-type MIDI plankton collector (5 net bags, 320 μ m mesh size, HydroBios, Germany) by oblique tows from a depth of 1000 m to the surface. Multinet casts were conducted at night (23:00-3:00 h) at six out of seven sites for biodiversity and included oblique 30-minute tows at 1.5 kn and five depth intervals (1000–800 m, 800–500 m, 500–300 m, 300–200 m and 100 m – surface). There is growing interest in animals and microbes subsisting above the brine layers that fill some of the Red Sea deeps. Hence, horizontal sampling of the zooplankton community above the brine layer at the Atlantis II deep was attempted using detailed multibeam bathymetric information from SP2 (Fig. B-5.1.2). Unfortunately, it was not overly successful. Only a few animals could be retrieved from the collectors. The cast could not be repeated because of the long time required for this type of operation, which would have spent too much of the time available for the remaining cruise. The casts above the

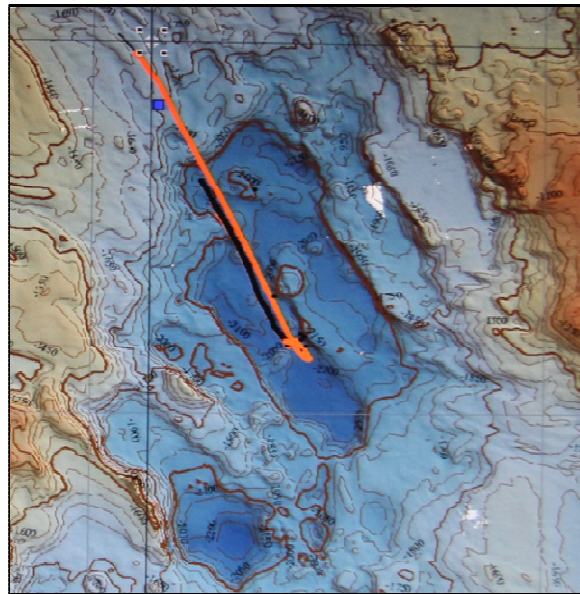


Figure B-5.1.2: Towing track of the multinet above the hot brine (1990 m depth) at the western basin of the Atlantis II deep.



Figure B-5.1.3: Chief-scientist Dr. Ali Al-Aidaros sorting life zooplankton for stable isotope analysis.

brine layer and as well as at the Nereus deep both failed because one of the nets became twisted, tangled and subsequently trapped at the opening of the net frame and thus blocked the entry. The reason for this can only be speculated on, and may be related to unsteady ship speed or deep water currents.

On-board sorting of zooplankton was conducted on life animals retrieved from the WP2 net and from the multinet casts. Animals were identified to the lowest practical taxonomic level, usually genus, sorted and placed in pre-weighed Sn capsules for later analysis of elemental composition and carbon and nitrogen stable isotope abundance. Sorting gave a preliminary overview of the diversity of species at each station. Overall, the zooplankton community was very diverse, consisting of many genera and species within a single genus. Copepods were particularly diverse. Stable isotope analysis (SIA) generates the key information to be linked with biological-oceanographic and nutrient stoichiometric information in order to explain patterns in trophodynamics.

For the analyses on trophodynamics approx. 450 isotope samples were isolated (Figure B-5.1.3), including 18 Copepoda genera (e.g. *Eucalanus* sp., *Pleuromamma* sp., *Candacia* sp., *Oncaea* sp., *Cosmocalanus* sp., *Candacia* sp. and *Macandrewella* sp.), 2 Ostracoda genera (*Cypridina* sp., *Conchoecia* sp.), Amphipoda, Mysida, Zoea and Megalopa stages of Decapoda (Anomura and Caridea), Cnidaria (Siphonophora), 5 Pteropoda genera (e.g. *Creseis acicula*, *Euclio pyramidata*), predatory Chaetognatha (*Sagitta* sp.) and small larvae of fish (Osteichthyes).

First results from SIA conducted after the cruise in Jeddah revealed increasing $\delta^{15}\text{N}$ signatures from the northern Red Sea (Duba, Mabahiss) towards the southern Red Sea (Farasan West; Fig. B-5.1.4). The data suggest that the source of nitrogen for the whole plankton community changes.

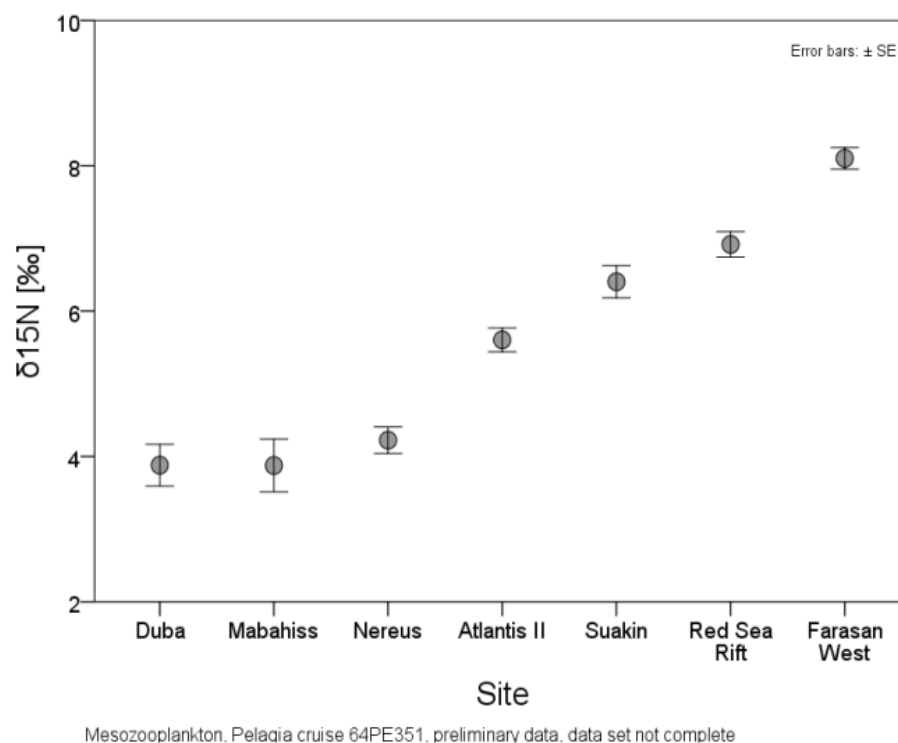


Figure B-5.1.4: Preliminary results from stable isotope analysis of nitrogen ($\delta^{15}\text{N}$) of mesozooplankton collected during RV PELAGIA cruise 64PE351.

To improve the understanding of ecohydrodynamics in the inflow region north of Bab-al-Mandab, SP3 and 4 collected samples along an East-West transect from the shallows of the southern Farasan Archipelago towards the deep waters at the border of Saudi Arabia with Eritrea where full plankton/ water sampling took place. ADCP measurements (SP4, see section 5.2.3) provided data on currents and particle distribution over depth during the E-W passage (Fig. B-4.1), supported by CTD profiling/ water sampling and collection of one phytoplankton net tow and one zooplankton net tow respectively for biodiversity assessments at the four sites (SP3). The upper water layer currents and water movements at lower depths could be distinguished both in magnitude and direction by ADCP (preliminary results). Whilst close to the Farasan Islands fluorescence, oxygen and salinity were homogenous over depth, CTD casts clearly indicated an inflow of water masses from the Indian Ocean at the other three transect sites and increased fluorescence at approx. 45 m depth (Fig. B-5.1.5).

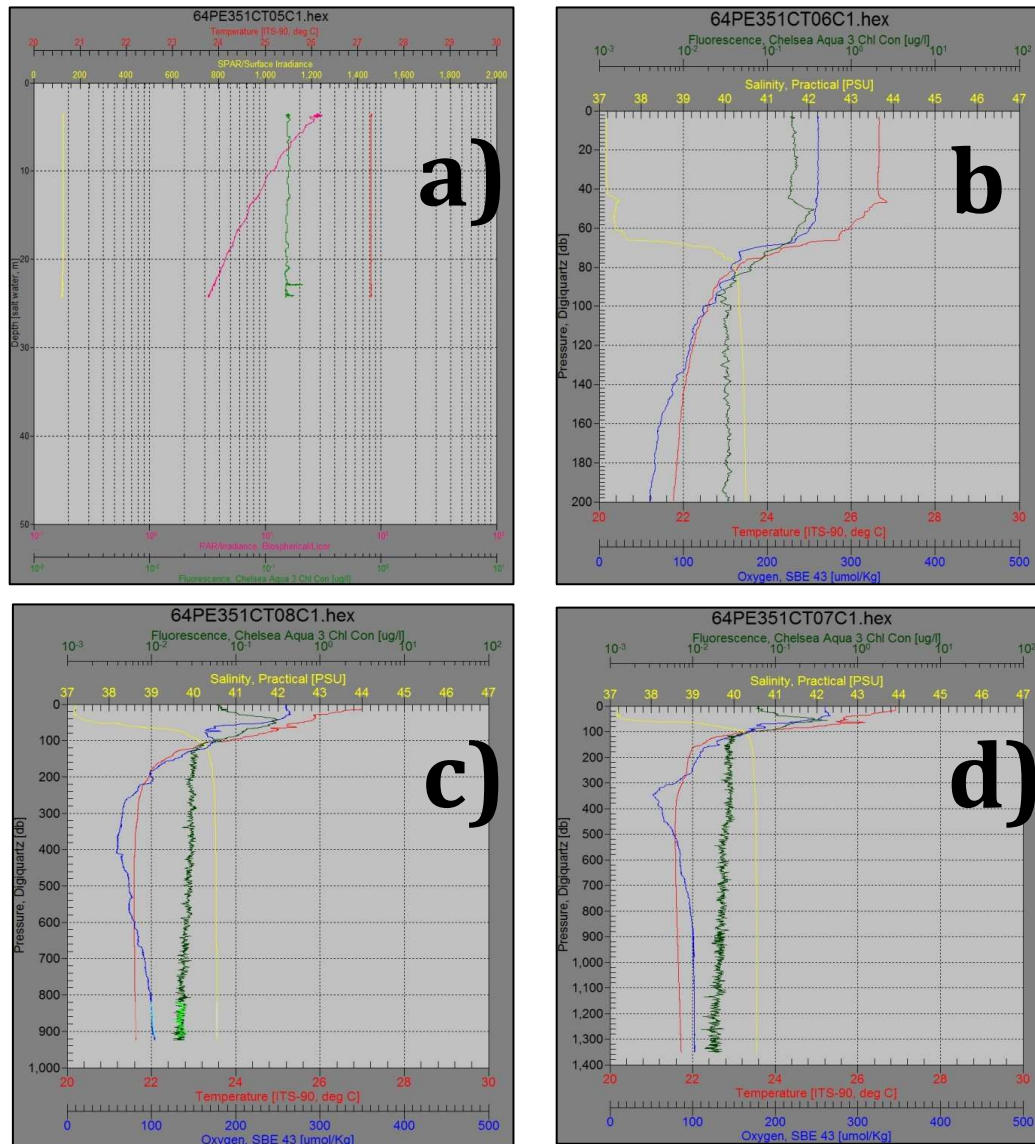


Figure B-5.1.5: CTD plots of the four East-West transect sites situated at (a) the shallow areas of the southern Farasan Archipelago, the transect sites (b) EW1 and (c) EW2, and Farasan West (d).

5.2. Subproject 4

David Pena, Gerd Bruss

Two members of subproject 4 (SP4), David Pena and Gerd Bruss, joined the second leg of RV PELAGIA cruise 64PE351. The main objectives were to deploy two survey buoys, to determine nutrient dynamics based on the analysis of water samples and several incubation experiments and to collect physical met-ocean data in terms of ADCP and light spectrum measurements.

5.2.1. Buoy deployments

At the beginning of leg 2 a mooring for a wave rider buoy and one larger buoy to collect met-ocean data (Fig. B-5.2.1) were deployed in the vicinity of Jeddah. Due to the highly structured seafloor topography in the shallow reef zones near Jeddah it was necessary to conduct pre-deployment surveys of the two mooring sites. For determination of the final release locations, a brief sea floor mapping was done by SP2 using the on-board multi-beam echo sounder. Based on this information the buoys were released at the following positions:

wave rider mooring @ N21.45683°, E39.04622° and 25m water depth

met-ocean buoy @ N21.65417°, E38.99850° and 51m water depth

SP2 also generated high-resolution topographic maps of the deployment sites. The maps will be used to improve the reproduction of the hydrodynamic conditions in the vicinity of the buoys with the HN modeling system developed in SP4.



Figure B-5.2.1: Deployment of the met-ocean buoy.

5.2.2. Nutrient dynamics

The main objectives of the nutrient dynamics sampling strategy were to improve the understanding of

- 1) the spatial distribution of nitrogen and phosphorus chemical species
- 2) their transformation in the uppermost layers of the Red Sea
- 3) the corresponding respiration rates

The strategy focused on the mineralization of the organic fraction of nutrients and the oxidation of ammonium.

To accomplish this objective, the following experimental design was carried out: For the spatial distribution of the nutrients, water samples were taken from six depths at all seven stations. The sampling depths were located at the surface (~25 m), the fluorescence maximum (~60-80 m), shortly below this layer (~120-150 m), and at depths of 300 m, 600 m and 900 m. The samples for the dissolved fraction were filtered instantaneously through a 0.2- μ m membrane and preserved with HgCl_2 (for DIN) or cooked with a digestion reagent (for DON). The preserved samples will be analyzed for total nitrogen, total phosphorus (TP, TN), ammonium, nitrite, nitrate (DIN), phosphate and dissolved organic nitrogen (DON) and phosphorus. To avoid redundant work, SP3 and SP4 agreed that nutrient analysis, which is required by both sub-projects, would mostly be performed at the FTZ. Comparative analysis of several duplicate samples will be done by SP3.

Experiments on the transformation of the nutrient chemical species due to nitrification and mineralization were carried out on samples of the three uppermost layers from five of the seven stations (3, 4, 5, 6 and 8). For the nitrification experiments, unfiltered water was poured into two 500-ml acid-washed aluminum-foiled polycarbonate bottles and incubated in a dark chamber with flowing surface seawater for ~24 h. At the end of the incubation, one sample of each bottle was filtered through a 0.2- μ m membrane and preserved with HgCl_2 for final DIN analysis. For the mineralization experiment in the surface layer, four treatments were carried out: incubation on deck for ~8 h exposed to solar light in 500-ml quartz bottles of unfiltered and 0.2- μ m-filtered samples (Fig. B-5.2.2).



Figure B-5.2.2: On-deck incubations for measurement of DON and DIN mineralization in surface waters due to UV light exposure.

In the other two treatments, unfiltered and 0.2- μ m-filtered samples were incubated in the dark with flowing surface water for ~24 h. For the other two depths, only the dark experiments were carried out. All experiments were done in duplicate. At the end of the mineralization experiments, a water sample from each bottle was filtered through a 0.2- μ m membrane and preserved with HgCl_2 for

final DIN analyses or filtered, cooked and refrigerated for final DON analyses. From the two first sampling stations (3 and 4) one bottle of each mineralization treatment and depth was incubated either in the light or in the dark for ~10 days for a medium term mineralization analysis. After the medium term incubation, samples were treated likewise. For the three uppermost sampling depths of all the stations, respiration incubations were carried out in the dark for ~24 h within a dark chamber with flowing surface sea water. Initial dissolved oxygen concentrations on Winkler 250 ml aluminum-foiled bottles were measured immediately after the CTD Rosette was on deck. The final dissolved concentration at the end of the incubation was also measured.

Light spectrum measurements

The spectrum of solar radiation within wave lengths from 270 to 730 nm was measured with a TRIOS Ramses probe (Fig. B-5.2.3). Information on the light spectrum is needed for estimation of mineralization rates due to solar radiation. Two types of light measurements were carried out: vertical profiles in the upper water column and



Figure B-5.2.3: The spectrum of solar radiation (wavelengths 270-730 nm) was measured down to a depth of to 45 m using a Ramses probe (TRIOS). Information on the light spectrum is needed for the estimation of mineralization rates due to solar radiation.

recordings in the air on deck. Vertical profiles of the light spectrum were measured from the surface to a water depth of approx. 45 m at the sampling stations and in close temporal proximity to CTD and water sampling profiles. A total number of 13 profiles were recorded covering the conditions of morning, noon and evening at different latitudes. A clear spatial variation of light penetration due to differences in the suspended matter concentrations could be observed. In addition to the vertical profiles in water, the light spectrum in the air was measured on deck from dawn till dusk. Variable meteorological conditions made it necessary to record as many measurements as possible in order to determine representative daily cycles throughout the Red Sea. Therefore the on-deck recordings were done more or less continuously in between the vertical profiles.

5.2.3.ADCP data recording

ADCP data was collected using the vessel-mounted RDI Ocean Surveyor. The ADCP operates at 75 kHz and detects backscatter up to a water depth of ~620 m.

On the one hand, the ADCP data will be used to assess large-scale currents within the Red Sea. The data will help in the model verification of the tide-surge model of SP4 and in the estimation of the water exchange between Red Sea and Indian Ocean, required by SP3. An East-West transect at 16.5° North was recorded at low ship speed to increase measurement accuracy. Upper layer currents and water movements at lower depths could be distinguished, both in magnitude and direction. Wind and tidal currents will also be analyzed along the rest of the entire cruise track. Postprocessing of the ADCP current data, including corrections for pitch and roll and filtering of data which are noisy due to increased ship speeds, will be performed after the cruise.

On the other hand, the Echo Amplitude of the ADCP was used to capture vertical migration patterns of plankton in the upper water body. Vertical movements of suspended matter could be observed very clearly in the intensity of the backscattered ADCP signal (Fig. B-5.2.4). A correlation between the intensity records of the ADCP, which *a priori* are only qualitative, and samples of suspended matter, to be done by SP3, is envisaged to derive quantitative information. A comparison of the 24-h recordings at each sampling station allows an assessment of regional variations. The expected diurnal vertical migration of zooplankton was confirmed in backscatter intensity data and displayed the behavior of two to four discrete zooplankton groups, which ascended at dusk to prey and descended at dawn to avoid visual predation (Fig. B-5.2.4). Some animal groups migrated to depths of approximately 470 m – below the oxygen minimum zone - whereas a second group only migrated below the deep chlorophyll maximum to a depth of approximately 150 m. There was a noticeable band of very high backscatter in the surface mixed layer, 30 m and above.

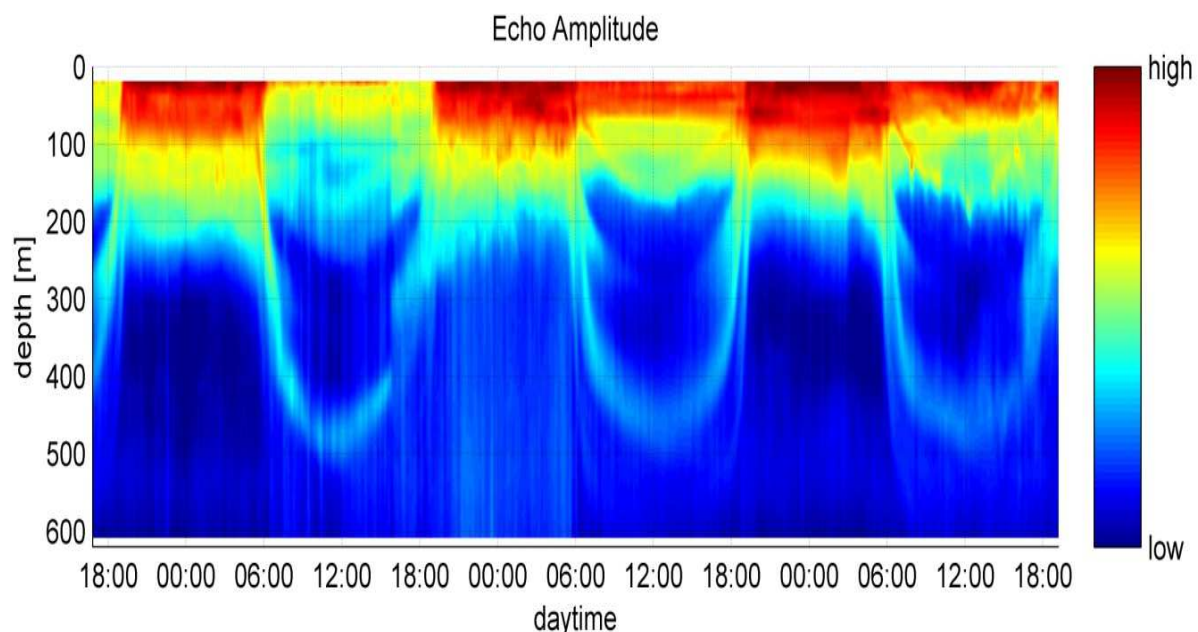


Figure B-5.2.4: Continuous measurements of backscatter intensity of the VMADC from 12 April to 14 April 2012.

5.3. Subproject 2

5.3.1. Sea Floor Imaging

N. Augustin

During RV PELAGIA cruise 64PE351, multibeam mapping was performed to collect bathymetric data of the Red Sea between 16°30'N and 25°30'N, including parts of the Red Sea Rift south of 19°30'N, bands of coastal regions close to Jeddah and the Farasan Archipelago, as well as parts of the Mabahiss Deep. In addition, bathymetric data were collected to increase the datasets existing from RV POSEIDON cruise P408 and RV PELAGIA cruise 64PE350. The mapping was carried out with a hull-mounted EM302 echo sounder system provided by Kongsberg Maritime AS. The EM302 multibeam echo sounder collects bathymetric, corrected backscatter and water column imaging (WCI) deep-water data over a wide swath with a maximum excess of 130° (2 x 65°). The configuration installed on RV PELAGIA operates in the 30-kHz frequency band at water depths of up to 7000 m. It has an across-ship swath width of up to 5.5x the depth, to approximately 8 km with 288 beams and 32 soundings per swath. Data acquisition was done using the Kongsberg Seafloor Information System (SIS) Version 3.7.5, Build 93, running in a Microsoft Windows XP environment. For details regarding the multibeam system and data processing see also part A of this cruise report.

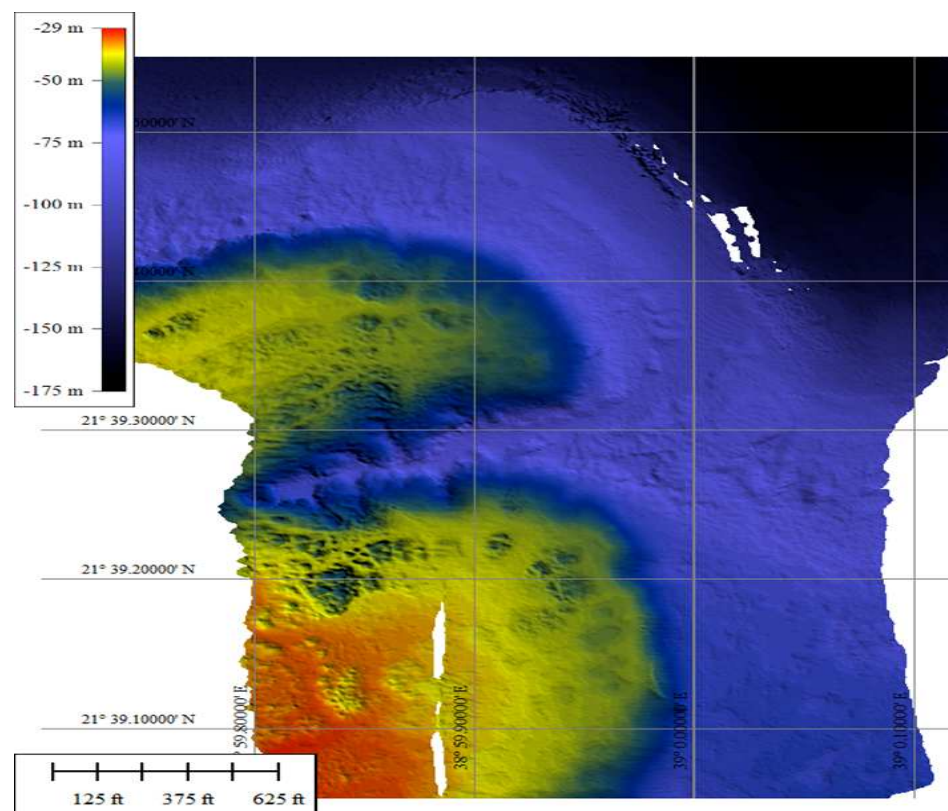


Figure B-5.3.1 Bathymetry of the MetOcean Buoy deployment site, southern Eliza Shoals Reef, Jeddah (KSA). The acoustic spatial resolution of this map is 1 m. The buoy was placed at the northern shallow reef part at a water depth of about 45 m.

Due to the high mapping speed of 9-10 kn the approximate spatial acoustic resolution of the data is about 30 m for the deeper parts. Additionally, higher resolution EM302 data (1-20 m) were collected from the shelf areas at the reefs of Jeddah (Fig. B-5.3.1), Farasan and Al-Wajh. A bathymetric survey of the Mabahiss Mons volcano in the Mabahiss Deep revealed a new and detailed view of the volcano, which measures about 6 km, with a caldera of 2 km in diameter (Fig. B-5.3.2).

Area-based editing of selected parts of the collected data was carried out using PFM container files created by DMagic as well as the 3DEditor modules included in the IVS 3D Fledermaus Professional software package. Processing the data with Kongsberg Neptune did not produce the needed results compared to area-based editing with the Fledermaus package. However, the cleaning and postprocessing aboard PELAGIA was selective and preliminary and will be finished ashore. By processing and calculating seafloor information mosaics of the Kongsberg backscatter data with the FMGT module, it was possible to distinguish between harder and more highly reflective seafloor (which was interpreted to be basaltic) from more sedimented or encrusted, restraining seafloor (B-5.3.2). Backscatter data were a major element in targeting rock-sampling stations (dredging) during cruise 64PE351. Combined with digital elevation models of the areas surveyed it improved the planning of seafloor sampling.

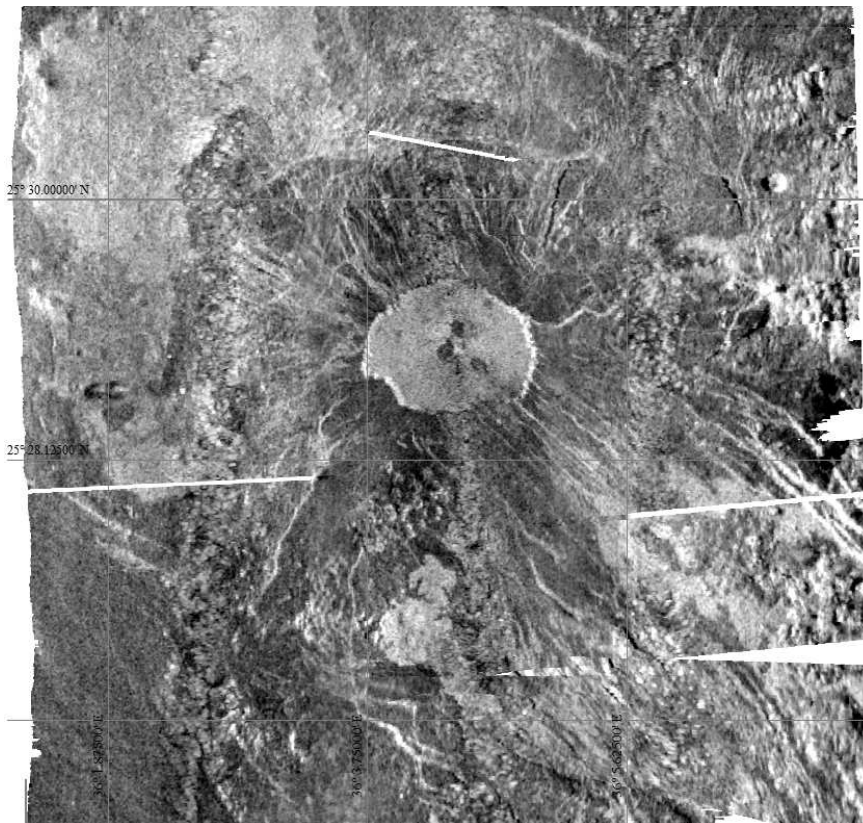


Figure B-5.3.2: Backscatter data of the Mabahiss Mons volcano. Bright reflectors at the flanks and inside the caldera mark most likely recent, lava flows, less covered by sediment and carbonate. While dark grey to blackish areas at the flanks of Mabahiss Mons represent carbonate encrustation, the grey area in the southwest corner of the picture represents sediments.

Preliminary gridding and bathymetric map production was realized using the Fledermaus DMagic module as well as Global Mapper. The data were mainly gridded with cell sizes of 15-30 m and exported in diverse needed data formats. More finely gridded bathymetric models with a spatial resolution of up to 1 m have been produced for the JAGO dive sites (see Fig. B-5.3.3), as well as the deployment sites of the oceanographic instrumentations (Figs. B-5.2.1, B-5.3.1) in order to provide more accurate navigational information in shallow waters near the coral reefs. The resulting maps could be used as layer in the OFOP navigation software, so the JAGO dives could be monitored, directed and navigated based on recent bathymetric charts instead of poor nautical maps or satellite images.

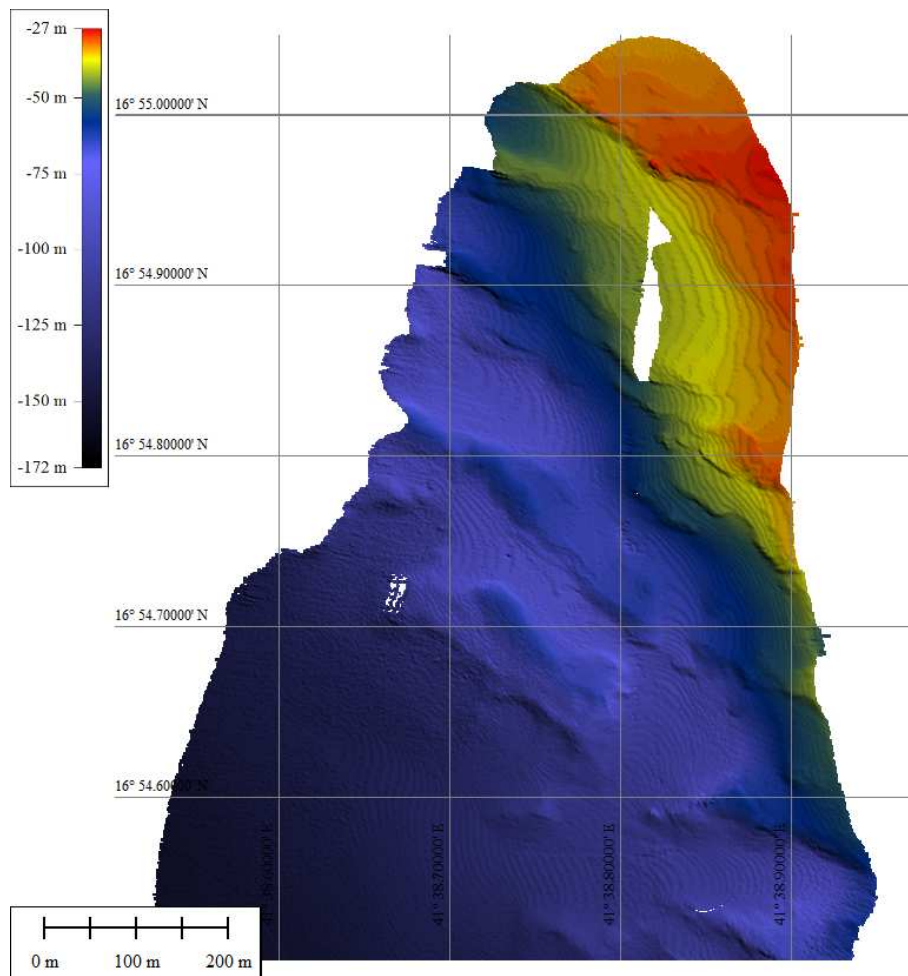


Figure B-5.3.3: Bathymetry of the JAGO dive site, at the Farasan Archipelago in the southern Red Sea. The acoustic spatial resolution of this map is 1 m.

5.3.2. Petrology and seafloor sampling

Froukje van der Zwan, Nico Augustin

Basaltic rock samples from different deeps and locations are required for (ongoing) chlorine investigations of basaltic samples which are performed within the Jeddah Transect Project (JTP) Subproject 2, which aims at tracing seawater infiltration into the crust and hydrothermal processes in the crust. In addition, studying basalts from the Red Sea is important for understanding the relation of the magmatism, tectonics, and southward evolution of the Red Sea spreading, e.g. different deeps may have a higher degree of melting or magma chambers at different depths/ temperatures/ compositions.

Earlier, basaltic glass had been obtained from Shaban Deep from other studies. During the JTP expeditions RV POSEIDON P408/1 in January 2011 and RV PELAGIA 64PE350, good basaltic samples had been recovered from all major deeps between 22°23' and 19°35' N. However, these cruises did not go further north and south. Therefore, the aim for expedition 64PE351 - from the petrological point of view - was to collect basalts from two sites in the southern Red Sea (Red Sea Rift at ~17° and 18°) and two from the northern Red Sea (Nereus and Mabahiss Deep) by dredging. For more details on dredge location targeting and sampling background, see part A of this report.



Figure B-5.3.4: Sample 14DR-1 from the Mahabiss Mons volcano offshore Al-Wajh. The sample from the south-eastern flank of the volcano represented a massive basaltic, folded sheet flow.

With four dredges deployed and an overall dredge station time of approx. 9 h, a total of nine individual basaltic samples (rocks and glass) were collected from the four sites and described (Fig. B-5.3.4). Apart from volcanic rocks (basalts with glass rims), carbonate crusts were collected at Nereus Deep, and a black crust at 17° N. The basalts collected are sheet lavas and blocky basalts with ½ - 1 cm-thick glass rims that are relatively fresh, only thin (<1 mm) palagonite alteration and some carbonate cover on the outside, apart from the basalt from Nereus which had no glass and was more heavily altered. An overview and description of all samples is given in Table B-5.3.1.

Table B-5.3.1: Dredge station list with sample descriptions (DR Chain bag dredge, BS backscatter image from multibeam).

Station	Latitude (°N)/ Longitude (°E)	Date/ Time (UTC)	Depth (m)	Sample descriptions and samples taken (TS = thin section/microprobe slide; GI = Glass; Mn = manganese; Qtz = quartz; Pl = Plagioclase; Ol = Olivine)
9 DR	16°46.980'/40°48.9	10.04.12	1389 -	4 dms rocks: sheet basalts + one black coated rock. + empty glass
North flank	65'	09:08 -	1341	bottle.
of volcanic	to	11:00		
cone at	16°46.831'/40°48.9			1: 20x17x18 cm: Basalt sheet flow. Semi-altered with palagonite +
16°47,	56'			carbonate on top. At bottom 'baked' sediment. ½ cm glass
slightly off				crust on top, <3 mm glass rims/flow edges on bottom. Flow
axis. Bright				structures/imprints on top and bottom. Rough bottom surface.
BS.				Large cm sized holes/gangs in bottom (~5%). Basalt ~30% <1
				mm vesicles and ~3% cm holes. Top more massive. No minerals
				visible.
				2: 27x13x3 cm: Basalt sheet flow. Semi-altered with palagonite and
				carbonate mud on top and bottom. Smooth surfaces, flowing
				patterns on top. Up to ½ cm thick glass crust. Massive, ~1%
				vesicle (<1 mm). ~15% <1 mm minerals: Pl?
				3: 9x7x7 + 11x8x3 cm + 3 smaller pieces: Black-yellowish
				crust/coating. Inside metallic (lead-copper) imprint/coating of
				metal object. Shiny black grains: sulfites? Many (~3%) 2-3 mm
				holes/gangs. Soft black streak.
				Extra rocks:
				1 sheet crust as 1: (extra 1)
				1 small piece of baked? sediment with glass (extra 2)
10 DR	17°58.323'/40°04.5	11.04.12	1670 -	Empty, cm sized glass fragments in sediment traps. Sieved for >1
Lava flow	86'	00:29 -	1630	mm and > 0.5 mm.
from central	to	03:28		
volcano at W	17°58.261'/40°04.6			
flank at RSR	02'			
18° N. Bright				
BS.				
13 DR	23°12.533'/37°16.0	16.04.12	1830 -	1 altered basalt; 1 carbonate rock; ~20 carbonate crusts. Small
Steep E flank	26' to	18:13 -	1417 -	black grains in sed. traps: glass? Sieved for >1 mm and >0.5
of Nereus	23°12.827'/37°16.3	20:51	11769	mm. Also black grains collected from carbonate crusts.
Deep. N of	55' to			1: 9x5½x4 cm: Basalt rock (no glass). Partially covered by hard
literature	23°12.478'/37°16.0			crystallized carbonate cover (brown, organic formed). Heavily
samples	47'			altered on outside: light brown to dark brown (Mn) to greenish
(bright BS)				grey alteration. Inside light grey: not fresh anymore. Vesicles
				(<1 mm, ~3%) and cracks filled with Fe-oxyhydroxyds: visible
				(but not heavily) LT seafloor alteration, on way to greenstone.
				2: 10x9x7 cm: Hard carbonate rock (breccia). Yellow brown to dark
				brown to whitish. Massive to mm-cm layers that are irregular
				and non-parallel (angled). Breccia fragments, some massive,
				some with fragments. Also glass fragments up to 3 mm +
				palagonite/glass rests on corner on surface. ~10% fossile
				fragments in patches (pteropods + shells). Some soft
				carbonate at side. 2x TS
				3: 10x6x2 cm: (soft) Carbonate crust. Vesicular: ~10%, <1-5 mm
				holes/gangs. White-yellow to yellow-grey-brown to dark brown
				(Mn). ~1% fragments of pteropods, forams, tubeworms.
				4: 7x5x ½ cm: Carbonate crust similar to 3. Bottom covered by mm
				black, brown and white grains (~20% cover).
				Extra rocks:
				22 1-10 cm pieces of carbonate crusts as 3, bagged together.

Table B-5.3.1 continued

14 DR	25°27.346'/36°05.8	19.04.12	1180 –	>10	10-49 cm pieces of glassy basalt: Sheet lavas + blocky basalt, palagonitization and a few carbonates on surface.
Mabahiss	41'	1:19 - 2:55	1100		
Deep South flank of caldera volcano (bright BS)	to 25°27.548'/36°05.5 91'				<p>1: 27x23x23 cm: Lobate basalt with glass on top and bottom. Large flowing structures. Blas up to 1 cm thick, fresh. Palagonite altered, little carbonate on top and in pockets. Some pockets 'collapsed' (round rim visible) with carbonate mixed with glass fragments as filling. Basalt up to 5% (1 mm) vesicular on rims, inside more massive. No minerals visible. GI.</p> <p>2: 17x10x9 cm: Sheetflow/lobate basalt with glass. Flowing structures. Core (bottom, folded to the inside) is basalt with large pockets, partially filled with yellow carbonate sediment. Top: lass up to 1 cm thick, in flowing/faulting patterns (like a front that broke through). Palagonite altered, Some carbonate crust on top. Basalts ~5% (<1-10 mm) vesicles. 1% needles of PI up to 3 mm long. GI.</p> <p>3: 10x9x5 cm: Basaltic glass rock around large pocket. Rock/glass up too 2 cm thick. On top 5 cm thick carbonate crust, mixed with 2-5 mm glass fragments. Palagonite altered + tubeworms. Flowing appearance. ~1% (1 mm) vesicles, no other features. GI</p> <p>4: 12x10x10 cm: Basalt block with glass at edges (Similar as 1). Palagonite altered, carbonate on top + tubeworms. One side: grey-white carbonate patch with some pterpods. Basalt has some 1-2 cm pockets.1 cm thick bands of high vesicularity: ~20% (1-2 mm). Rest ~3%. 3% PI (needles) up to 5 mm long. GI.</p> <p>Extra rocks:</p> <p>1 blocky basalt with glass as 1 (extra 1)</p> <p>2 basaltic glass rocks as 3 (extra 2, 3)</p> <p>1 blocky basalt with little glass, altered. As 4 (extra 4)</p>

5.4. Subproject 3.2

5.4.1. Submersible JAGO Dives

Yvonne Sawall, Abdulmoshin Al-Sofyani, Tom Kwasnitschka, Jürgen Schauer, Karen Hissmann

The manned research submersible JAGO of GEOMAR was mobilized on board of RV PELAGIA and prepared for diving during the last week of RV PELAGIA cruise 64PE350 (see part A of this report). JAGO can take the pilot and a scientist to a maximum depth of 400 m. It was planned to use the submersible for video/ photo documentation, photogrammetry and sampling of photosynthesizing scleractinian corals and other biota from the mesophotic zone below scuba diving depth at different sites along the Saudi Arabian coast whenever the working program along the central transect would allow inshore excursions. Unfortunately, regular time-consuming transits between the plankton sampling sites and suitable JAGO dive sites closer to the shelf were not possible.

During 64PE350, JAGO was deployed at two different sites that were at a steaming distance of 3-4 h from the main transect stations. Multibeam mapping prior to the dives provided information on the bathymetry. JAGO-Dive 1181 took place at depths between 95 and 40 m at the southern side of Ad Dissan Island, Farasan Archipelago (16°54'N, 41°38'E). The location appeared worth exploring on the little detailed sea charts. The gradually rising slope, however, was found to be mainly covered with soft sediment, like the rocky outcrop ridges that were crossed while moving upslope. The diversity and abundance of benthic organisms colonizing these rocky structures were low, and mainly restricted to sponges, few small asymbiotic stony corals (small orange colonies of most likely *Dendrophyllia* sp. and solitary (*Desmophyllum* sp.) and soft corals, some of which were collected. *Leptoseris* sp. corals (Fig. B-5.4.7), the prioritized scleractinian genus for incubation experiments (see below), were not found. The benthic community obviously struggles with the high sedimentation rate in this area.

The exploration of the Al-Wajh site (25°23'N, 36°40'E) had originally been planned for 19 April. Due to a bad weather forecast, the offshore program was interrupted and the reef approached already in the afternoon of 18 April. JAGO-Dive 1182 took place at the fringing reef of Al-Wajh, at depths between 145 and 75 m, first along a very steep, partly overhanging carbonate wall with a rugged edge texture and almost no benthos. The slope angle then started to decline to ca. 60° at a depth of about 100 m. Numerous *Leptoseris* sp. corals were collected at depths between 95 and 77 m at the upper edge of the wall around a huge reef boulder of ca. 10 m in height that was densely colonized mainly by gorgonians and encrusting red algae.

Leptoseris sp. specimens had also been collected by JAGO during the previous RV PELAGIA cruise 64PE350 (see part A) at the edge of a steep reef drop-off northwest of Jeddah (Shi'b Al Kabir, 21°40'N, 38°50'E). During RV PELAGIA cruise 64PE351, deployment and recovery of the submersible over the ship's stern went very well thanks to the professional teamwork between the deck crew and the teams in the workboat and on the bridge.



Figure B-5.4.1: Recovery of submersible JAGO on board RV PELAGIA after a dive at the reef of Al-Wajh.



Figure B-5.4.2: Rocky outcrop ridge with low benthos coverage at a depth of 48 m at Farasan Archipelago.



Figure B-5.4.3: Sponges on soft sediment, 88m, Farasan dive.

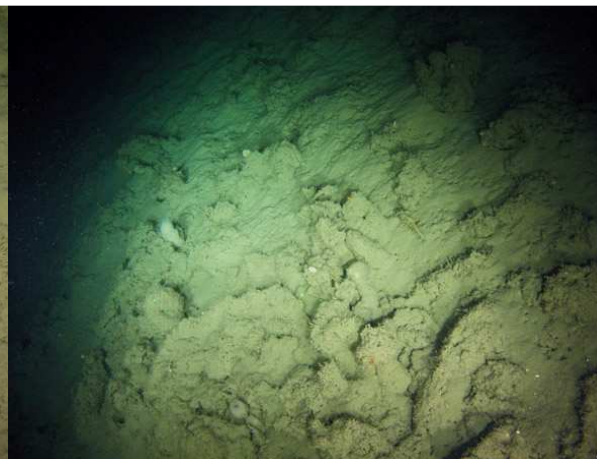


Figure B-5.4.4: Outcrop ridge at 85 m, Farasan Islands.



Figure B-5.4.5: Steep wall at 145 m, Al-Wajh.



Figure B-5.4.6: Benthic community on boulder at 75 m, Al-Wajh.



Figure B-5.4.7: Photosynthesizing *Leptoseris* sp. coral at a depth of 85 m, Al-Wajh reef. *Leptoseris* sp. corals occur below the euphotic zone; they bear endo-symbiotic algae that photosynthesize at extremely low light levels.

Table. B-5.4.1: Overview of JAGO dives during 64PE351

JAGO Dive #	Date	Location	Submerged Surfaced [UTC] Total time	Min-Max Depth [m]	Pilot Observer
1181 (4)	09-04- 12	Farasan Islands 16°54.69'N, 41°38.71'E	05:50- 07:56 126 min	44-93	Jürgen Schauer Yvonne Sawall
1182 (5)	18-04- 12	Al-Wajh Reef 25°23.39'N, 36°40.75'E	13:12 - 16:06 174 min	75-145	Jürgen Schauer Tom Kwasnitschka

CTD and water sampling

At the stations Shi'b Al Kabir (see part A, chapter 4.5), Farasan Islands and Al-Wajh a CTD profile was taken up to depths of 100/ 150 m and water samples were retrieved from a depth of 100 m. The water samples were used for water quality analyses (filtration: chl *a*, POM, DOC) and to keep the organisms collected by JAGO.

Incubations of Leptoseris spp.

The photosynthesizing deep water coral *Leptoseris* spp. was collected with JAGO at Shi'b Al Kabir (dive 1179) and Al-Wajh (dive 1182). The specimens were incubated on board during the following two days. By this, the photosynthesis and respiration rates of the corals were measured and water samples (initial and end) were taken for total alkalinity measurements to determine calcification rates. Furthermore, measurements with a Pulse Amplitude Modulation Fluorometer (PAM) were conducted on the corals (and on the endolithic algae) to evaluate the photosynthetic efficiency and hence photoacclimation processes. After the measurements, the coral tissue was taken off the skeleton and frozen for further analyses (e.g. pigments, proteins, biomass etc).

Organisms for reference collection

Some organisms collected by JAGO were preserved in Formalin (24 h) and Ethanol (long-term fixation). In total: Shi'b Al Kabir: 1 soft coral, 4 gorgonians, 1 hard coral; Jizan: 3 soft corals, 1 gorgonian; several small organisms attached to rocks, such as sponges, hydrozoans, worms etc. Furthermore, 3 gorgonians were dried, as well as some rocks covered by crustose red algae.

Photographic documentation

The dives were documented using an array of multiple cameras mounted inside as well as outside the submersible hull. All dives were surveyed using one or two GoPro HDhero II cameras mounted to the upper front bar of JAGO. The cameras were set to a two-second interval photo mode to provide uninterrupted overview mapping of the surveyed outcrops. Additionally, a camera was run inside the submersible. During dive 1179, two Canon Powershot G12 cameras were mounted outside on the upper front

bar. They were set to a capture interval of four seconds. On later dives they were not deployed since the existing GoPro cameras provided sufficient coverage. During dive 1181 we used a High definition camcorder with tele-zoom capability. During dive 1182, a RED One digital cinema camera with a hemispheric fisheye lens was carried to provide enhanced overview documentation functionality. This photographic data will be used to derive three-dimensional models of the reef slopes surveyed, to form a basis for later habitat mapping and biodiversity studies in context to the local seafloor relief.

6. Acknowledgements

The scientists on board highly acknowledge the professional, friendly and sustainable support of the RV PELAGIA crew during 64PE351. In particular, we also acknowledge the protection by the Royal Saudi Arabian warship Al-Riyadh.

7. References

- Aberle D, Hansen T, Böttger-Schnack R, Burmeister A, Post AF, Sommer U. (2010) Differential routing of 'new' nitrogen toward higher trophic levels within the marine food web of the Gulf of Aqaba, Northern Red Sea. *Marine Biology* 157:157-169.
- Acker J, Leptoukh G, Shen S, Zhu T, Kempler S (2008) Remotely-sensed chlorophyll *a* observations of the northern Red Sea indicate seasonal variability and influence of coastal reefs. *Journal of Marine Research* 69:191-204.

Appendix

1. Dive log for ROV dive 1

Dive log for ROV dive 1

Ocean Modules V8 Offshore ROV Dive Log			
Client: GEOMAR	Job No: 1		Date: 09-03-2012
	Location: Red Sea, N 21°34.35'; E 38°49.58		Vessel: R/V PELAGIA
	Conditions:		
Supervisor:	Pilot: Tomas Lundälv	Observer: Peter Linke Mark Schmidt	Deck Hand:
Dive No.: 1	Consumables:		
Dive Task: Observation			

Time	Heading	Depth	Description
06:50	308°	42m	63m of wire with depressor weight
06:53	303°	81m	83m of wire (winch speed 0,27 m/s)
06:56	290°	118m	116m of wire (winch speed 0,2 m/s); ROV Pitch 5°-9°
06:59	300°	150m	152m of wire (winch speed 0,25 m/s); Vessel Heading: 211°
07:02	299°	180m	180m of wire (winch speed 0,23 m/s); Vessel Heading: 222°
07:06	299°	215m	215m of wire (winch speed 0,25 m/s); Vessel Heading: 227°
07:15	300°	300m	305m of wire
07:21	304°	367m	372m of wire (winch speed 0,25 m/s)
07:24	309°	404m	406m of wire; Vessel Heading: 238°; PCB Temperature, °C: 0F (Option Board, Surface control unit): 38° 05 (Option Board, ROV): 32,5° 00 (Control Board, ROV): 57,5° 01 (Option Board, ROV): 49,5°
07:31	295°	449m	460m of wire, Vessel Heading: 224°

07:37	319°	507m	510m of wire, Vessel Heading: 232°
07:46	306°	566m	569m of wire, Vessel Heading: 232°, LED: Front-Portside – not able to turn off
07:53	307°	630m	635m of wire, Vessel Heading: 219°, LED: Aft - not able to turn off
07:58	326°	667m	670m of wire, Vessel Heading: 226°
08:03	311°	709m	714m of wire, Vessel Heading: 236°
08:10	190°	770m	Large number of small fish appearing
08:11	245°	781m	Mismatch in MRU and IMU heading readings – IMU:244°, MRU:287°
08:16	246°	798m	Visual contact with bottom
08:18	246°	798	Still large number of small fish all around
08:26	257°	799m	Beginning of transect. Soft mud with signs of bioturbation. Small fish and some shrimps.
08:30	282°	799 m	HD-camera, short loss of video signal
08:33	268°	799 m	Marks of deposit feeder on sediment surface
08:34	313°	799 m	Wedge-shaped small flatfish on bottom
08:35	277°	798m	Pan & Tilt – reluctant, in fully down position, not able to move up Vessel – moving West (Velocity: 0,3kn); Vessel Heading: 258°
08:40	238°	798m	HD Camera- short loss of video signal
08:41	241°	798 m	HD-camera - 10 min loss of video signal
08:52	282°	798 m	Video signal back. Mud with evidence of bioturbation and deposit feeding
08:55:40	280°	799 m	Fragments of plastic
09:00	255°	798m	Error - > one or more thrusters failure
09:02	310°	798 m	Aluminium can and metal garbage
09:04	290°	798m	Metal can
09:07	268°	799m	Small fish with long undulating tail
09:07:40	285°	799m	Pair of red shrimps with long antennae
09:08	302°	800m	Pan & Tilt – functioning
09:12	281°	799m	Plastic garbage?
09:16	277°	799m	Plastic garbage

09:19	247°	799m	Rusted metal?
09:19:50	261°	799m	Small mounds from infauna
09:23	280°	799m	Medium-sized fish
09:27	276°	799m	A couple of shrimps
09:29	270°	799m	Sparse population of shrimps
09:30	267°	798m	Vessel Heading: 257°
09:30:30	268°	799m	Plastic debris?
09:31	272°	799m	Medium sized fish
09:32	263°	799m	Trawl marks?
09:32:30	273°	799m	Plastic mug
09:34:10	267°	798m	Mounds from infauna
09:36	261°	798m	Vessel Heading: 256°, Vessel Velocity: 0,3kn
09:37	272°	798m	Plastic debris
09:37:50	266°	798m	Lost shoe
09:39:15	262°	798m	Lost slipper
09:40	278°	798m	Medium sized dark fish resting on bottom
09:48:20	287°	797m	Plastic debris
09:50:43	242°	797m	Pelagic shrimp with long tentacles passing
09:51	244°	796m	Vessel Heading: 255°, Vessel Velocity: 0,4kn
09:56	233°	796m	Vessel Heading: 266°, Vessel Velocity: 0,2kn
09:59:30	243°	796m	Aluminum can
10:11:15	228°	795m	Rusty steal bar
10:12:50	257°	795m	Depression in seafloor with large amounts of plastic and metal garbage
10:14	296°	793m	Changing Vessel Heading to 30°; Observation of depression of bottom surface, filled with garbage
10:16	100°	795m	Changing Vessel Heading to 30°
10:16:15	58°	795m	Plastic mug
10:21	95°	796m	
10:25	72°	796m	Medium-sized dark fish
10:26:30	71°	796m	Very thin small fish moving backwards

10:31:40	81§	797M	Aluminum can and bottle
10:33	30°	796m	
10:33:40	31°	797m	Pelagic shrimp with long tentacles
10:34:20	22°	797m	Bottle
10:35	23°	797m	Hermit crab in odd shell
10:39:57	77°	797m	Large squid passing by
10:41:20	80°	797m	Depression in seafloor with plastic and metal garbage. Ceranthid anemones
10:45:00	58°	797m	Plastic debris
10:46:10	54°	797m	Small shark passing by
10:46:20	52°	797m	Pelagic shrimp with long tentacles passing
10:47:50	75°	798m	Plastic debris
10:51:10	56°	797m	Trawl/dredge-marks
10:52:09	62°	798m	Plastic spoon
Time	Heading	Depth	Description
10:54:55...	53°	798m	Good views of unknown deposit feeder
10:56:40	53°	798	Pebbles?
10:57:30	39°	798m	Plastic debris
10:59:17	29°	797m	Rusty wire, aluminum can and plastic debris
11:02:24	103°	798m	Metal and plastic garbage
11:03	74°	797m	Changing Vessel Heading: 28°
11:10	47°	797m	Vessel Heading: 20°, Vessel Velocity: 0,2kn
11:11:36	47°	797m	Plastic spoon
11:13:56	35°	797m	Aluminum can and small dark/shiny fish
11:20:40	99°	798m	Glass bottle
11:21	89°	797m	Vessel Heading: 12°, Vessel Velocity: 0,2kn
11:24:35	38°	798m	Plastic/rubber? Debris
11:30	40°	797m	Bottle
11:31:04	44°	796m	Plastic debris
11:34:26	133°	797m	Plastic knife

11:36	111°	797m	Plastic debris
11:38	359°	797m	Plastic pen
11:38:20	338°	797m	Rusty metal barrel
11:40:38	25°	797m	Plastic spoon
11:41:45	27.1	797m	Nodule?
11:43:55	106°	797m	Aluminum can
11:45:35	92°	796m	Ink from escaping squid? Dark medium sized fish passing to left
11:46	89°	796m	Plastic spoon
11:46:35	108°	796m	Dark stain with white spots in the distance
11:53:28	214	797m	Upon closer inspection dark stain appears to be heap of dung with white plastic strings
11:54	233°	797m	Plastic spoon
11:55:40	21°	797m	Dredgemarks?
11:57:20	300°	796m	Bottle
11:57	330°	795m	Changing Vessel Heading: to 270° PCB Temperature, °C: 0F: 39,5° 05: 31,5° 00: 56° 01: 48,5°
11:58:56	241°	797m	Aluminum cans and plastic bar
12:01:10	297°	796m	Plastic debris
12:02:10	325°	796m	Plastic plate
12:03:24	288°	797m	Plastic debris
12:05	352°	796m	Vessel Heading: 262°
12:08	40°	787m	Take off from bottom contact
12:15	42°	747m	Umbilical multiply twisted around wire
12:51	340°	603m	
13:15	11°	563m	

13:57	350°	523m	
15:44	140°	402m	515m of wire; not able to use wire winch, started recovery using fixing ropes and deck crane
15:54	85°	383m	
16:05	105°	366m	
16:12	115°	353m	
16:30	102°	315m	
16:46	112°	270m	
17:00	173°	228m	
17:15	254°	190m	
17:47	88°	117m	
18:30			ROV at the surface
18:57			ROV on deck
			Total Time and Maximum Depth:
			12:07 (hh:mm)
			800 m

GEOMAR Reports

No.	Title
1	FS POSEIDON Fahrtbericht / Cruise Report POS421, 08. – 18.11.2011, Kiel - Las Palmas, Ed.: T.J. Müller, 26 pp, DOI: 10.3289/GEOMAR_REP_NS_1_2012
2	Nitrous Oxide Time Series Measurements off Peru – A Collaboration between SFB 754 and IMARPE –, Annual Report 2011, Eds.: Baustian, T., M. Graco, H.W. Bange, G. Flores, J. Ledesma, M. Sarmiento, V. Leon, C. Robles, O. Moron, 20 pp, DOI: 10.3289/GEOMAR_REP_NS_2_2012
3	FS POSEIDON Fahrtbericht / Cruise Report POS427 – Fluid emissions from mud volcanoes, cold seeps and fluid circulation at the Don-Kuban deep sea fan (Kerch peninsula, Crimea, Black Sea) – 23.02. – 19.03.2012, Burgas, Bulgaria - Heraklion, Greece, Ed.: J. Bialas, 32 pp, DOI: 10.3289/GEOMAR_REP_NS_3_2012
4	RV CELTIC EXPLORER EUROFLEETS Cruise Report, CE12010 – ECO2@NorthSea, 20.07. – 06.08.2012, Bremerhaven – Hamburg, Eds.: P. Linke et al., 65 pp, DOI: 10.3289/GEOMAR_REP_NS_4_2012

For GEOMAR Reports, please visit:

https://oceanrep.geomar.de/view/series/GEOMAR_Report.html

Reports of the former IFM-GEOMAR series can be found under:

https://oceanrep.geomar.de/view/series/IFM-GEOMAR_Report.html

Das Helmholtz-Zentrum für Ozeanforschung Kiel (GEOMAR)
ist Mitglied der Helmholtz-Gemeinschaft
Deutscher Forschungszentren e.V.

The Helmholtz Centre for Ocean Research Kiel (GEOMAR)
is a member of the Helmholtz Association of
German Research Centres

Helmholtz-Zentrum für Ozeanforschung Kiel / Helmholtz Centre for Ocean Research Kiel

GEOMAR
Dienstgebäude Westufer / West Shore Building
Düsternbrooker Weg 20
D-24105 Kiel
Germany

Helmholtz-Zentrum für Ozeanforschung Kiel / Helmholtz Centre for Ocean Research Kiel

GEOMAR
Dienstgebäude Ostufer / East Shore Building
Wischhofstr. 1-3
D-24148 Kiel
Germany

Tel.: +49 431 600-0
Fax: +49 431 600-2805
www.geomar.de